ARMY RESEARCH LABORATORY

Modeling Body Joint Loads During Equipment Decontamination Operations

Richard W. McMahon
Tariq Shams

ARL-TR-1332 JULY 1997

The findings in this report are not to be construed as an official Department of the Army position unless so designated by other authorized documents.

Citation of manufacturer's or trade names does not constitute an official endorsement or approval of the use thereof.

Destroy this report when it is no longer needed. Do not return it to the originator.

Army Research Laboratory
Aberdeen Proving Ground, MD 21005-5425

ARL-TR-1332 July 1997

Modeling Body Joint Loads During Equipment Decontamination Operations

Richard W. McMahon
Human Research & Engineering Directorate

Tariq Shams
General Engineering and Systems Analysis Company

Abstract

The General Engineering and Systems Analysis Company (GESAC), Inc., under contract with the Human Research and Engineering Directorate of the U.S. Army Research Laboratory (ARL), (contract number DAAL01-94-P-0906) estimated body joint loading using a computer simulation program called DYNAMAN. This work was performed in support of the U.S. Army Chemical and Biological Defense Command (CBDCOM) modular decontamination system (MDS) development program.

The objective of this effort was to model the loading imposed by each of five different scrub brush systems on various human body joints and compare the resulting force and torque values. Of primary interest was information concerning how electric motor placement affected joint loading and how the joint loads of the powered brush systems compared with those of the manual brush.

The results of this modeling effort identified several limitations with the current model, identified several key aspects of power scrub brush design and operator interface, and were used to aid in the selection of brush designs for continued development. In addition, the results indicate that the counterweight offered by attaching the motor to the brush helps to slightly reduce the torque imposed on the operator's body.

It is recommended that future efforts to model the effects of force and torque on humans include a highly definitive description of simulation conditions to allow for improved comparison. Finally, it is recommended that a research effort be undertaken to improve our understanding of the biodynamical tolerance of human joints to external loading. This effort should include determinations of human joint safety as well as comfort tolerance to joint loading.

PREFACE

The modeling work described in this report was performed by General Engineering and Systems Analysis Company (GESAC), Inc. under contract with the Human Research and Engineering Directorate (HRED) of the U.S. Army Research Laboratory (ARL) (contract number DAAL01-94-P-0906). Body joint loads were estimated using a computer simulation program called DYNAMAN.

The contract was awarded to support the U.S. Army Chemical and Biological Defense Command (CBDCOM) modular decontamination system (MDS) development program. The MDS pumper-scrubber module, including its electrically powered scrub brush, entered engineering design testing (EDT) in November 1994.

The objective of this contract was to model the loading imposed by each of five different scrub brush systems on various human body joints and compare the resulting force and torque values. Of primary interest was information concerning how electric motor placement affected joint loading and how the joint loads of the powered brush systems compared with those of the manual brush. The results of this modeling effort will be used to aid in the selection of brush designs for continued development.

The joint loads of each brush system were simulated using DYNAMAN. This computer simulation program can be used to model the dynamics of linked bodies exposed to the forces of acceleration. GESAC, Inc., modified the program to incorporate the data necessary to model the balancing effects of muscles in the waist and other joints in order to stabilize the model for use with external loads.

The authors would like to acknowledge the engineering and technical assistance provided by Mr. Dave Harrah, HRED, ARL, and Nagarajan Rangarajan, Ph.D., GESAC, Inc.

CONTENTS

TABLES

MODELING BODY JOINT LOADS DURING EQUIPMENT DECONTAMINATION OPERATIONS

INTRODUCTION

Current U.S. Army detailed equipment decontamination procedures as described in Field Manual (FM) 3-5 (Headquarters, Department of the Army, 1993) require that soldiers use mops and brooms or the decontaminating apparatus, M13, to apply and scrub decontamination solution No. 2 (DS2) on the contaminated surfaces of vehicles. The scrubbing action, although highly labor intensive, is considered to be necessary to mix the DS2 with the chemical or biological agent on the vehicle surface, thus effecting decontamination.

In an effort to reduce the soldier's workload, the U.S. Army Chemical and Biological Defense Command's (CBDCOM) modular decontamination system (MDS) program has developed a diesel-powered DS2 application system (XM21). This system includes two DS2 spray wands and two electrically powered scrub brushes. Conceptually, the powered scrub brush is intended to eliminate the labor-intensive action of manually using mops and brooms to mix the DS2 and chemical agent. This mixing action will be automated by the electrically powered rotating brush. However, the powered scrub brush assembly is heavier than the manual broom and the soldier still has to physically guide it over the vehicle surface and thus, he or she is exposed to load forces that contribute to fatigue.

The objective of this effort was to model the loading imposed by each of five different scrub brush systems on various human body joints and compare the resulting force and torque values. Of primary interest was information concerning how electric motor placement affected joint loading and how the joint loads of the powered brush systems compared with those of the currently used manual brush. A computer simulation model was used to determine the physical stresses imposed on the soldier by the MDS scrub brush systems. This report describes the results of this simulation. General Engineering and Systems Analysis Company (GESAC), Inc., under contract with the U.S. Army Research Laboratory (ARL) (contract number DAAL01-94-P-0906), modeled body joint loads for the different brush systems using a program called DYNAMAN.

Using the physical properties (weight, length, motor torque, handle location, and an estimate of brush contact friction) of each brush system as input, DYNAMAN was used to calculate the force and torque values imposed on the elbows, shoulders, hips, and knees of the user. This effort supported the MDS program by identifying the advantages and disadvantages related to joint loading, for various sub-system design considerations.

OVERALL MODEL AND SIMULATION INTERACTION

A model of a 50th percentile human male using one of four powered scrub brushes (PSB) or a manual scrub broom (MSB) against a vertical flat surface has been developed (see Figure 1). The model is used by the simulation program DYNAMAN to calculate forces and torques at various body joints. Table 1 describes the five different brush systems used in the model.

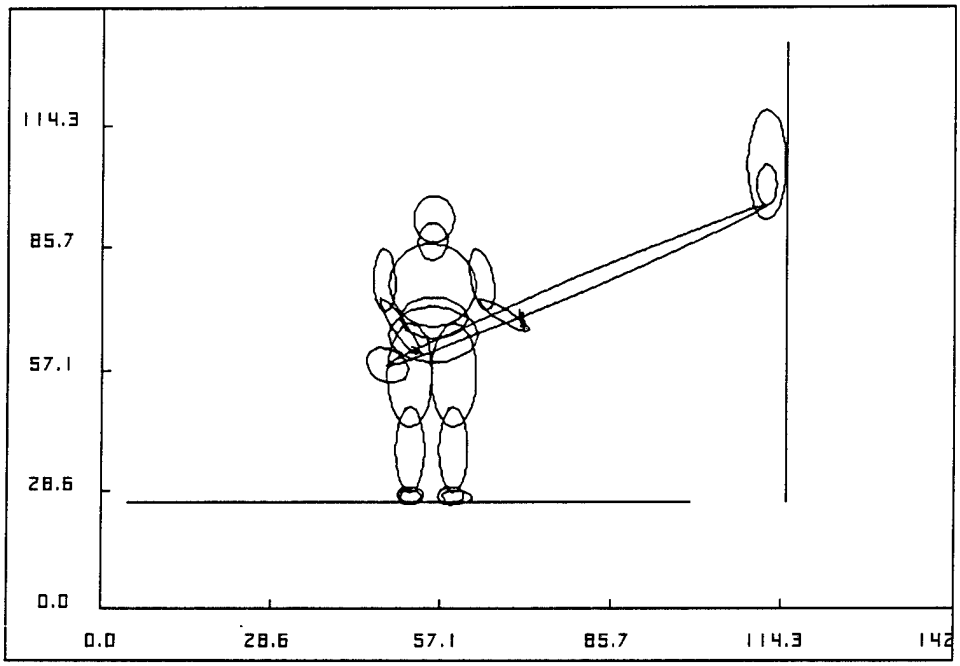

Figure 1. 50th percentile male Hybrid II human figure holding scrub brush.

Table 1

Description of Brush Systems

Brush No.	Brush type	Brush nomenclature	Motor location	Brush length (inches)
01	Manual	Manual brush	N/A	60
02	Powered	Redesign-attach	Attached to PSB	Short (85)
03	Powered	Config C-attach	Attached to PSB	Long (140)
04	Powered	Redesign-unatt	Back of operator	Short (85)
05	Powered	Config C-unatt	Back of operator	Long (140)

For each brush (01 through 05), simulations were run to examine joint loads when the operator holds the brush at different angular orientations. The basic design of the model is described in the following four sections along with a description of the assumptions made in generating the model.

Model of the Human Operator

The scrub brush operator is a Hybrid II dummy (Shams et al., 1992) developed using U.S. Air Force anthropometric survey data for a 50th percentile male person. Table 2 is a listing of the anthropometric measures from which the Hybrid II dummy is constructed.

Table 2

List of Antropometric Measures for Hybrid II Dummy

Weight
Standing height
Shoulder height
Armpit height
Waist height
Seated height
Head length
Head breadth
Head to chin height
Neck circumference
Shoulder breadth
Chest depth
Chest breadth
Waist depth
Waist breadth
Buttock depth
Hip breadth, standing
Shoulder to elbow length

DYNAMAN was originally intended to be used in automobile crash reconstruction to determine impact forces on the Hybrid II dummy vehicle occupant. For this use, the dummy is not required to model active musculature or simulate standing balance, carry external loads, or be used for analyzing static external loading effects. If this dummy were required to hold even

minimal weight (2 pounds) outside its "body," its center of gravity (CG) would be affected to the point where it would fall. For this reason, the Hybrid II dummy data set required several changes to allow for proper behavior of the dummy when it is made to stand and hold the various brush systems. Since DYNAMAN does not model active musculature or simulate strength responses, it was necessary to balance the dummy in a state of equilibrium by moving the dummy's CG (originally located within the lower torso segment) slightly forward, so that the torques produced by the contact of the feet with the ground while the dummy holds the brush would be as small as possible. In addition, all the joints in the dummy were permanently locked so that various segments would not begin rotating with each other when external torques began to act.

To improve the balance of the dummy further, each foot was modeled by using an ellipsoid to model the heel in addition to the regular ellipsoid that modeled the front of the foot. This controlled, to some extent, the rotation of the body in the anterior-posterior direction (about the lateral axis).

Model of Brush

Model of Brush Nos. 02 and 04 (PSB)

Some modeling assumptions were made regarding the No. 02 and 04 PSBs. The brushes were modeled as consisting of four separate segments joined together, roughly corresponding to the physical segments in the actual PSB. The various segments and their properties, and their correspondence with the actual brush properties are as follow:

Brush:

Model:
- shape - ellipsoidal
- half-length - 18 inches (only half of ellipsoid relevant to model)
- diameter - 6 inches
- weight - 0.9 pound

Actual PSB: shape - conical
- length - 12 inches
- diameter - varied (6 inches to 2 inches)
- weight - 0.92 pound

Angled Extension (approximately at 60° to straight extension):

Model:
- shape - ellipsoidal
- length - 9 inches

diameter - 3 inches
weight - 0.3 pound (estimated from proportional length)

Actual PSB: shape - cylindrical
length - 9 inches (est.)
diameter - 2 inches
weight = 0.3 pound (est.)

Extension rod:

Model: shape - long, thin ellipsoid
length - 70 inches
diameter - 3 inches
weight - 3.6 pounds (including handle)

Actual PSB: shape - long cylindrical rod
length - 70 inches (estimated, excluding angled extension)
diameter - 2 inches
weight - 3.98 pounds

Motor:

Model: shape - ellipsoidal
length - 6 inches
diameter - 8 inches
weight - 7.5 pounds

Actual PSB: shape - roughly cylindrical
length - 6.25 inches
diameter - 8 inches
weight - 7.5 pounds

Total weight

Model - 12.3 pounds
Actual - 12.4 pounds

Total length

Model - 85 inches
Actual - 84.5 inches

Model of Brush Nos. 03 and 05 (PSB)

The models of the No. 03 and 05 PSBs were developed in the same way as the No. 02 and 04 PSBs. These brushes also consisted of four separate segments joined together, roughly corresponding to the physical segments in the actual PSB. In these configurations, however, an additional extension length of 41.7 inches was added to the segment corresponding to the extension rod along with a corresponding additional mass of about 1 pound. The various segments and their properties and their correspondences with the actual brush properties are as follow:

Brush:

Model: shape - ellipsoidal
half-length - 10 inches (only half of ellipsoid relevant to model)
diameter - 6 inches
weight - 1.0 pound

Actual PSB: shape - conical
length - 10.5 inches
diameter - 6 inches
weight - 1.0 pound

Angled Extension (approximately at 60° to straight extension):

Model: shape - ellipsoidal
length - 9 inches
diameter - 3 inches
weight - 0.3 pound (estimated from proportional length)

Actual PSB: shape - cylindrical
length - 9 inches (est.)
diameter - 2 inches
weight = 0.3 pound (est.)

Extension rod:

Model: shape - long, thin ellipsoid
length - 115 inches
diameter - 3 inches
weight - 5.8 pounds (including two handles)

Actual PSB: shape - long cylindrical rod
length - 114.7 inches (estimated, excluding angled extension)
diameter - 2 inches

weight - 5.8 pounds (including two handles)
(* Center extension weight estimated from weights of other segments)

Motor:

Model: shape - ellipsoidal
length - 6 inches
diameter - 8 inches
weight - 7.5 pounds

Actual PSB: shape - roughly cylindrical
length - 6.25 inches
diameter - 8 inches
weight - 7.5 pounds

Total weight

Model - 14.6 pounds
Actual - 14.6 pounds

Total length

Model - 140 inches
Actual - 140.7 inches

Model of Brush No. 01 (MSB)

The MSB (brush No. 01) was modeled using two separate segments joined together. The various segments and their properties and their correspondences with the actual brush properties are as follow:

Broom:

Model: shape - approximately rectangular (hyper-ellipsoid)
dimensions - 4 inches x 18 inches x 5.6 inches
(this includes bristle length + width)
weight - 1.8 pounds

Actual MSB: shape - approximately rectangular
dimensions - 4 inches x 18 inches x 5.6 inches
(includes bristle + width)
weight - 1.8 pounds

Handle:

Model:	shape - long, thin ellipsoid length - 60 inches diameter - 1 inch weight - 1.1 pounds
Actual MSB:	shape - long cylindrical rod length - 60 inches diameter - 0.94 inch weight - 1.1 pounds

(The broom was placed at 45° [pitch] with respect to the handle.)

Total weight

Model - 2.9 pounds
Actual - 2.9 pounds

Total length

Model - 64 inches
Actual - 64 inches

Interaction of Operator and Brush

In the DYNAMAN model, no individual segments correspond to the hands. The brush was attached to the operator using a set of spring dampers that connected each lower arm with the extension rod, approximately modeling the pull that would be exerted by the hands on the rod. This was a purely artificial method of keeping the rod from moving away from the hands. A single spring was initially modeled to connect each arm to the rod, but it produced relatively large oscillations, and the direction of the spring changed rather easily. Two springs were then used, which improved the model stability significantly. The positioning of the springs was somewhat arbitrary but was selected to crudely approximate a grasping of the rod by a hand where the upper and lower surfaces of the rod are connected to the hand (in the model, actually to the end of the forearm). Additional springs would probably improve the stability even further, but we felt that the added complexity of the model would not increase the overall performance of the model (i.e., the stability of the complete human model). The strength of the spring was selected to provide as small a deflection as feasible (so that it appeared as if the rod were tightly grasped), without producing too high a reaction force. The spring strength was increased in test simulations until at a value of 2000 pounds per inch (lb/in.), stability in the

response appeared to be adequate. The damping coefficient (20 lb/[in/sec]) was selected to produce a quickly damped response from the spring, so that over a period of about 1 second, an approximately constant force appeared to be acting at the hand location. These spring parameters had no direct correlation with any human physiological responses, and other combinations of spring constant and damping coefficient may have produced acceptable results. We simply selected the first set of values that provided reasonable responses.

We also examined the optimum locations of the end points of the springs relative to the lower arm and the extension rod. The positioning of the arms was such that the right arm was attached to the rod closer to the body (6 inches from the motor end), and the left arm was attached somewhat farther ahead along the rod (about 20 inches to 24 inches, depending on the orientation of the rod). This positioning is similar to a right-handed person's grip on a gasoline-powered "weed-wacker" device and allows for maximum practical reach for all brush systems.

The position of the springs had to be slightly modified for the more angled orientations studied because the simple spring model did not produce the desired constant response and oscillations were more pronounced. This is discussed in greater detail in the section entitled "Limitations of the Present Analysis." We modified the position of the springs for these angled orientations to create a more stable environment (i.e., the hand stayed in the same orientation for about a second). For the different orientations studied, a different set of spring constant and damping coefficient may have produced better results. However, we did not perform such a detailed optimization for this study, since the main aim was to see if the model provided a way of obtaining reaction forces and torques at the joints and what the limitations were of using such a dynamic model for this purpose.

Modeling Rotation of Brush and Contact with Surface

The brush segment in the PSB was given a prescribed motion to model its rotation. Mechanical property data indicated that the brush has a rotational speed of 330 revolutions per minute (rpm) or 1980° per second with an applied torque of 7.5 inch-pound (in.-lb). We assumed a rotation speed of 2000° per second when the brush was pushed against a flat vertical surface, thus producing a normal load of 5 pounds and a frictional load of 5 pounds. We assumed a constant reaction force acting on the brush from the contacting surface. To obtain a simple estimate of this force, we assumed that the brush is held horizontally and that there is an equilibrium of forces and moments because of the weights of the different components of the PSB (motor, rod, and brush), the reaction forces at the hands, and the reaction force at the contact

surface. We assumed that there was no additional moment acting at the hands and that the motor was placed at the end of the rod. Under these conditions, the equilibrium conditions are

Horizontal Forces: $N=R^x$

Vertical Forces: $R^y + f = W_m + W_r + W_b = W$

Moment at motor location: $fL - W_rL/2 - R^yh = 0$

in which

W_m = weight of motor

W_r = weight of rod

W_b = weight of brush

N = normal reaction force at surface

f = friction reaction at surface = mN

R^x, R^y = X and Y components of the hand reaction forces

L = length of rod

h = average position of hands from end of rod

m = friction coefficient between brush and surface

W = total weight of brush

From the equations, the reaction force, R^y, can be obtained:

$$R^y = ([W - W_b]L - W_rL/2) / (L + h)$$

Substituting for the approximate dimensions of the PSB and assuming an average hand position of h = 15 inches from the end, we obtain

$$R^y = ([12.5 - 1]\ 85 - 4 * 85/2) / (85 + 15) = 8 \text{ pounds}$$
$$f = W - R^y = 12.5 - 8 = 4.5 \approx 5 \text{ pounds}$$

The normal reaction force would then be given by

$$N = f/\mu$$

The friction coefficient depends on the two surfaces in contact, that is, the brush and the contact surface, and would likely depend on the degree of contact, that is, how hard the brush is pushed against the surface because of the deformation on the brush surface. To simplify the model for this preliminary study, we assumed a friction coefficient of $\mu = 1.0$ to describe the contact between the brush and the surface, since it would usually be a high friction contact.

Then the normal force is given by

$$N = 5 \text{ pounds}$$

We think these values would be representative of the contact made by the actual brush against a surface.

DYNAMAN allows one to model a moving object with effectively infinite mass and moments of inertia. The motions of these objects are called "prescribed motions." Once defined, they are not altered by interactions with other objects of normal masses. (An example is the interaction of a human occupant of a vehicle with the vehicle itself. In this case, the impact of the occupant with the vehicle will not alter the motion of the vehicle in any measurable way.) It was necessary to model the motion of the brush as a prescribed motion, even though the mass of the brush was quite finite. This was because, in DYNAMAN, it is not possible to model the operation of the motor, and a constant rate of rotation could only be maintained as a prescribed motion (otherwise, the brush rotation would slow upon the application of external torque from the contact with the surface). We assumed that for the loads being considered, the rotational speed of 330 rpm would remain approximately constant.

Because the brush motion is described as a prescribed motion, it does not react to the forces produced from the contact with the surface. Therefore, we had to apply external forces in the normal and tangential directions to model the contact force acting on the rest of the brush assembly. These forces were applied to the extension rod at the end point of the angled brush. There would be a small error in the exact location of the applied force since it was not being detected at the actual point of contact. The error would be approximately of the order of 1/80 inch or 1%, however (this is the error in the position of the applied force). Thus, this error would be equivalent to an error of about 0.05 pound when the applied load is 5 pounds. We think that such an error would not appreciably change the results for the joint forces and torques.

Motor Attachment

A set of simulations was run for brushes 02 and 03, which have the motor attached to the end of the extension rod. Another set of simulations was run for brushes 04 and 05, which have the motor placed on the back of the operator. The exact location of the motor for brushes 04 and 05 was at the upper half of the upper torso segment. This position will only affect the forces and torques at the joints because of the change in the inertial properties of the PSB. There is no direct dynamic effect because of the torque imparted by the motor through the extension rod.

Brush Orientations

To examine the variation of the joint forces and torques when the extension rod is held at different angles, simulations were conducted with the rod placed at different yaw and pitch angles. The orientations at which the rod was held were

1. Rod kept straight (0° yaw)
2. Rod at 15° yaw (right)
3. Rod at 30° yaw (right)
4. Rod at 30° pitch (up)
5. Rod at -30° pitch (down)

For each different orientation, the forearms were moved to allow for the most logical contact (anatomically) between the arms and the extension rod. The spring attachment points were also recalculated, since, as the orientation changed, the point on the rod where the arms would make contact also changed.

All simulations were run using these five basic orientations. Illustrations of the initial setup of each brush configuration for each of the angular orientations are given in Appendix A. Figures A-1 through A-5 are the initial positions of the operator using brush No. 02 (PSB) for the five angular orientations given previously and with the motor attached to the extension rod. Figures A-6 through A-10 are the corresponding pictures for brush No. 04, with the motor attached to the back of the operator. Figures A-11 through A-15 are the pictures for the initial position using brush No. 03 with the motor attached to the rod. Figures A-16 through A-20 are the corresponding initial positions for brush No. 05 with the motor attached to the back of the operator. Figures A-21 through A-25 are the initial positions with brush No. 01 (manual broom).

COORDINATE SYSTEMS FOR CALCULATING FORCES AND TORQUES

The DYNAMAN program can compute the forces and torques at designated joints in a user-specified coordinate system. For the simulations conducted, the joint loads and torques were computed about the local axes of the corresponding segments. This axis system was selected since it corresponds to the anatomical axes of the dummy segments. The axes definitions are

1. For the right and left shoulders (RS and LS), the joint forces and torques are computed in the local system of the corresponding upper arms. In this system, the axes are delineated as follows:

X-axis: along the width of the upper arm (wider dimension); points forward when the upper arm is pointing down.

Y-axis: along the lateral width of the upper arm; points to the right when the upper arm is pointing is down.

Z-axis: along the length of the upper arm; points down when the upper arm is pointing down.

2. For the right and left elbows (RE and LE), the joint forces and torques are computed in the local system of the corresponding lower arms. The axes are essentially along the same directions as for the upper arm, that is,

X-axis: along the width of the lower arm (wider dimension); points forward when the lower arm is pointing down.

Y-axis: along the lateral width of the lower arm; points to the right when the lower arm is pointing is down.

Z-axis: along the length of the lower arm; points down when the lower arm is pointing down.

3. For the right and left hips (RH and LH), the joint forces and torques are computed in the local system of the corresponding upper legs. When the legs are maintained in the standard anatomical position, that is, they are not rotated at the hips or knees, the axes are defined as follows:

X-axis: points forward
Y-axis: points to right
Z-axis: points downward

4. For the right and left knees (RK and LK), the joint forces and torques are computed in the local system of the corresponding lower legs. The coordinate system in the lower legs is defined the same as for the upper legs.

RESULTS

Comparison with Simple Static Analysis

To verify what we may expect from a simple static analysis, we can consider the forces at the elbows for the straight case (0° yaw) for a simple configuration. We can assume that the lower arms are held horizontal and the right hand is placed about 6 inches from the motor end and

the left hand placed 24 inches from the right hand. For equilibrium, the reaction force at the elbow supports the weight of the whole brush system, and the total torque calculated about each hand has to be zero.

The total weight of the brush system is 12.4 pounds. The external forces acting are

Vertical Forces:

1. Weight of rod: 4 pounds: @ CG
   Location: 10 inches from left-hand location
   34 inches from right-hand location

2. Weight of brush: 1 pound: @ end
   Location: 50 inches from left-hand location
   74 inches from right-hand location

3. Weight of motor: 7.5 pounds: @ end
   Location: 30 inches from left-hand location
   6 inches from right-hand location

Horizontal Forces:

1. Normal reaction at surface: 5 pounds
   Location: about 10 inches vertically below line of rod

If:

F_L = vertical force (up) at left hand
F_R = vertical force (up) at right hand

then, total torque at the right hand is composed of

Counterclockwise:

$7.5 \times 6 + F_L \times 24$ (from motor weight and reaction at left hand)

Clockwise:

$4 \times 34 + 1 \times 74 + 5 \times 15$ (from weight of rod and brush and horizontal reaction at surface)

For equilibrium, the clockwise torque must equal the counterclockwise torque. Equating the two, we find

$$F_L = (4 \times 34 + 1 \times 74 + 5 \times 15 - 7.5 \times 6) / 24$$

Or:

F_L = 9 pounds (up)

F_R = 3.5 pounds (up) (from equilibrium of forces)

We then analyzed the results of the simulation for brush No. 02 (PSB with motor attached) and the straight configuration (in this case, the arms are not held straight; we had the hands placed at an angle as seen in Figure A-1 in Appendix A). If we examine the results of this analysis, we find that the value for Fz at the RE is 4 pounds and the value for Fz at the LE is 10 pounds, both in the up direction. This is relatively close to the numbers we found in the static analysis presented before. The total upward forces at the elbows is 14 pounds, which is somewhat higher than the static value of 12.5 pounds. The additional force in the simulation total arises from part of the weight of the lower arms that also has to be supported at the elbow and which we did not include in the simple static analysis. Because the left arm is placed closer to the CG of the rod and the right arm is near the end, most of the load in the Z-direction is carried by the left elbow.

Similarly, the total force in the Fx direction that supports the push against the vertical surface (about 5 pounds) is about 4 pounds and the total force in the Fy direction is about 1 pound. The reason for the low value of the lateral force is that there is no direct way for the body in DYNAMAN to counteract this force, and the body will begin to move in the direction of the applied force rather than produce a counteracting force. Although it may be possible to define a set of springs that attach the feet to the ground and can generate these restoring forces artificially, we have not examined this procedure for this study.

From this analysis, it is also seen that when the motor is not present, an increase in the force acting at the left hand and a decrease of the force at the right hand is experienced. This is because there is no counteracting torque from the motor attachment to reduce the force at the left hand (as seen in the equation given previously). Thus, there would usually be an increase in the difference of the magnitude of the forces acting at the two hands and correspondingly at the two elbows and two shoulders. Depending on the reaction force at the surface, this difference may be large enough to produce a difference in the direction of force acting at the two hands. Physically, this means that the operator would have to push up or support the rod with his or her left hand and push down with the right hand to counteract the torques.

Results of Simulations

Bar charts displaying the comparison of forces and torques at the various joints for the different brush systems (including the manual broom) are given in Figures B-1 through B-48 of Appendix B. Each page contains two charts that give the forces and torques for both the right (top of page) and left (bottom of page) sides of a specific joint. Within each graph are displayed the values for the five different brush systems used at the five angular orientations. The bars representing the five different brush systems are drawn next to each other. Their hatching patterns are described in the legend attached to each graph. These legends use brush nomenclature (see Table 1) to identify the different brush systems.

We feel that because of the limitations described in the next section, the data presented in Appendix B contain some degree of variability in calculating the appropriate forces and torques at a joint. A more appropriate way of combining the information in the graphs and improving the statistical reliability of the results is by determining, for each brush configuration, the largest magnitude recorded (either positive or negative) force or torque at each joint for the different orientations. The figures in Appendix C present this analytical approach. The graphs of the largest forces and torques at the various joints are displayed in Figures C-1 to C-48. These graphs show the greatest magnitude of a force or torque component at a specific joint for the five different brush systems.

The following general results are seen in the graphs in Appendix C (remember that the actual values depend on the coordinate system defined for each joint as described previously). There is some degree of variability for specific configurations (i.e., a brush system at a specified orientation), which is being neglected in the following observations.

General Features

For the shoulders, the joint forces along the local Z axis (along length of upper arm) showed greatest uniformity. This corresponded to the fact that for most orientations, the weight was borne at the shoulders in this direction. The range of values for all brush systems and directions was -5 to -10 pounds (negative sign corresponds to the force acting at the shoulder).

The greatest force variability was in the X and Y directions where the magnitudes varied from 0 to 10 pounds. This is because of the reaction forces transmitted by the brush at the contact surface.

The maximum torque was about the local Y axis at the left shoulder, where the torque varied from 100 to 300 in.-lb for the various orientations. This corresponds to a torque that causes flexion of the upper arm because of the weight of the system.

For the elbows, there was greater variability in the forces along different directions. This was because of the different angles at which the lower arms were kept for the various brush orientations. The force along the X-axis appeared to be most uniform and varied from about 5 to 10 pounds. This component usually corresponded to the force reacting to the weight of the brush system.

The maximum torque was also about the local Y axis at the left elbow and varied in the range of 100 to 200 in.-lb for the various orientations. This also corresponds to a torque that causes flexion of the lower arm because of the weight of the system.

The principal force acting at the hips and knees was along the Z axis and corresponds to the support of the upper body at these two locations. These forces are fairly uniform, regardless of brush system and orientation. The hip Z force is about 50 pounds at each hip and the knee Z force is about 70 pounds at each knee.

Torques along the local X and Y axes at the hips and knees are substantial. The torques at the hips are in the 100- to 200-in.-lb range, while the torques at the knees are somewhat less and in the 50- to 100-in.-lb range. These torques tend to topple the operator in the anterior-posterior direction (about Y axis) and in the lateral direction (about X axis) and arise mostly from the reaction forces generated at the contact surface.

Dependence on Orientation

The magnitude of the forces and torques is usually much larger (100% to 300% larger) for the yawed orientations (15° and 30°) than the straight configuration (0° yaw) for all brush systems. The forces in the local X direction at the right and left shoulder increase as do the forces in the local Y direction at the right and left elbow.

The torque along the local Z axis increases at the right shoulder (this tends to twist the upper arm), as do the torques about the X and Y axes at the right and left elbow. There is a slight increase of the torques acting along the X and Y axes at the right and left knees and right and left hips. These probably correspond to the greater imbalance produced when the rod is held at a yawed position.

The magnitude of the torque is usually larger for the -30° pitch (pitched down) orientation than the straight or the +30° pitch orientation. This is probably because torques produced by the horizontal reaction from the surface augment the torque produced by the weight of the rod and the brush. On the other hand, in the +30° orientation, the reaction force at the surface counteracts the weight of the brush system and helps to lower the magnitude of the torques.

The force in the Y direction at the right shoulder and along the Y and Z directions at the right elbow, for this pitched orientation, shows some increase compared to the straight or the +30° orientation. Similarly, the torques about the X axis at the left shoulder also show an increase.

Dependence on Brush Design

The forces (when all three components are examined) acting at the shoulder and elbow decrease when the motor is removed from the extension rod. For some orientations, however, there is an increase in the torques along some of the joint axes. This increase is in the 10% to 40% range for the torques about the local X and Y axes at the shoulder and elbow. Because of the change in orientation of the arms for the various brush orientations, the cause of this increase is not obvious.

There is also a slight increase in the torques acting along the X and Y axes at the hips and knees when the motor is removed. This probably corresponds to the lack of a counterbalancing torque when the motor is not attached, since both the upper and lower legs are maintained in the same configuration for all the simulations.

There appears to be an anomaly in the results for some of the forces and torques for brushes 03 and 05 when compared to the results for brushes 02 and 04. For some of the component forces and torques, the results for 03 and 05 are less (10% to 50%) than those for 02 and 04. One would expect from general engineering science, that the torques would be higher for a longer rod. One possible explanation for this counter-intuitive result may be that the greater inertia of the 03 and 05 PSBs (weight is 2 lb heavier; moments of inertia about the transverse axes are about 2 times greater) makes it more difficult to move during the duration of the simulation and thus appears to generate smaller loads. A longer simulation may produce a more stable equilibrium (as long as the body can be maintained in an erect posture) and thus more intuitive results.

LIMITATIONS OF THE PRESENT ANALYSIS

One limitation of the present analysis is that there is some degree of guesswork at the initial placement of the hands relative to the extension rod for the various orientations. The hands were placed so that they looked physically reasonable for a given orientation, but small changes can be made in the angles of the arms while still maintaining a reasonable posture. We have not examined the variation of the forces and torques for small variations of the initial placement conditions. We do not think it will be significant, since the overall results are within the range expected from the static engineering analysis results. One way of eliminating this limitation is to define a strict procedure for changing the angles at the shoulder and elbow for each orientation. This may not always lead to the most human-like orientation but would allow for a consistent way of comparing various brush designs and brush orientations.

Another limitation of the analysis is that a number of simulations are required for each configuration to determine the optimum position of the human model that will minimize the drift that occurs when the external forces from the brush are transmitted to the body (trial and error technique). Since DYNAMAN is a dynamic model without muscle response, it is not possible to eliminate the drift, but it is possible to minimize it for a reasonable amount of time (usually about 1 second).

For some configurations, we found that the body remained fairly steady for as long as 1 second. We also found that the plot of the joint forces and torques oscillated about a mean value before drifting. For these cases, it was relatively easy to estimate the mean values from the plots. An example of a plot for brush No. 02 is given in Figure 2. This represents the plot of the X-component force at the right shoulder with yaw angle of 15°. Notice that after a rapid oscillation (because of the spring damper system attaching the arms to the extension rod), the curve remains steady for about 1 second before drifting, which corresponds to whole body movement because of the change in equilibrium from the external forces.

For some orientations, however (usually for yaw = 30° and for pitch = -30°), the drift begins earlier and the body is approximately stationary for a shorter period of time (from 400 to 500 msec). For these situations, the plots are not as regular and may have a large time variation effect. In these cases, it was necessary to make an estimate of the best mean value based on the component force at the right shoulder for brush No. 02 with yaw angle of 30° (see Figure 3). We think that by appropriate placement of the body and by the addition of new forces that counteract the forces from the surface (e.g., by using additional springs or by external forces acting at the joint between the feet and the ground), the situations when there is greater

movement of the body can also be made more stable. Because of the large number of configurations examined in this study, we have not attempted to do this case-by-case analysis at the present time.

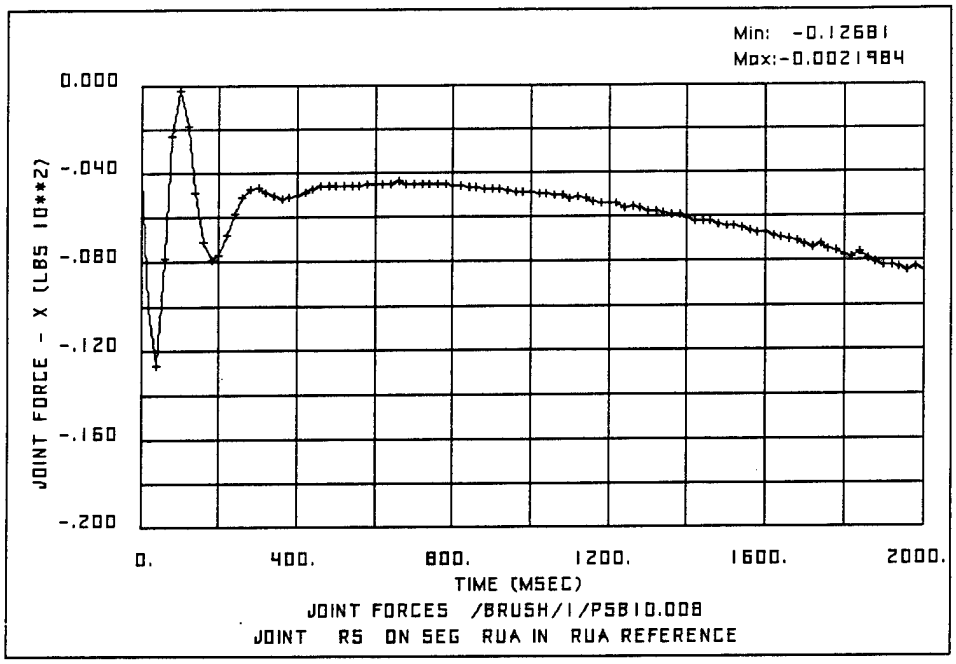

Figure 2. Plot of right shoulder X-component force (yaw = 15°).

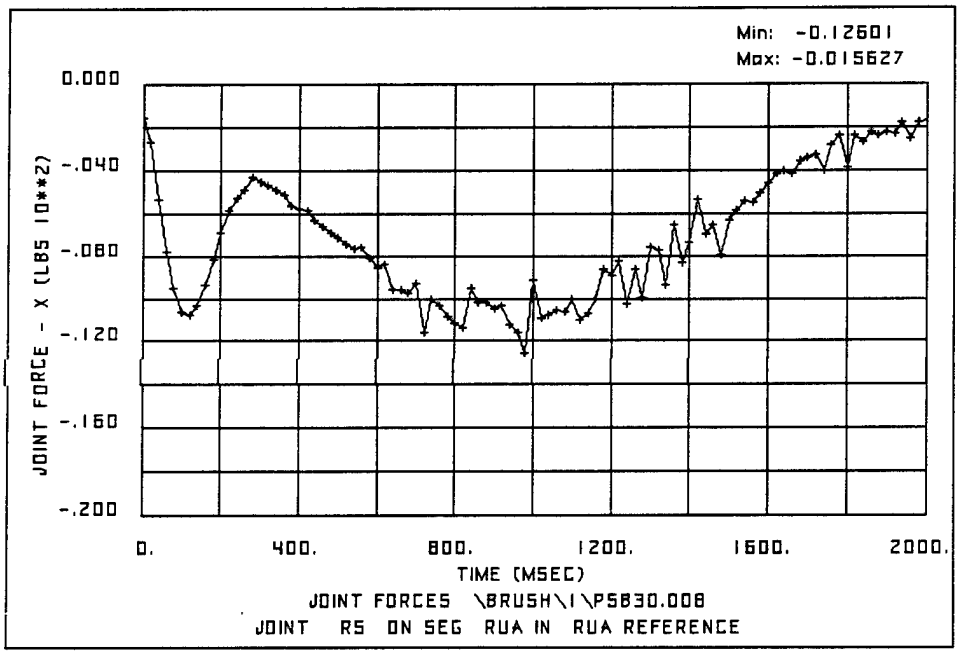

Figure 3. Plot of right shoulder X-component force (yaw = 30°).

CONCLUSIONS

The results of this simulation indicate that torques are usually larger for those orientations in which the moment arms are greatest. This effect is seen for the yawed cases and the -30° pitch case. One way of mitigating this effect may be to provide some kind of pivoting at the junction of the brush and the extension rod, which would allow an operator to change the location of the area of contact for different orientations.

It would appear that the counterweight offered by the attached motor helps to slightly reduce the torques on the whole. The present analysis does not show any significant decrease at the shoulders and elbows compared to the motor being mounted on the user's back. However, there is a reduction at the hips and knees, although this effect may be offset by the strong muscles in this region and the stability of the lower half of the body.

Without an understanding of the actual biodynamical tolerance to external forces and torques at the different joints (tolerance with regard to magnitude, as well as to duration), it is not possible to categorize any of the values as being within or outside a person's level of comfort or safety.

Because of the dynamic nature of the solutions offered by the current simulations, it is important to set up a more definitive procedure for describing the initial conditions of each configuration, so that they may be compared properly. For a more in-depth analysis, it is probably necessary to add an option to DYNAMAN to perform a static analysis for each modeled configuration which would remove some of the uncertainties that have appeared because of the drift in the position of the body over time.

RECOMMENDATIONS

Based on the results of this simulation, recommendations concerning both the modular decontamination system electrically powered scrub brush and the DYNAMAN simulation approach are offered. First, it is recommended that the motor for the powered scrub brush be located on the user's end of the brush to aid in counterbalancing the torque generated by the system. In addition, in order to minimize the forces and torque generated during use, it is recommended that the operator be trained to hold the system in a "straight" (0° yaw) orientation (see Figure A-1 of Appendix A).

Because of limitations in the present simulation approach, a conclusive result regarding the preferred length of the powered scrub brush system could not be determined. Therefore, it is recommended that future efforts attempt to perform longer simulations, which may produce a more stable equilibrium condition and allow for a better system comparison. It is also recommended that future simulation efforts include a more definitive procedure for describing initial conditions (including static analysis) in order to improve the analyst's ability to make comparisons.

Finally, it is recommended that an effort be undertaken to improve our understanding of the biodynamical tolerance of human joints to external loads. This effort should consist of a review of existing data, an identification of data voids, and additional simulation or experimentation. The objective of such an effort would be to determine the human joint safety and comfort tolerance to loading with regard to magnitude and duration.

REFERENCES

Headquarters, Department of the Army (1993, November 17). NBC decontamination (Field Manual 3-5). Washington, DC: Author.

Shams, T., Weerappuli, D., Sharma, D., Nurse, R., Rangarajan, N. (1992). DYNAMAN user's manual version 3.0 (AL-CF-TR-1993-0076). Air Force System's Command, Armstrong Laboratory.

APPENDIX A

INITIAL SETUP OF VARIOUS BRUSH ORIENTATIONS

INITIAL SETUP OF VARIOUS BRUSH ORIENTATIONS

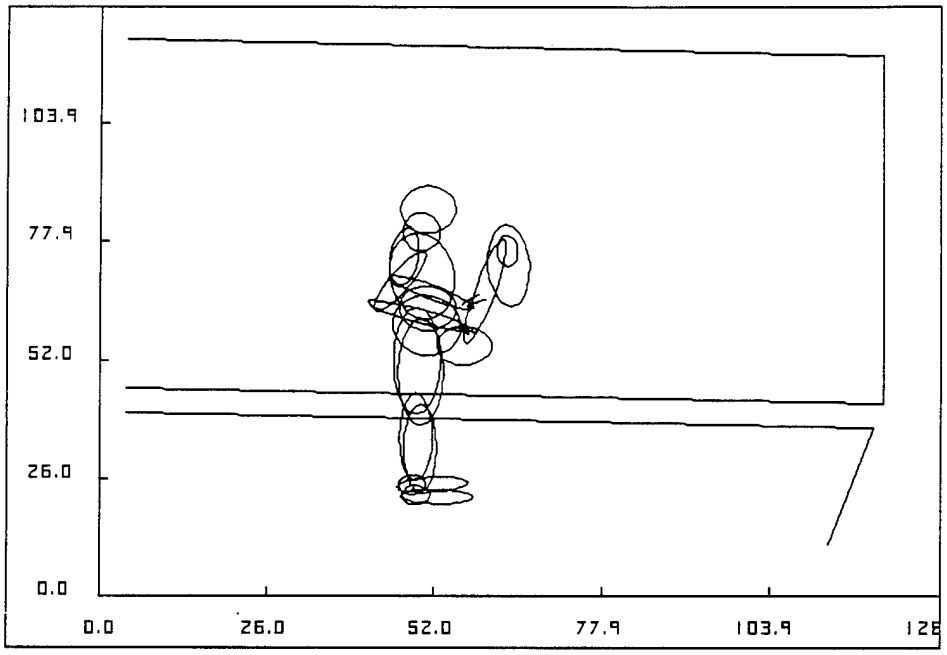

Figure A-1. Setup of brush #02-PSB with motor attached for straight orientation.

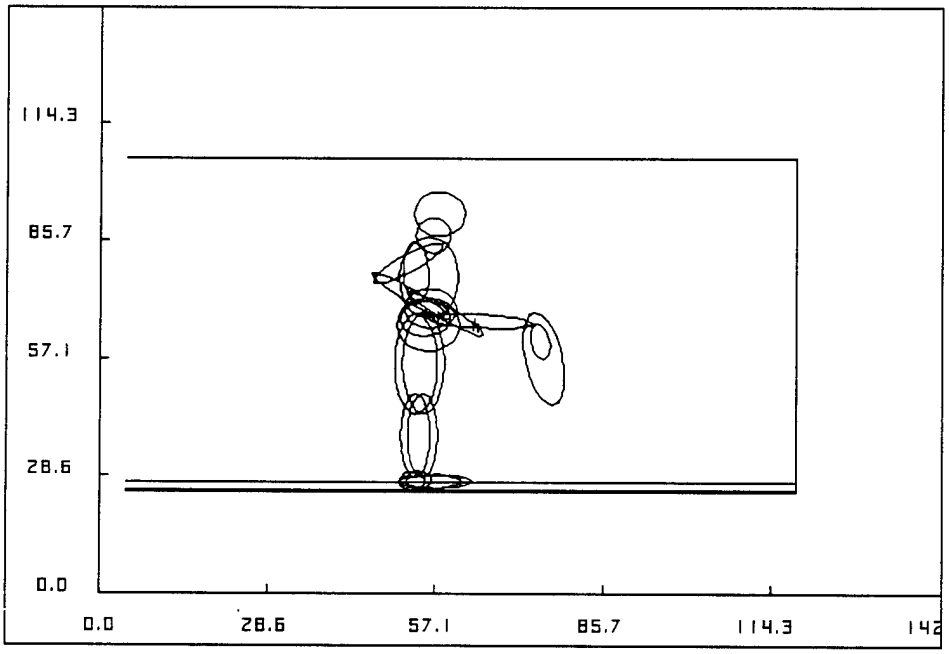

Figure A-2. Setup of brush #02-PSB with motor attached for yaw = 15° orientation.

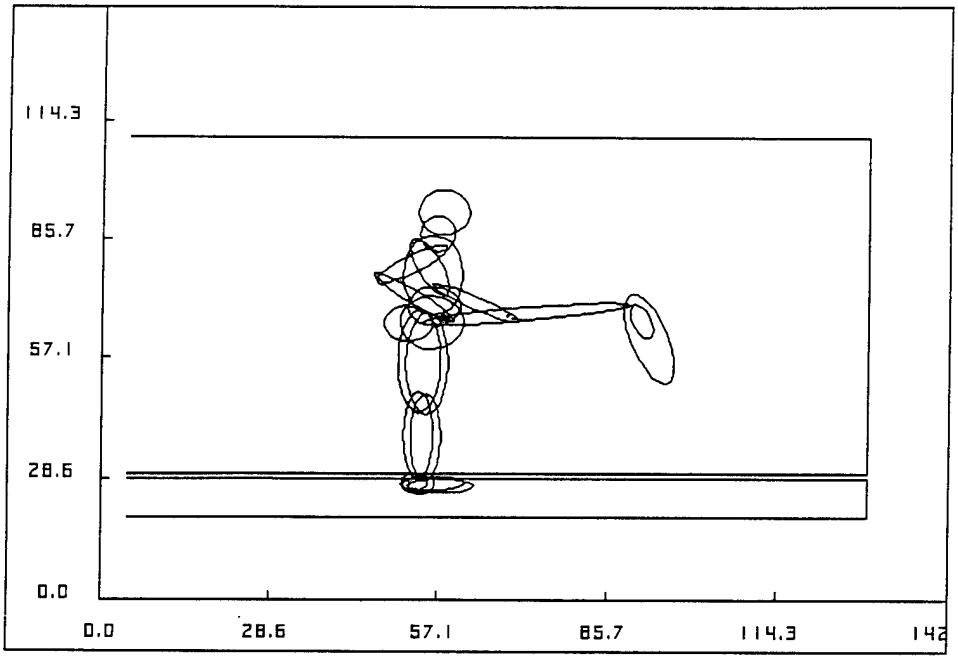

Figure A-3. Setup of brush #02-PSB with motor attached for yaw = 30° orientation.

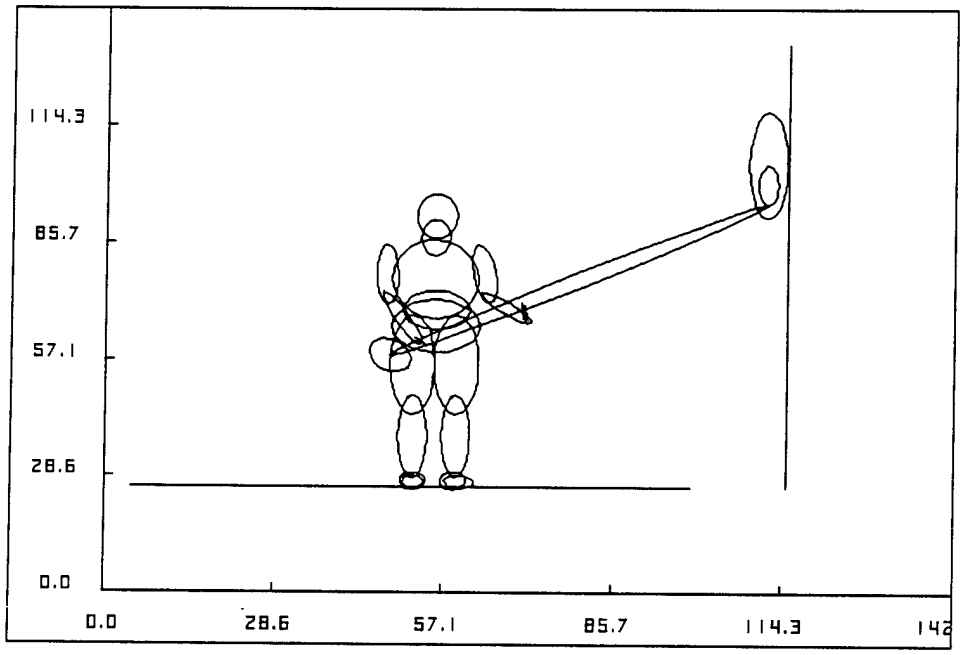

Figure A-4. Setup of brush #02-PSB with motor attached for Pitch = 30° orientation.

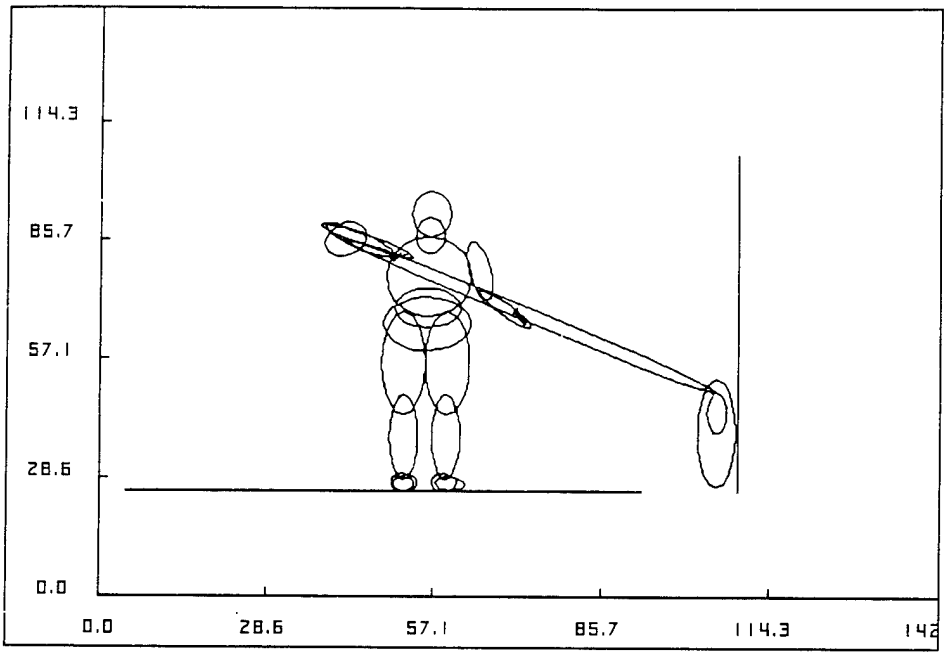

Figure A-5. Setup of brush #02-PSB with motor attached for Pitch = -30° orientation.

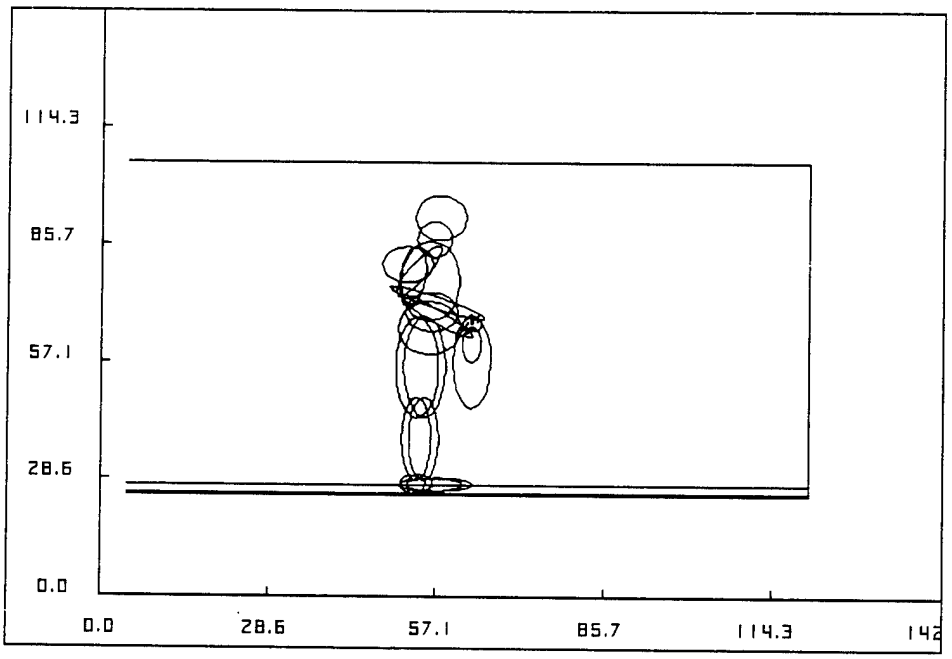

Figure A-6. Setup of brush #04-PSB with motor separated for straight orientation.

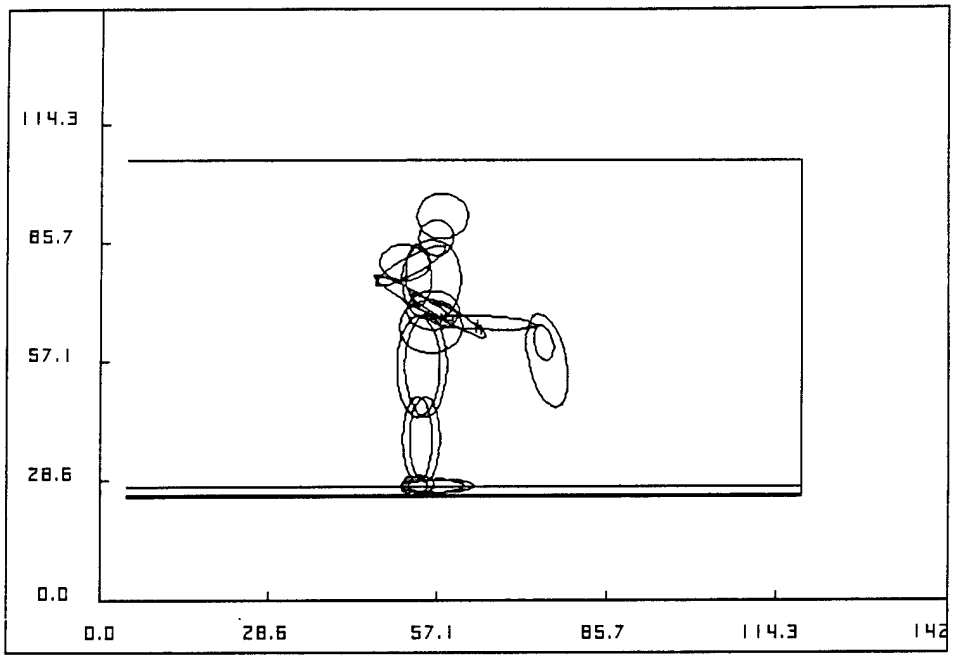

Figure A-7. Setup of brush #04-PSB with motor separated for yaw = 15° orientation.

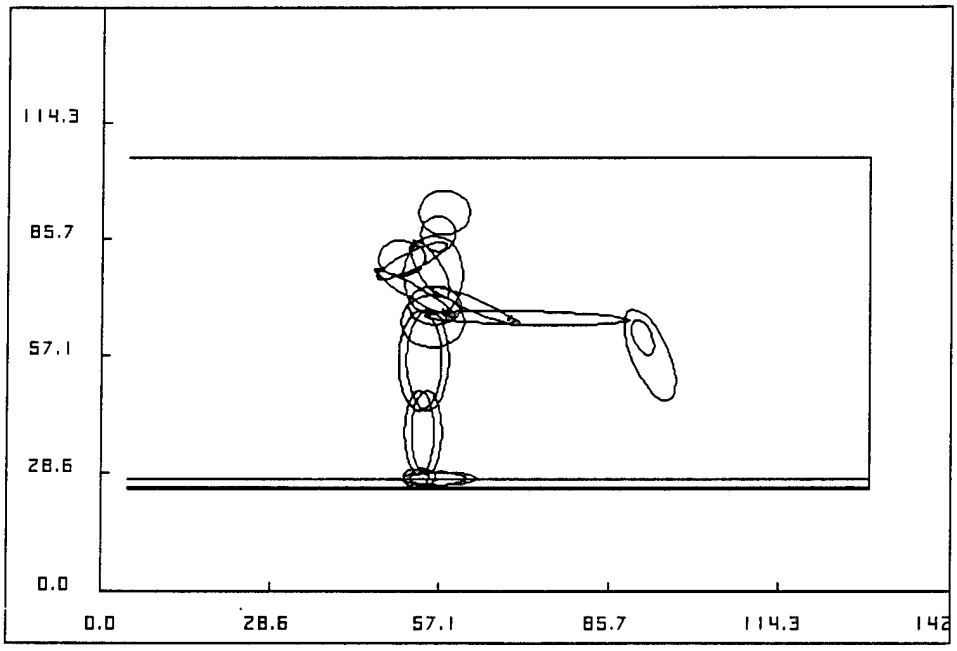

Figure A-8. Setup of brush #04-PSB with motor separated for yaw = 30° orientation.

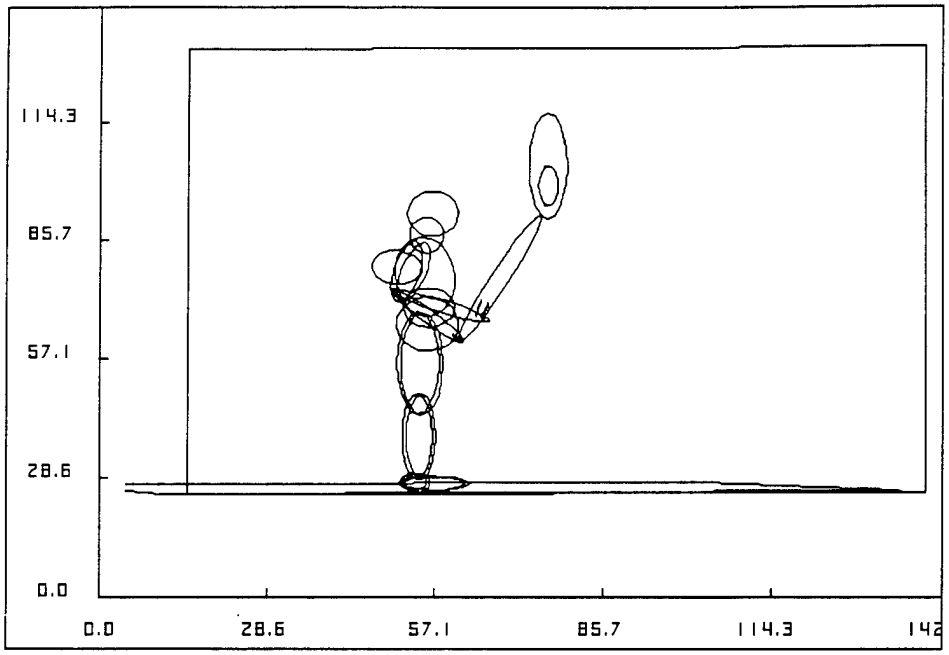

Figure A-9. Setup of brush #04-PSB with motor separated for Pitch = 30° orientation.

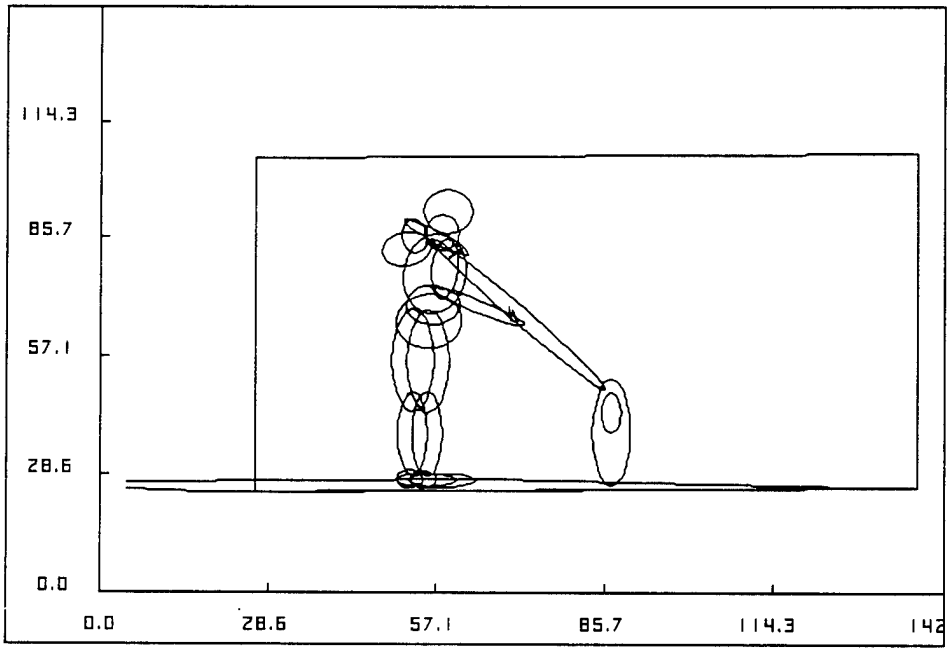

Figure A-10. Setup of brush #04-PSB with motor separated for Pitch = -30° orientation.

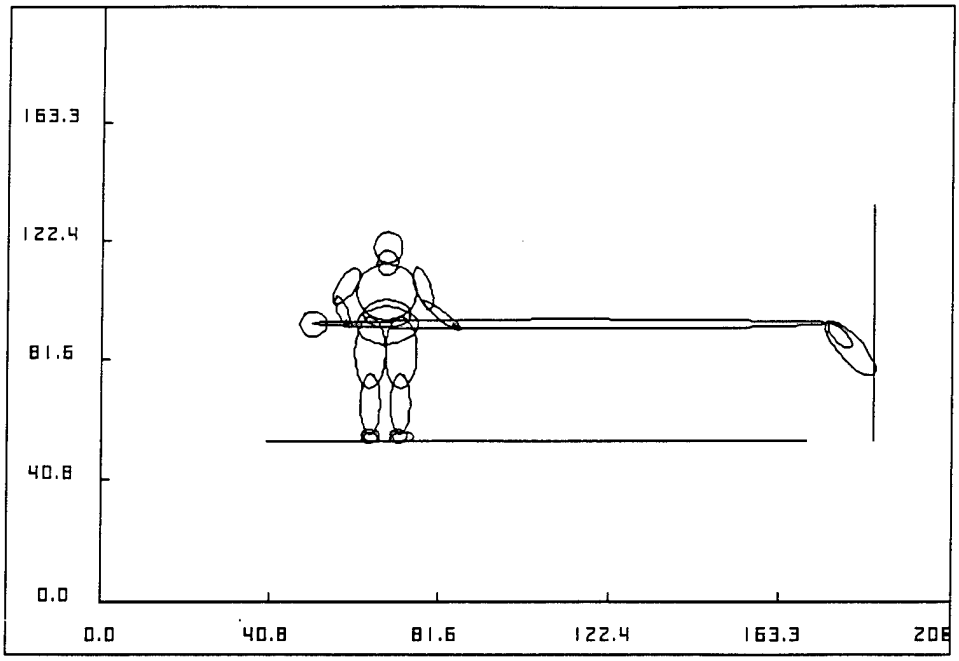

Figure A-11. Setup of brush #03-PSB with motor attached for straight orientation.

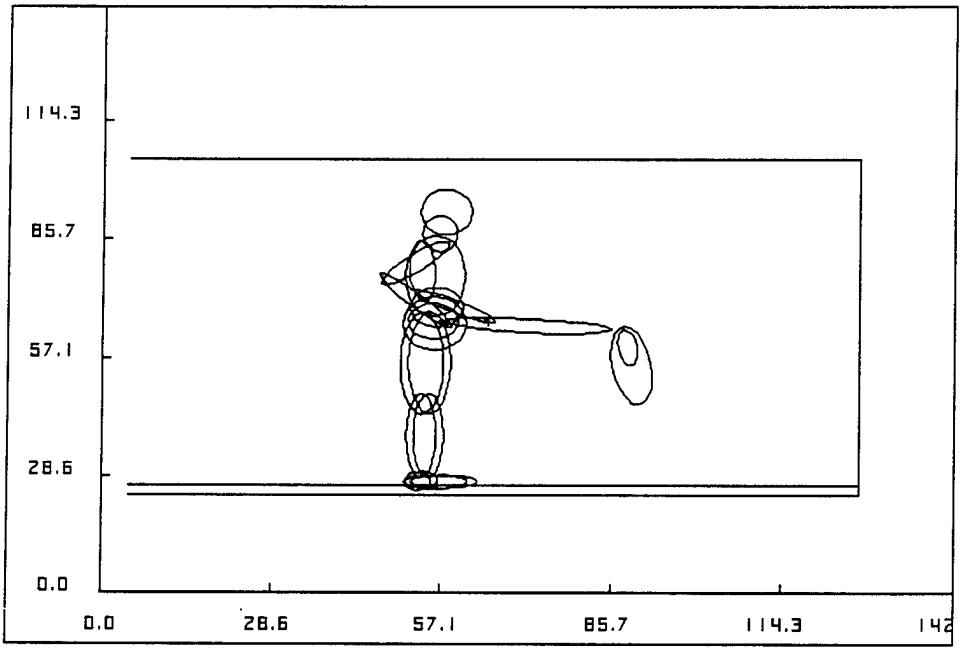

Figure A-12. Setup of brush #03-PSB with motor attached for yaw = 15° orientation.

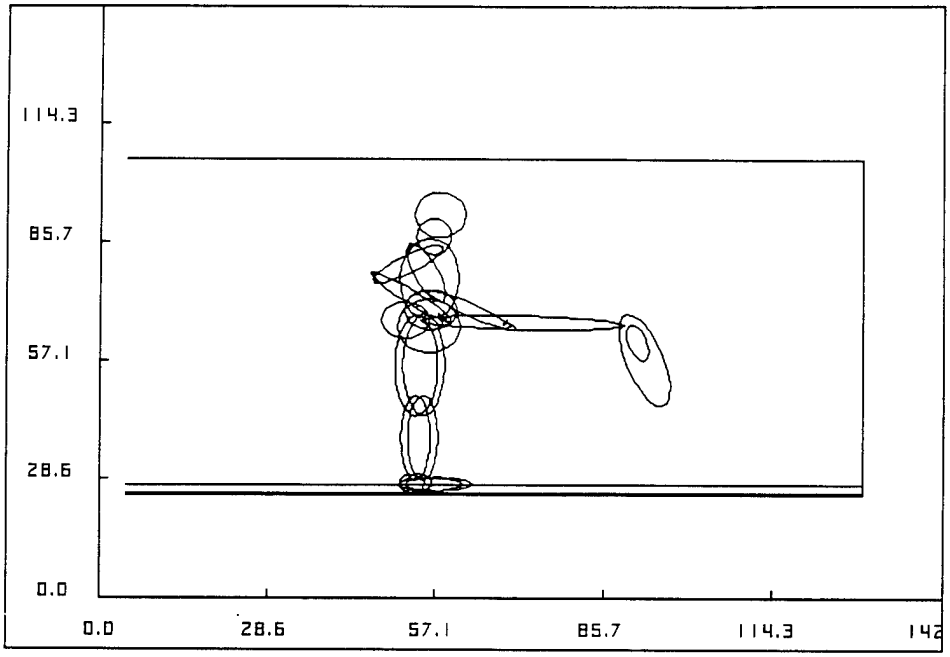

Figure A-13. Setup of brush #03-PSB with motor attached for yaw = 30° orientation.

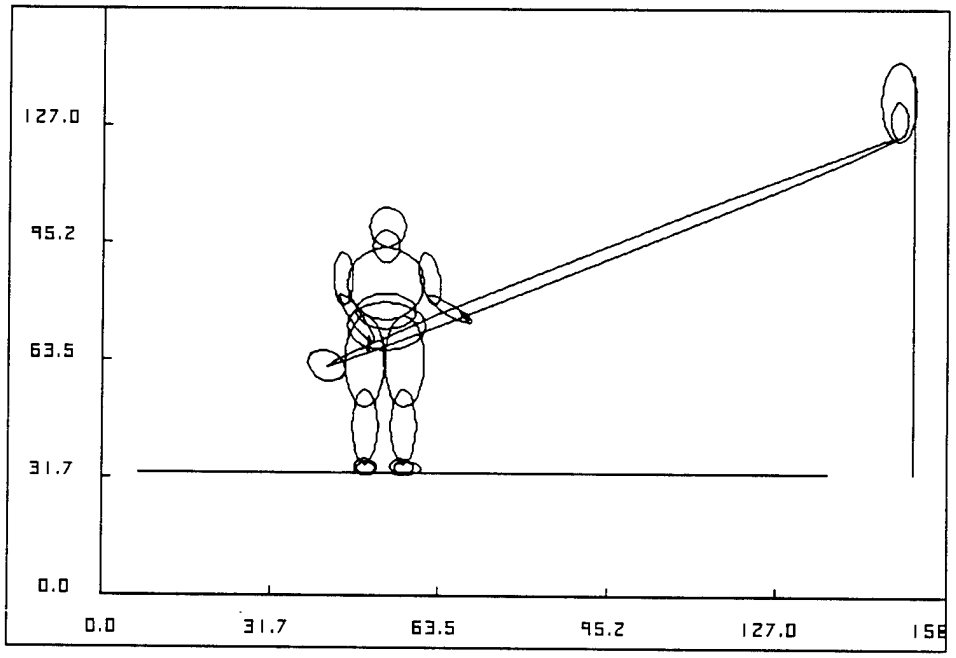

Figure A-14. Setup of brush #03-PSB with motor attached for Pitch = 30° orientation.

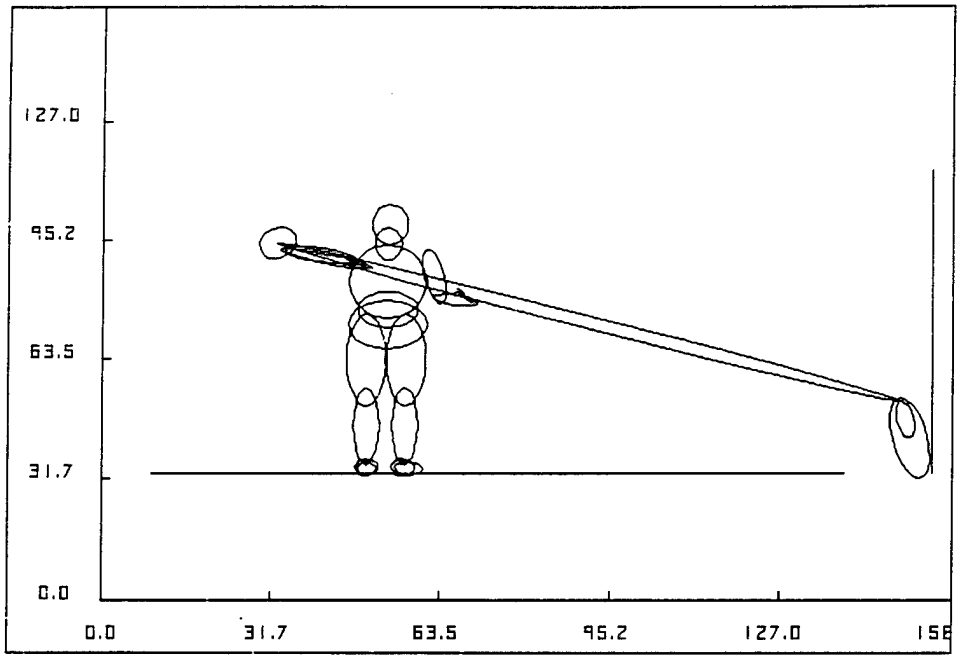

Figure A-15. Setup of brush #03-PSB with motor attached for Pitch = -30° orientation.

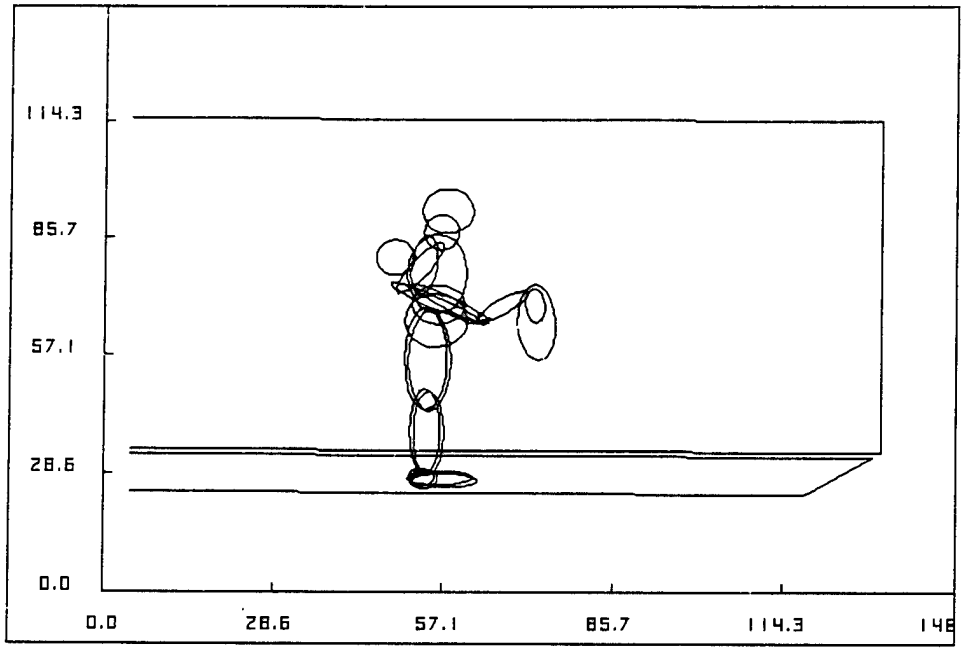

Figure A-16. Setup of brush #05-PSB with motor separated for straight orientation.

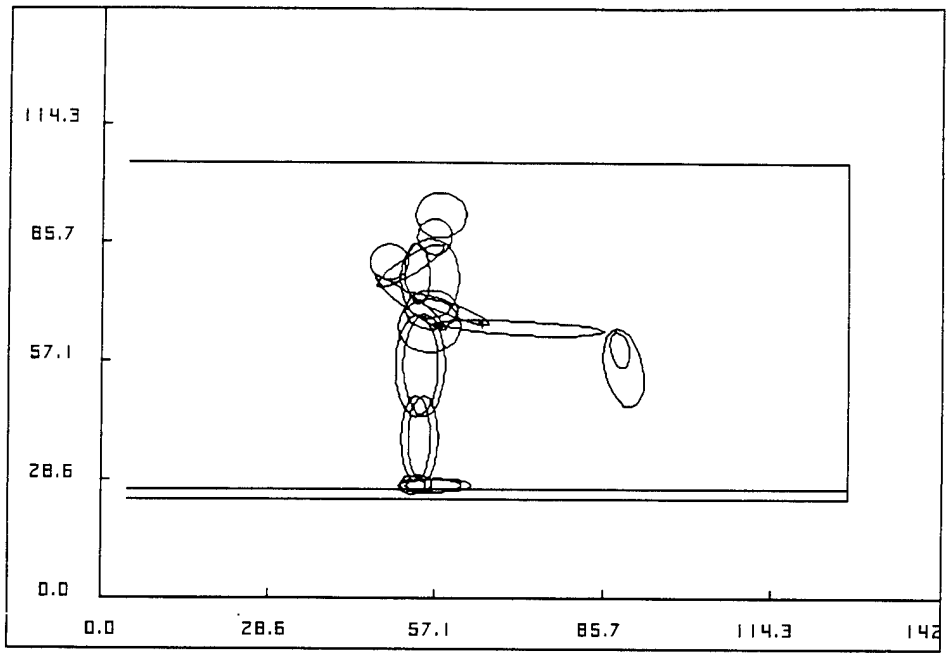

Figure A-17. Setup of brush #05-PSB with motor separated for yaw = 15° orientation.

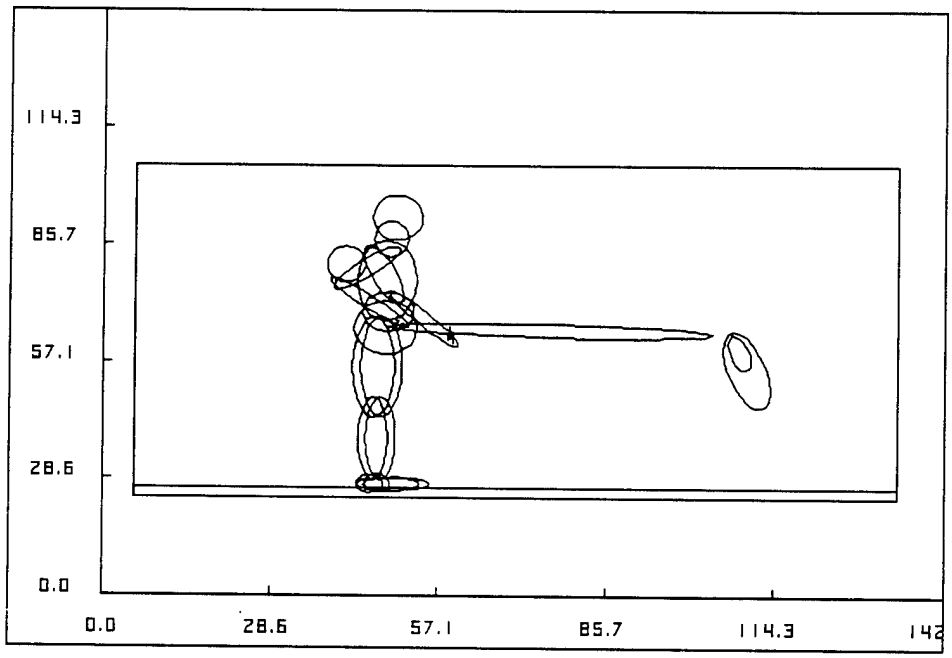

Figure A-18. Setup of brush #05-PSB with motor separated for yaw = 30° orientation.

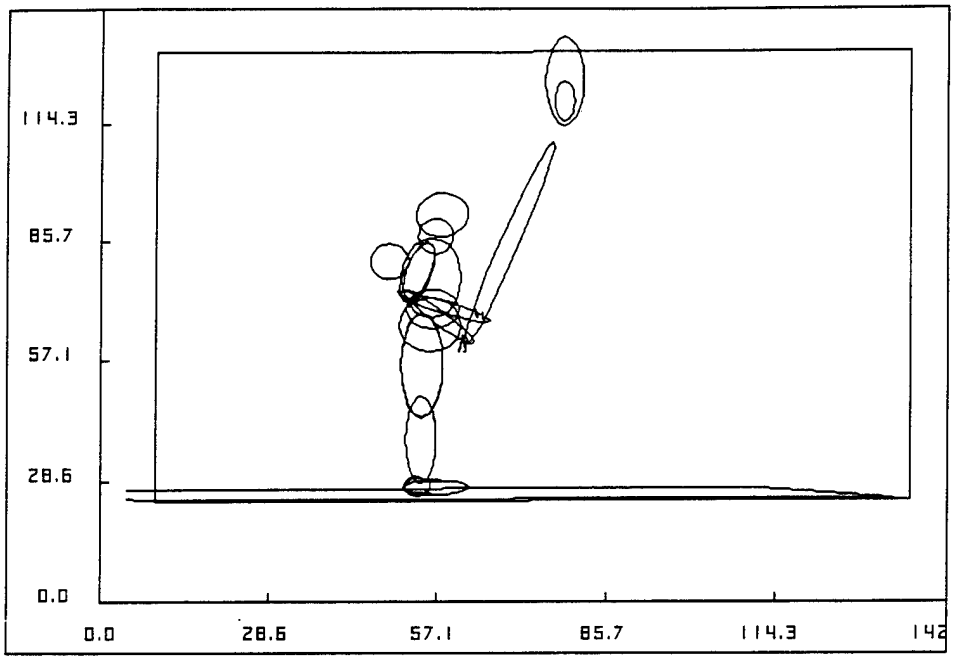

Figure A-19. Setup of brush #05-PSB with motor separated for Pitch = 30° orientation.

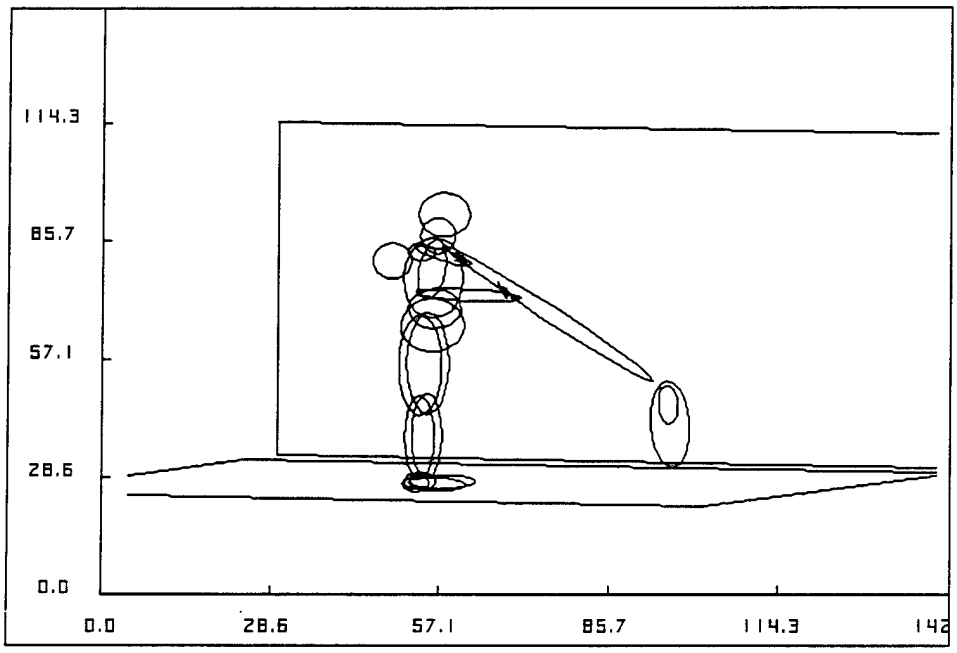

Figure A-20. Setup of brush #05-PSB with motor separated for Pitch = -30° orientation.

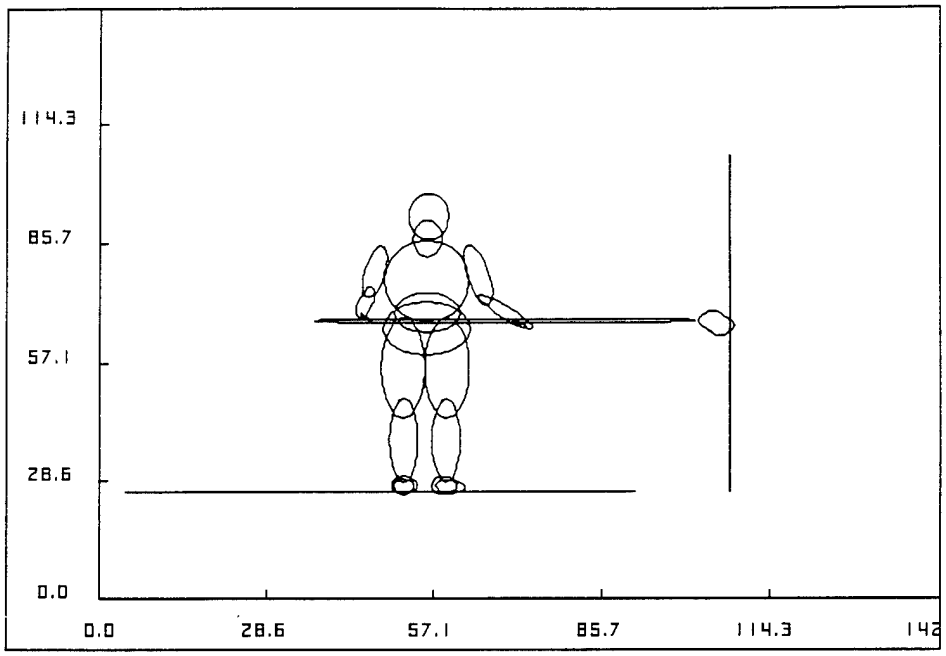

Figure A-21. Setup of brush #1-Manual Scrub Broom for straight orientation.

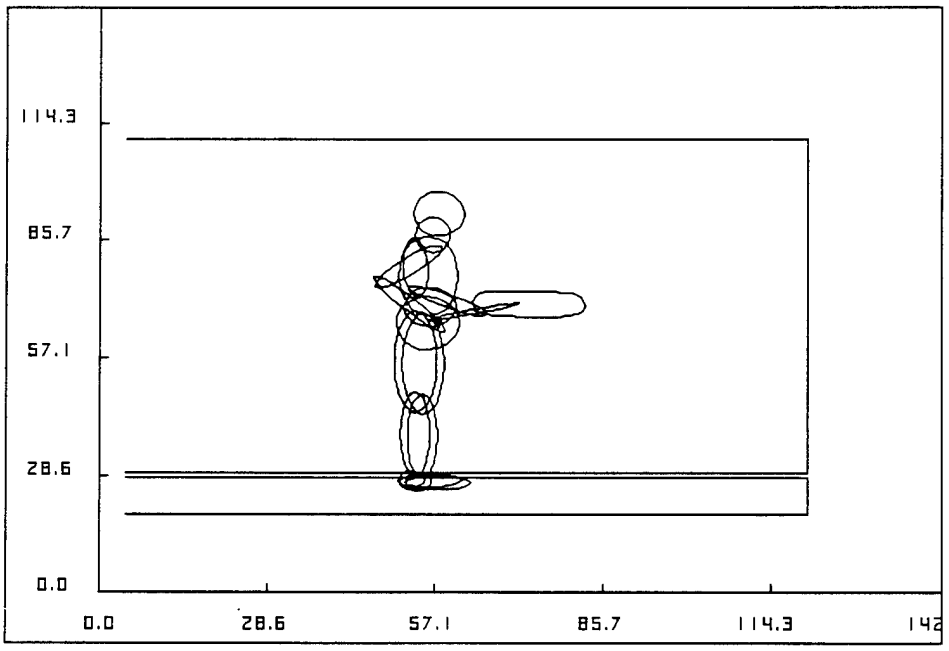

Figure A-22. Setup of brush #1-Manual Scrub Broom for yaw = 15° orientation.

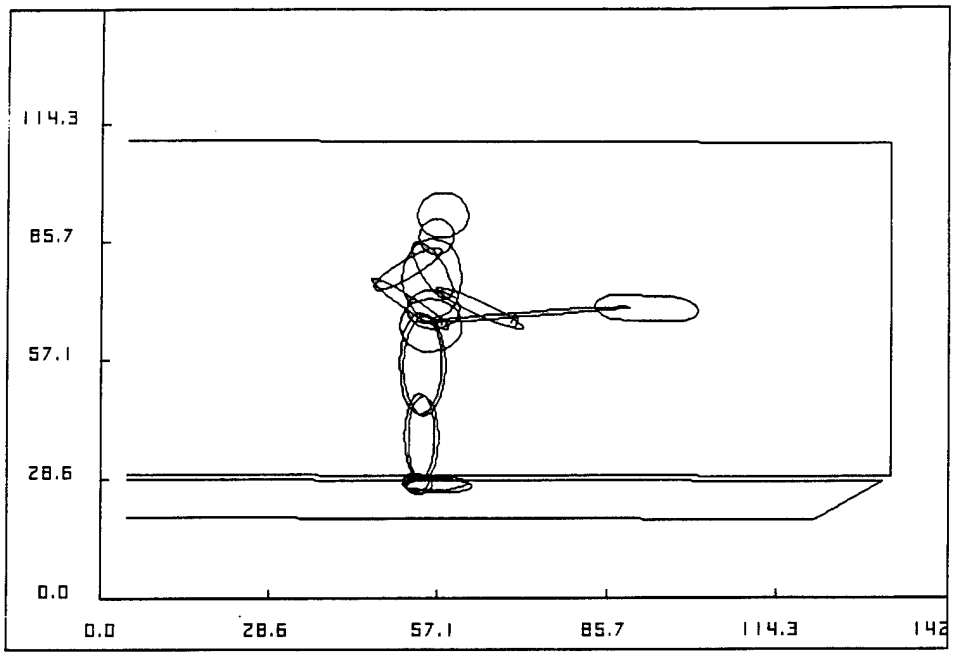

Figure A-23. Setup of brush #1-Manual Scrub Broom for yaw = 30° orientation.

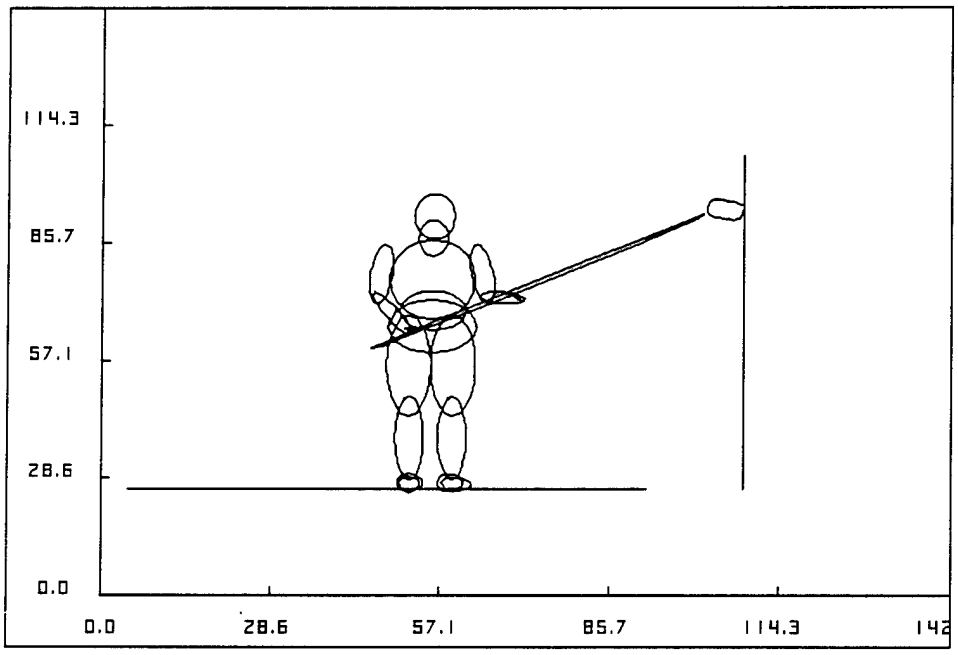

Figure A-24. Setup of brush #1-Manual Scrub Broom for Pitch = 30° orientation.

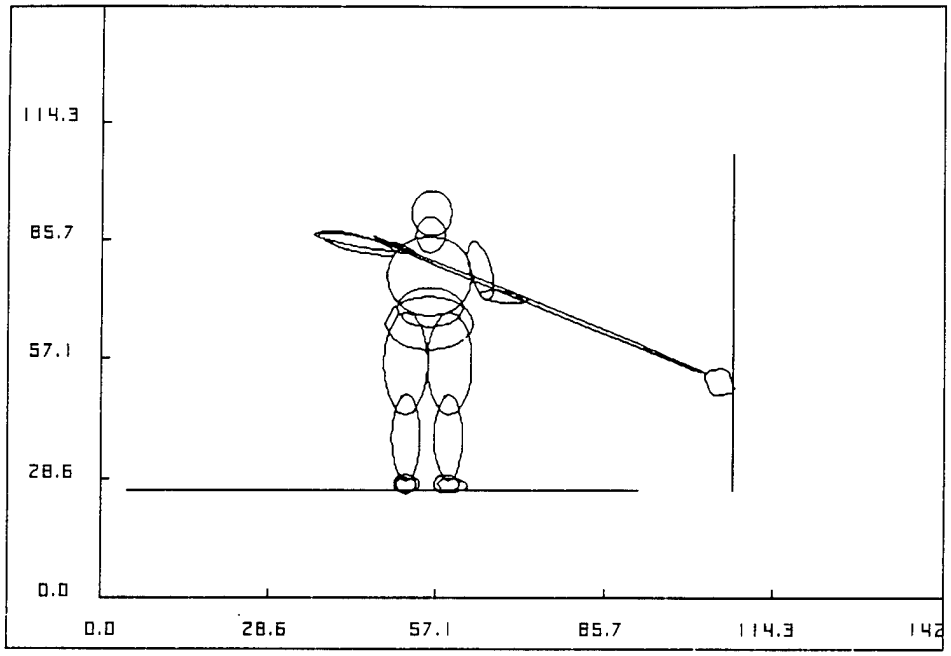

Figure A-25. Setup of brush #1-Manual Scrub Broom for Pitch =-30° orientation.

APPENDIX B

PLOTS OF COMPARISON OF FORCES AND TORQUES AT JOINTS

PLOTS OF COMPARISON OF FORCES AND TORQUES AT JOINTS

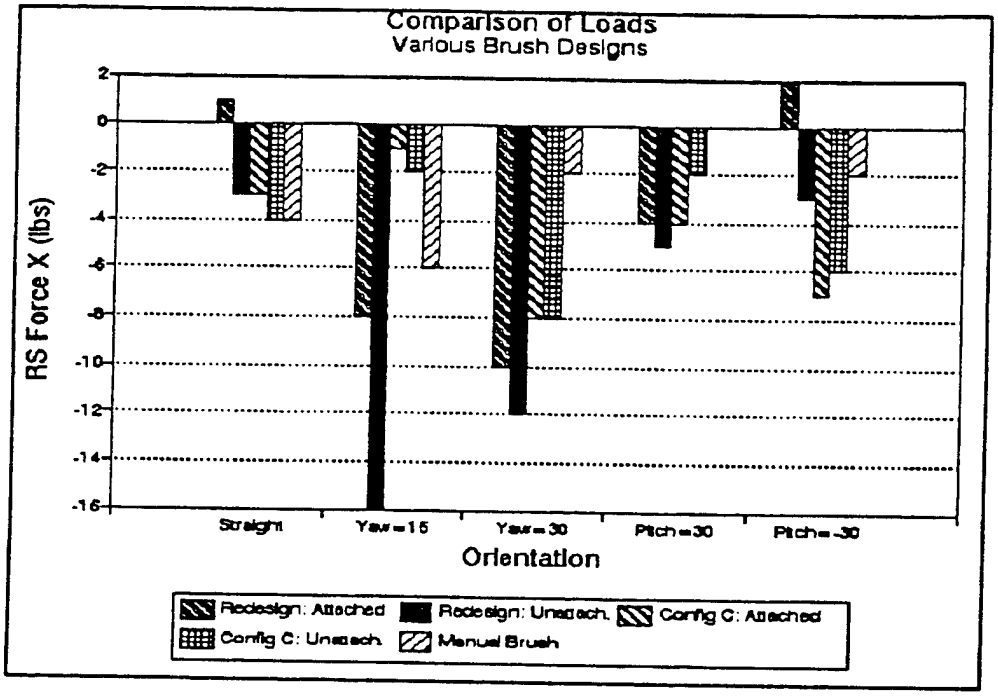

Figure B-1. Comparison of various brush configurations. Force - X at right shoulder.

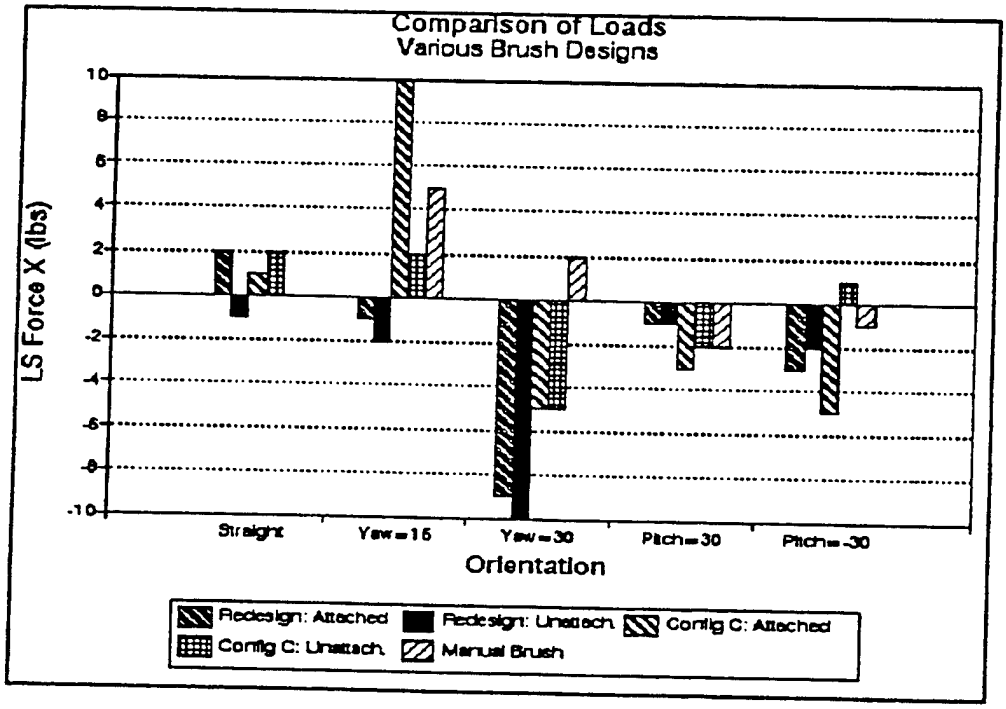

Figure B-2. Comparison of various brush configurations. Force - X at left shoulder.

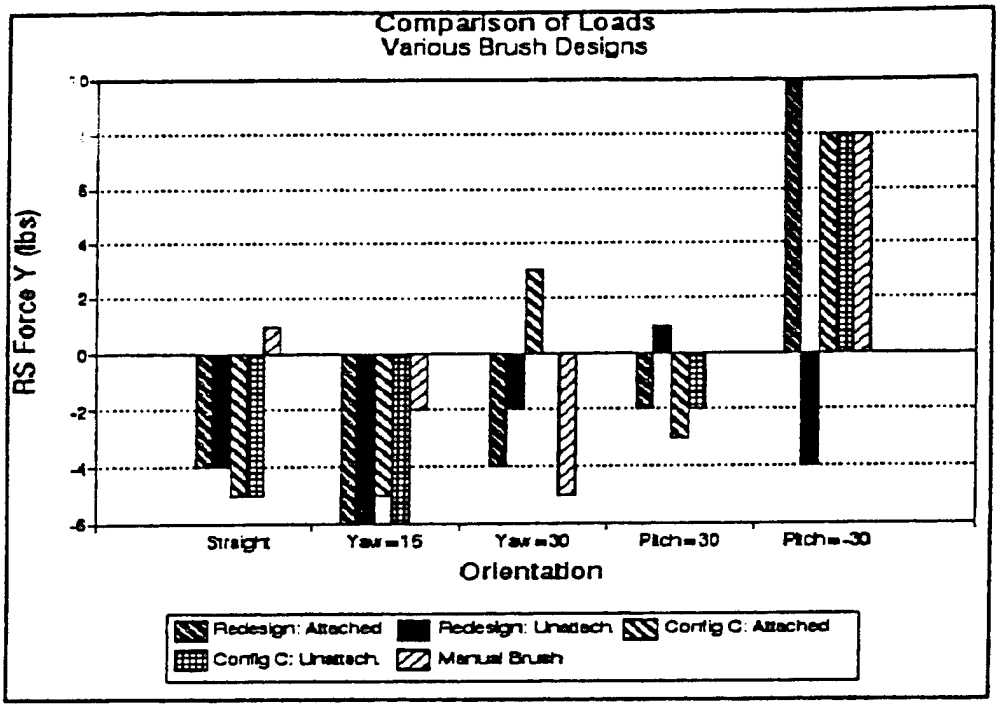

Figure B-3. Comparison of various brush configurations. Force - Y at right shoulder.

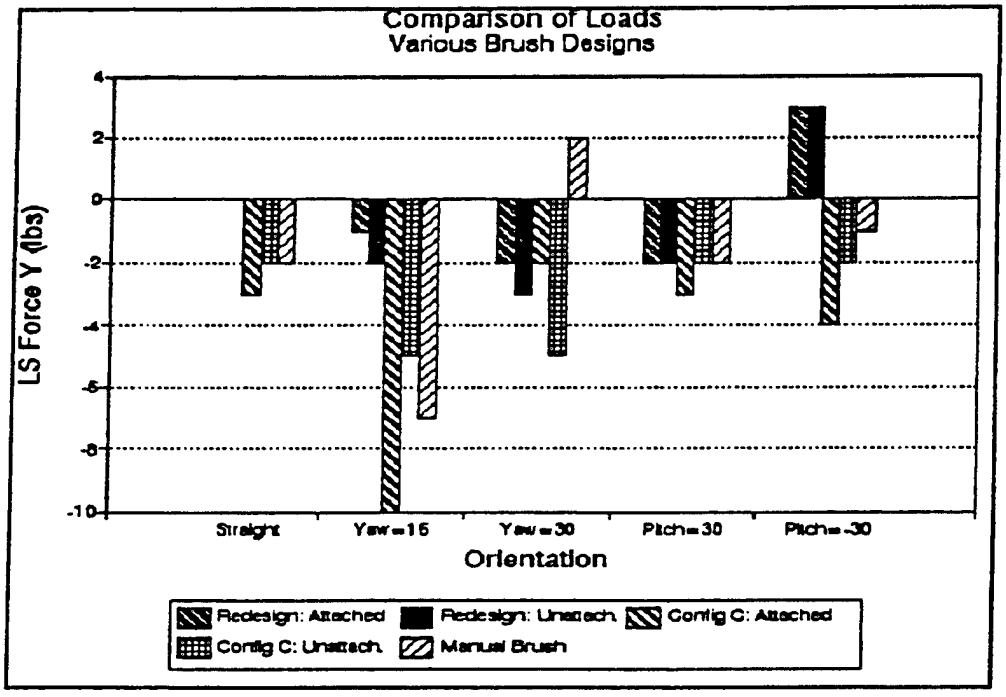

Figure B-4. Comparison of various brush configurations. Force - Y at left shoulder.

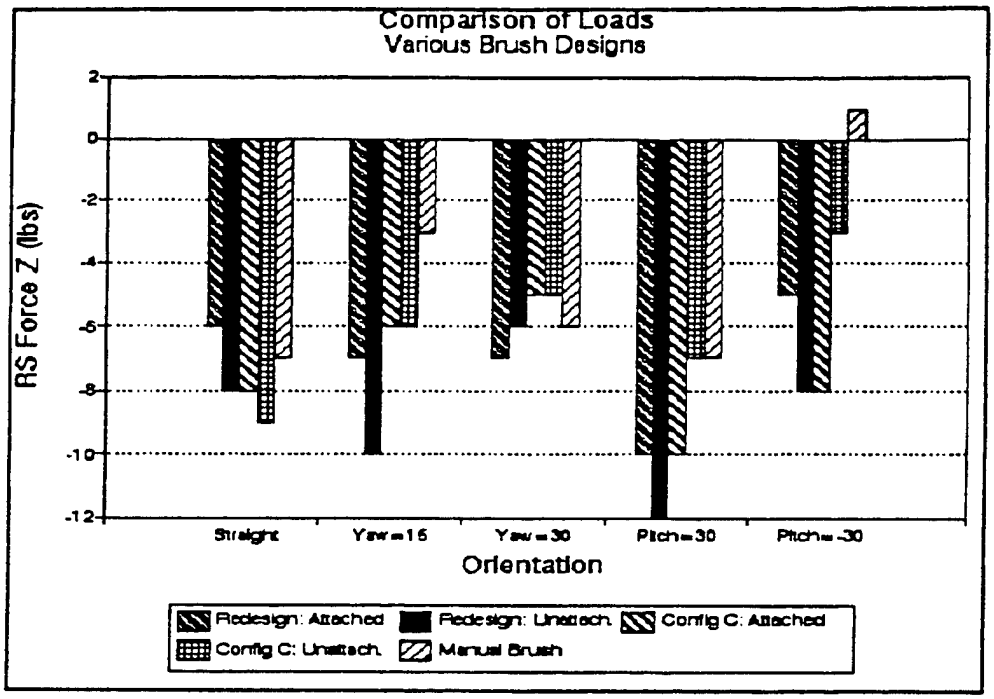

Figure B-5. Comparison of various brush configurations. Force - Z at right shoulder.

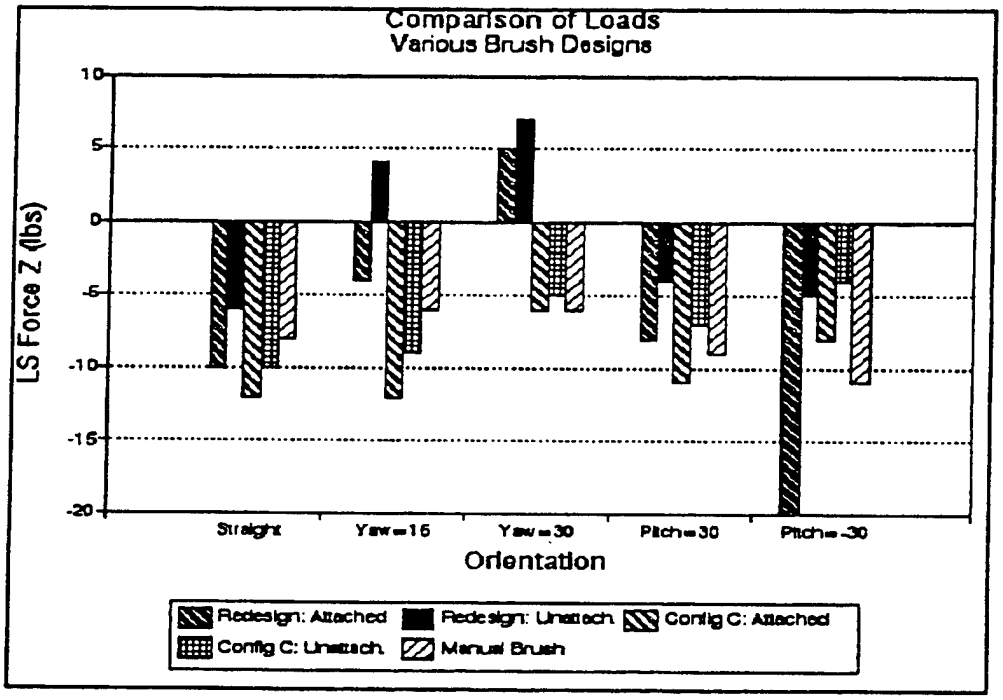

Figure B-6. Comparison of various brush configurations. Force - Z at left shoulder.

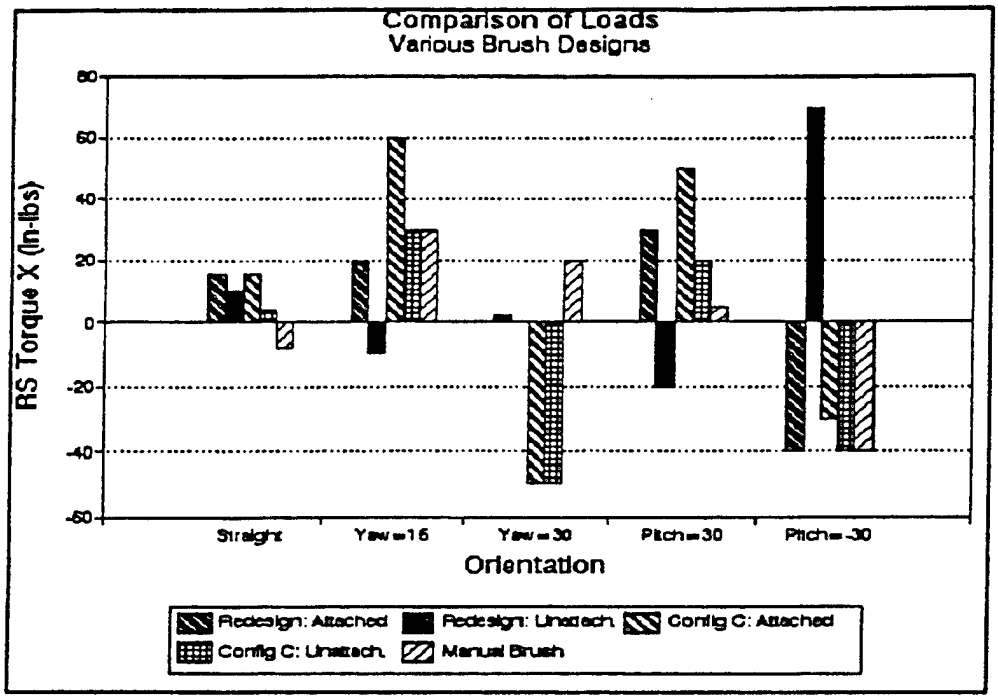

Figure B-7. Comparison of various brush configurations. Torque - X at right shoulder.

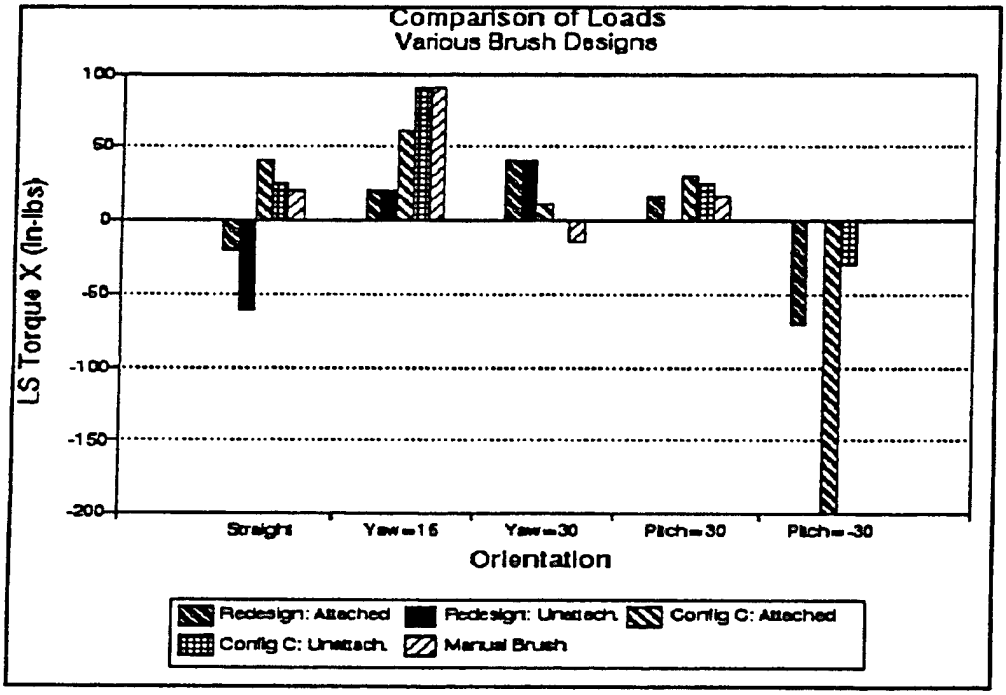

Figure B-8. Comparison of various brush configurations. Torque - X at left shoulder.

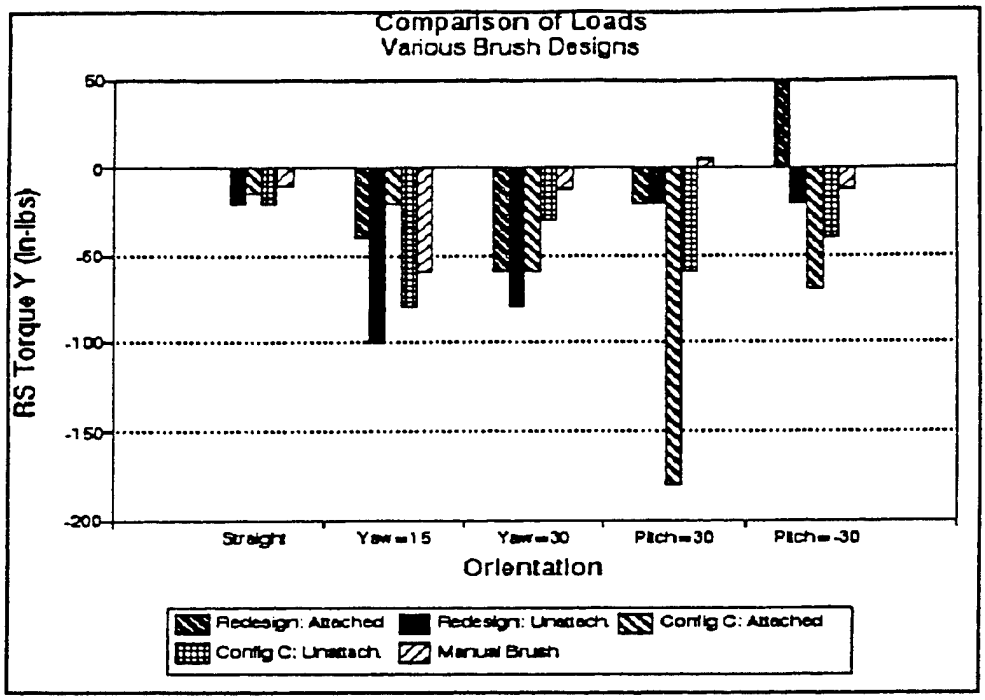

Figure B-9. Comparison of various brush configurations. Torque - Y at right shoulder.

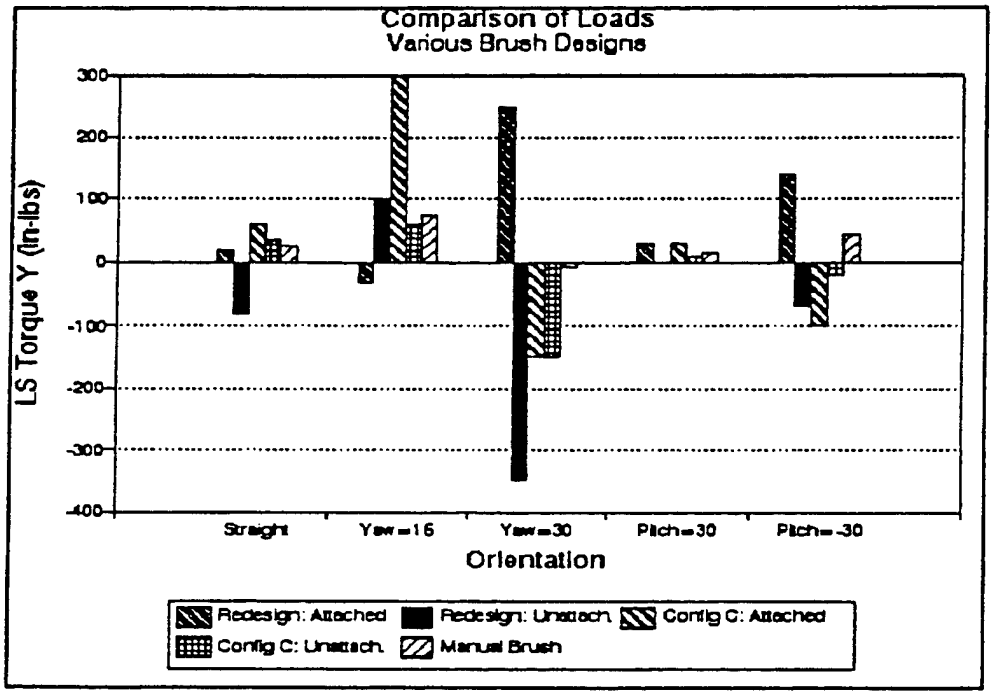

Figure B-10. Comparison of various brush configurations. Torque - Y at left shoulder.

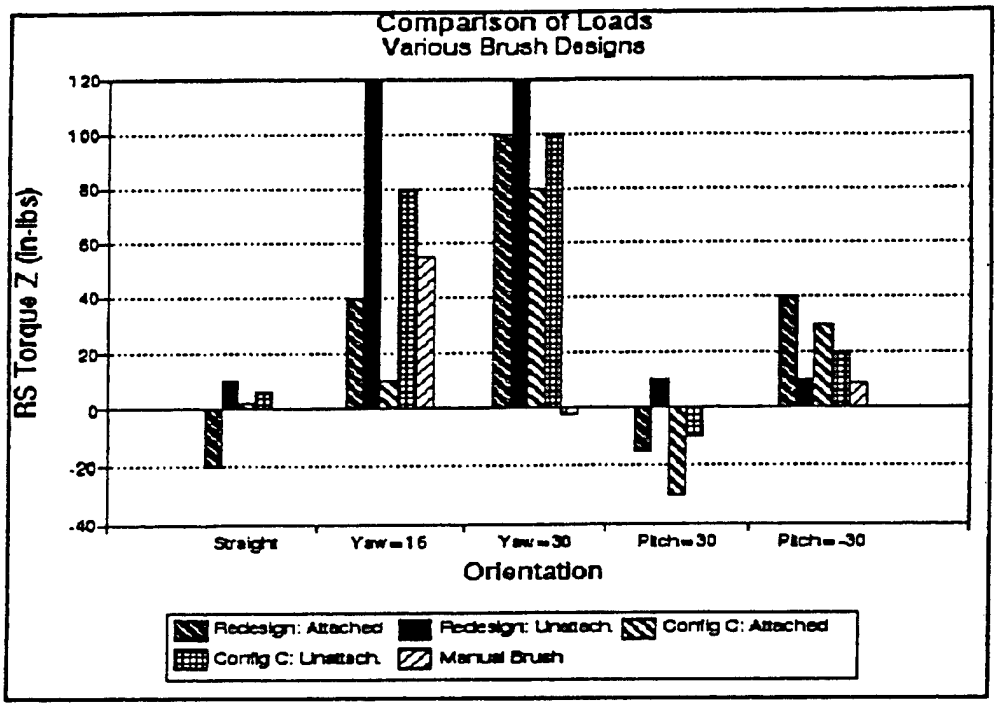

Figure B-11. Comparison of various brush configurations. Torque - Z at right shoulder.

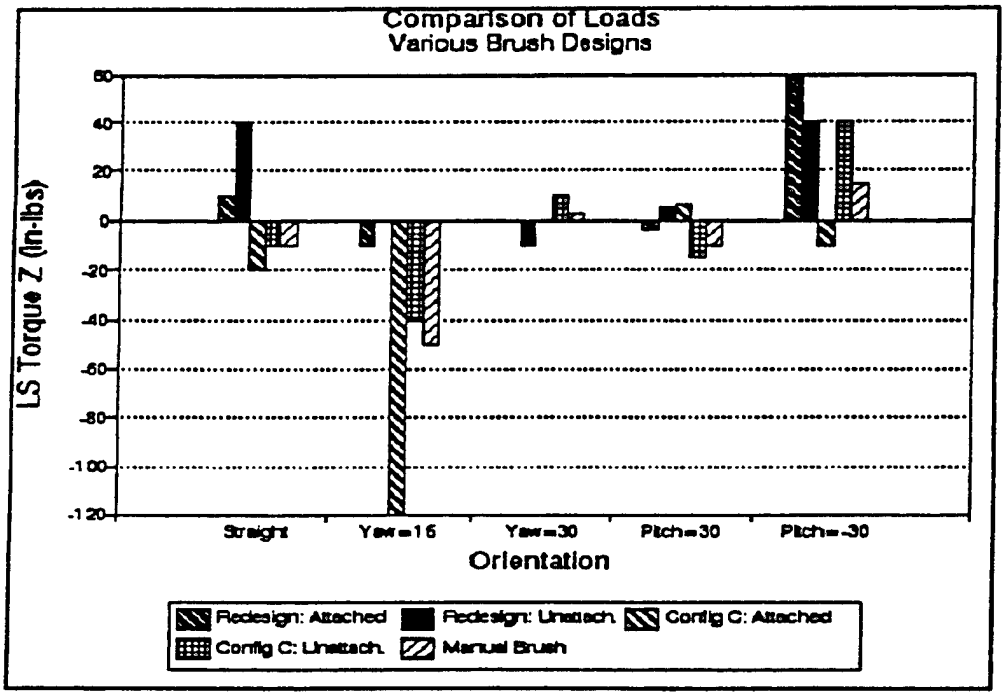

Figure B-12. Comparison of various brush configurations. Torque - Z at left shoulder.

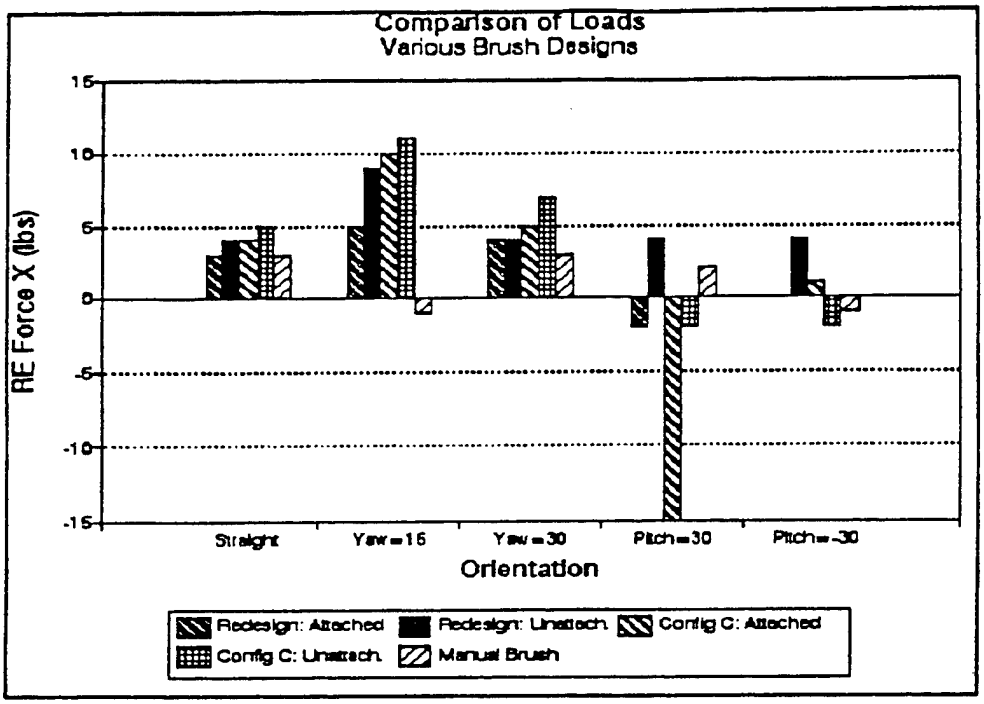

Figure B-13. Comparison of various brush configurations. Force - X at right elbow.

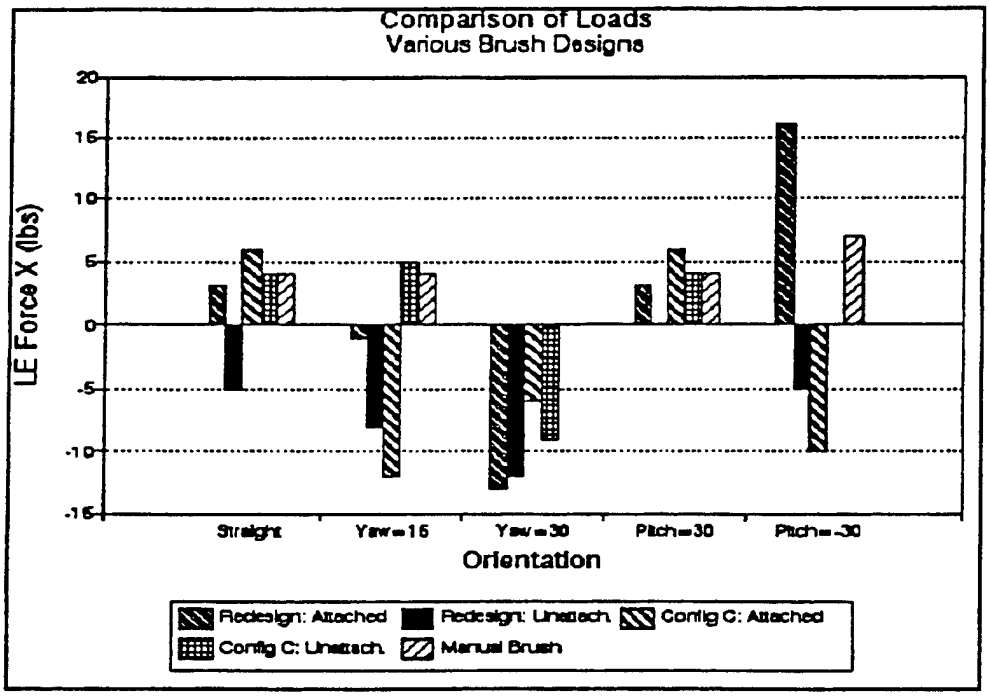

Figure B-14. Comparison of various brush configurations. Force - X at left elbow.

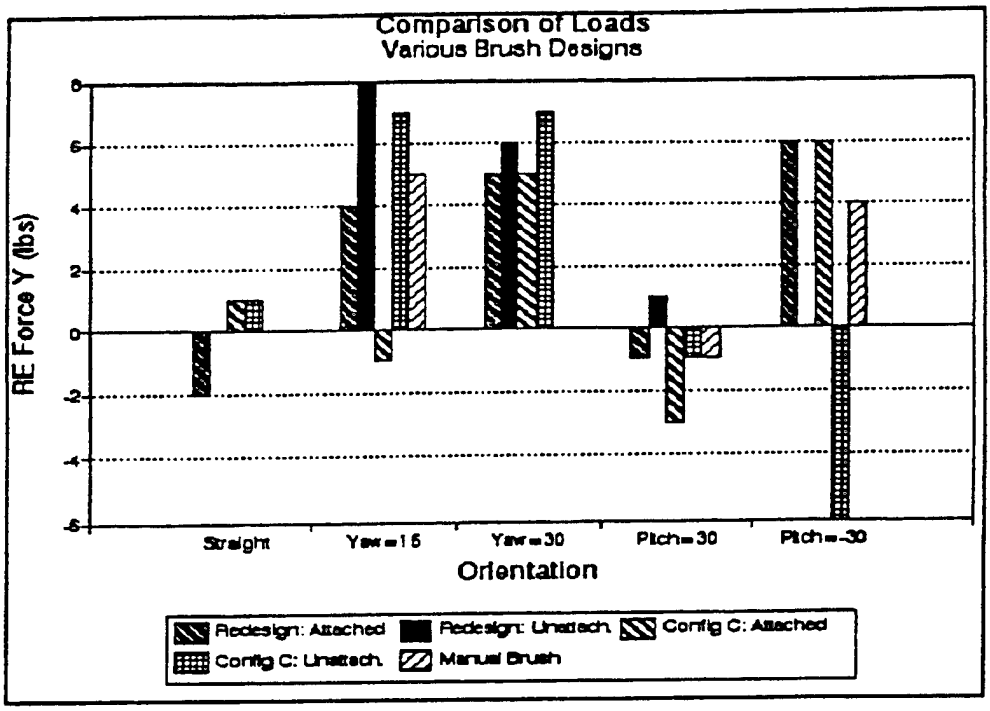

Figure B-15. Comparison of various brush configurations. Force - Y at right elbow.

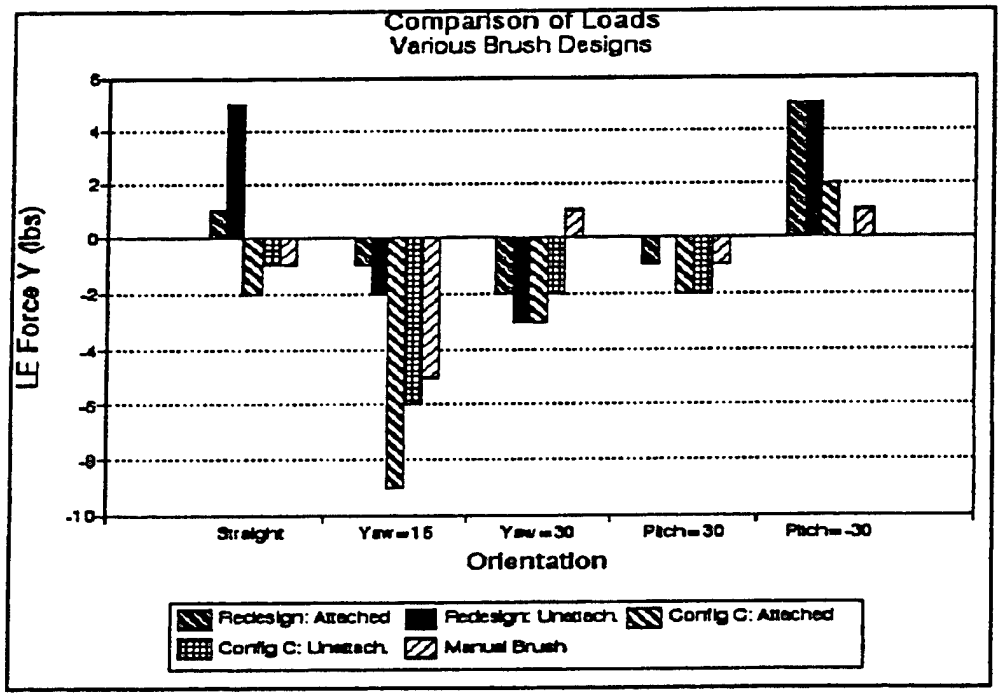

Figure B-16. Comparison of various brush configurations. Force - Y at left elbow.

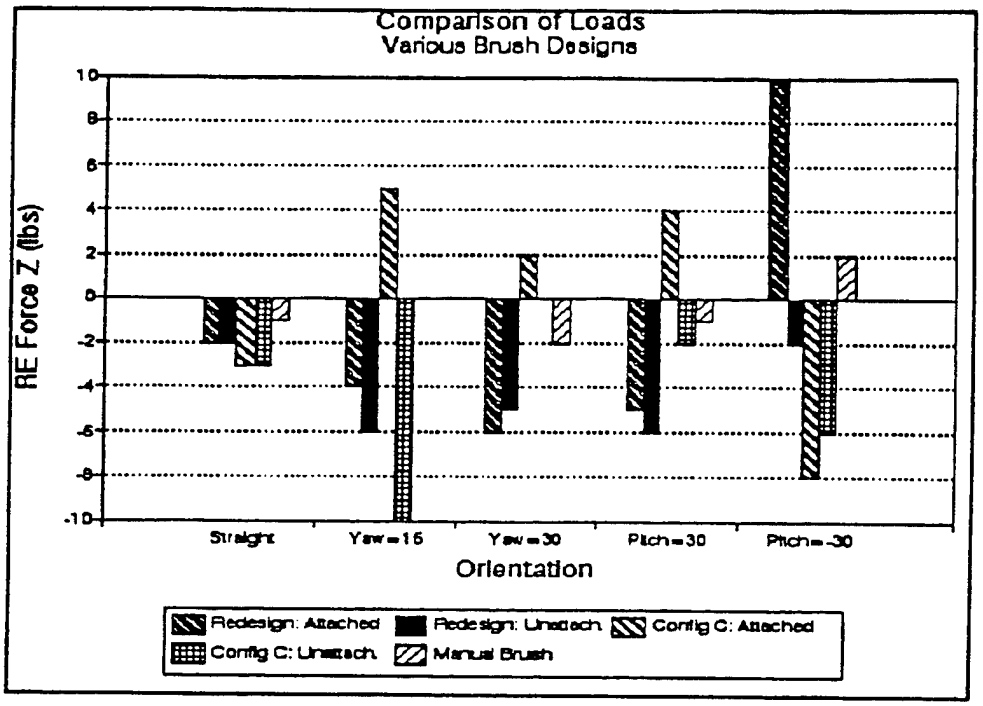

Figure B-17. Comparison of various brush configurations. Force - Z at right elbow.

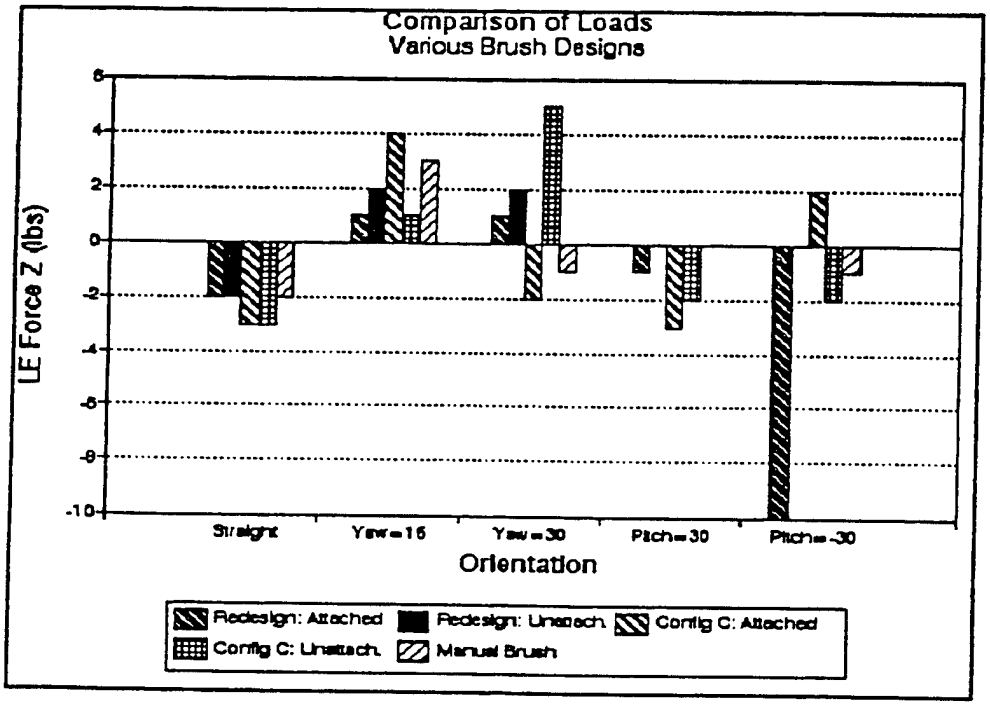

Figure B-18. Comparison of various brush configurations. Force - Z at left elbow.

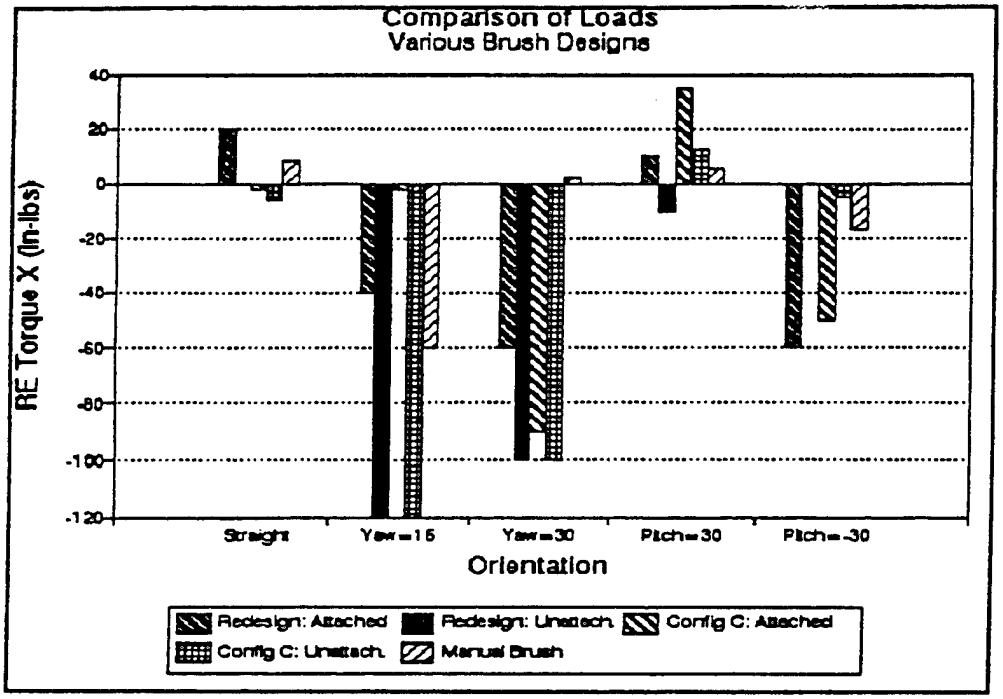

Figure B-19. Comparison of various brush configurations. Torque - X at right elbow.

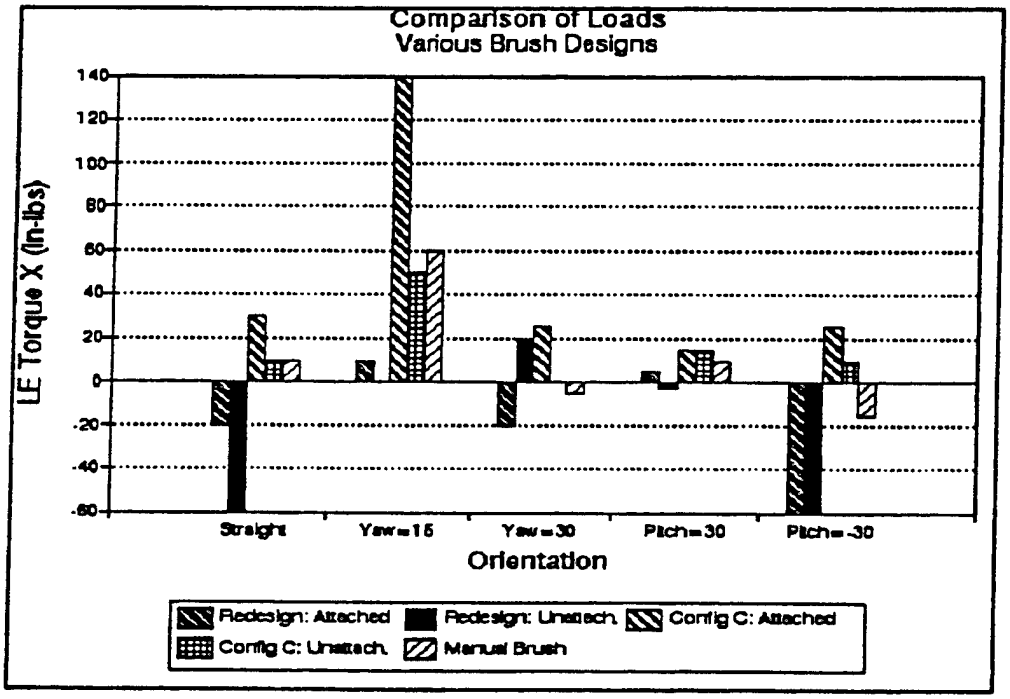

Figure B-20. Comparison of various brush configurations. Torque - X at left elbow.

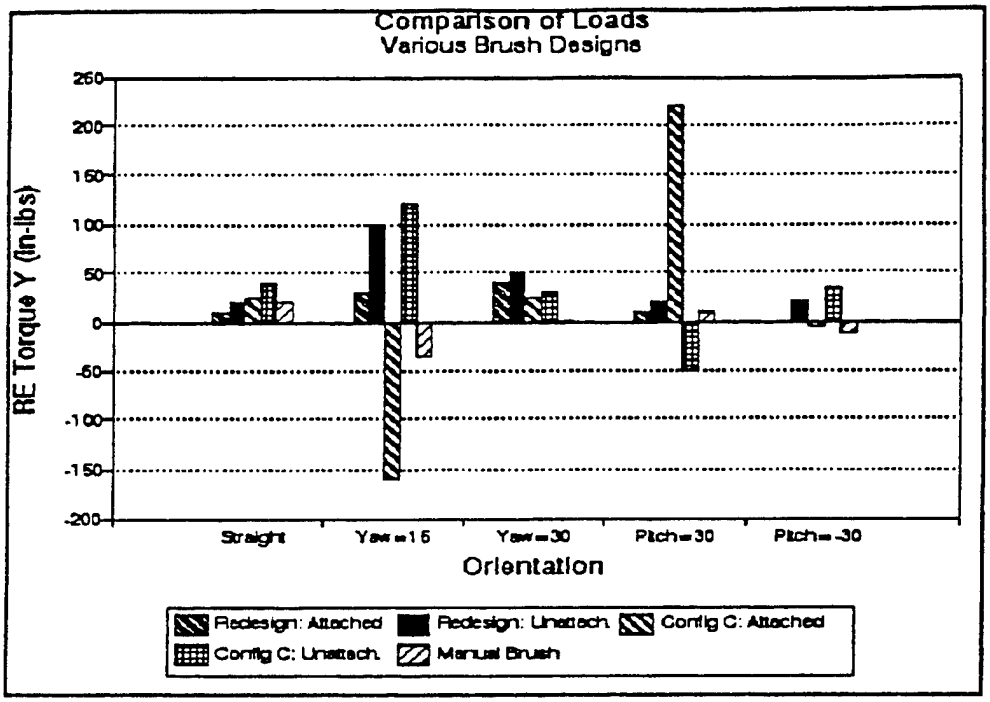

Figure B-21. Comparison of various brush configurations. Torque - Y at right elbow.

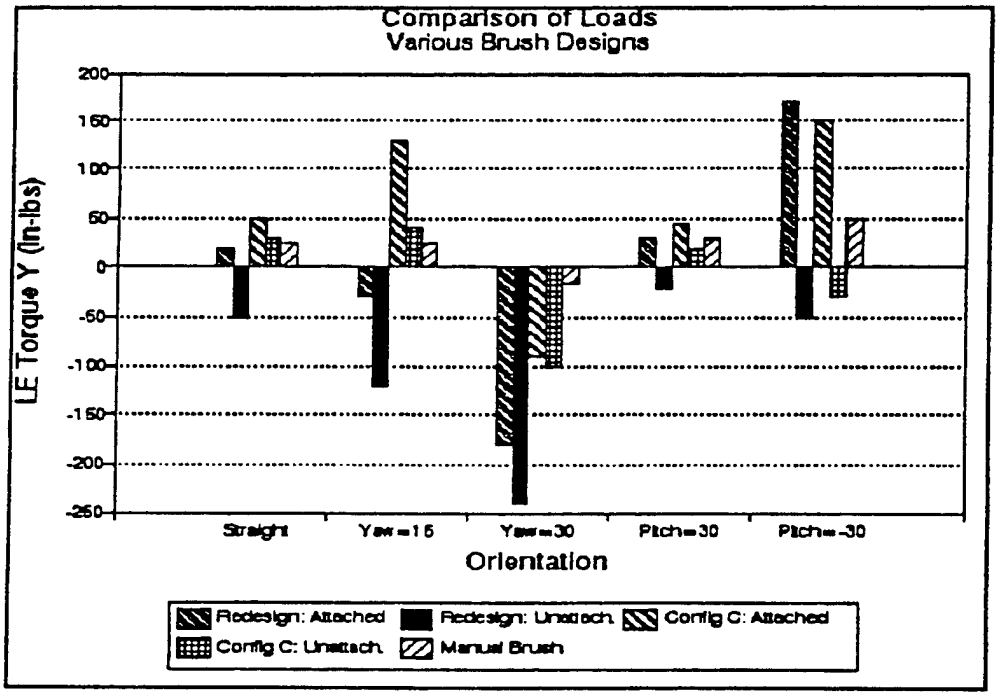

Figure B-22. Comparison of various brush configurations. Torque - Y at left elbow.

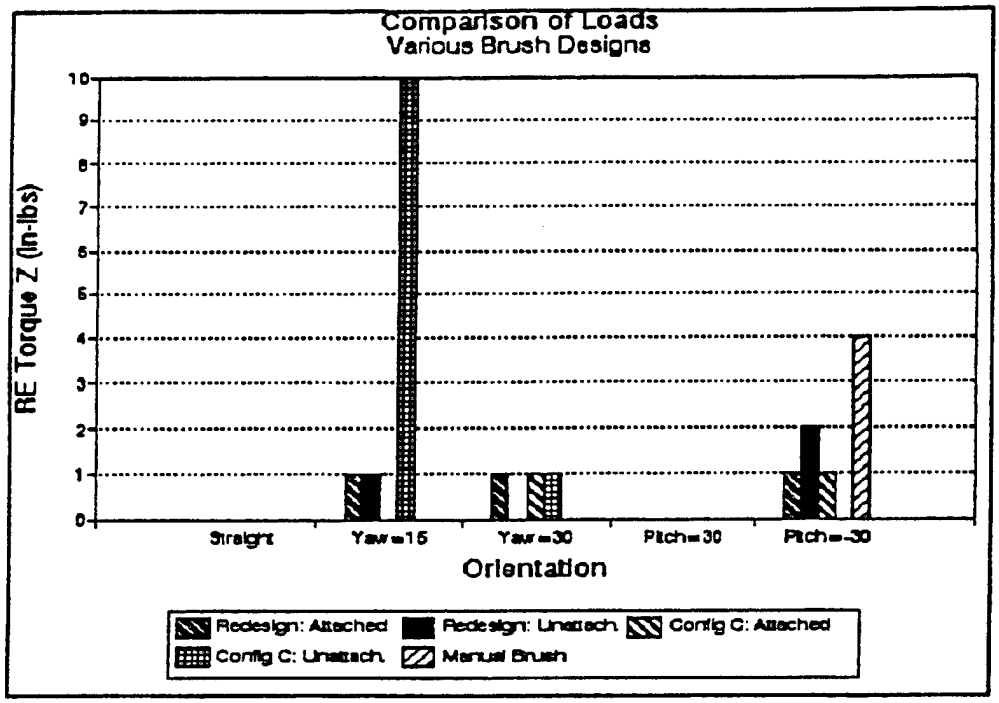

Figure B-23. Comparison of various brush configurations. Torque - Z at right elbow.

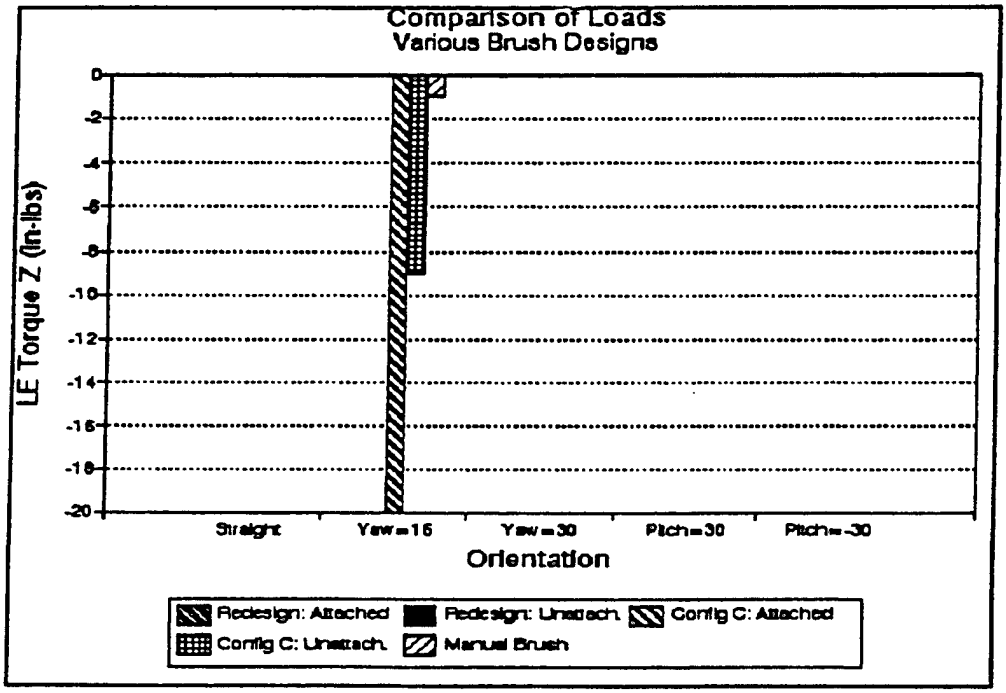

Figure B-24. Comparison of various brush configurations. Torque - Z at left elbow.

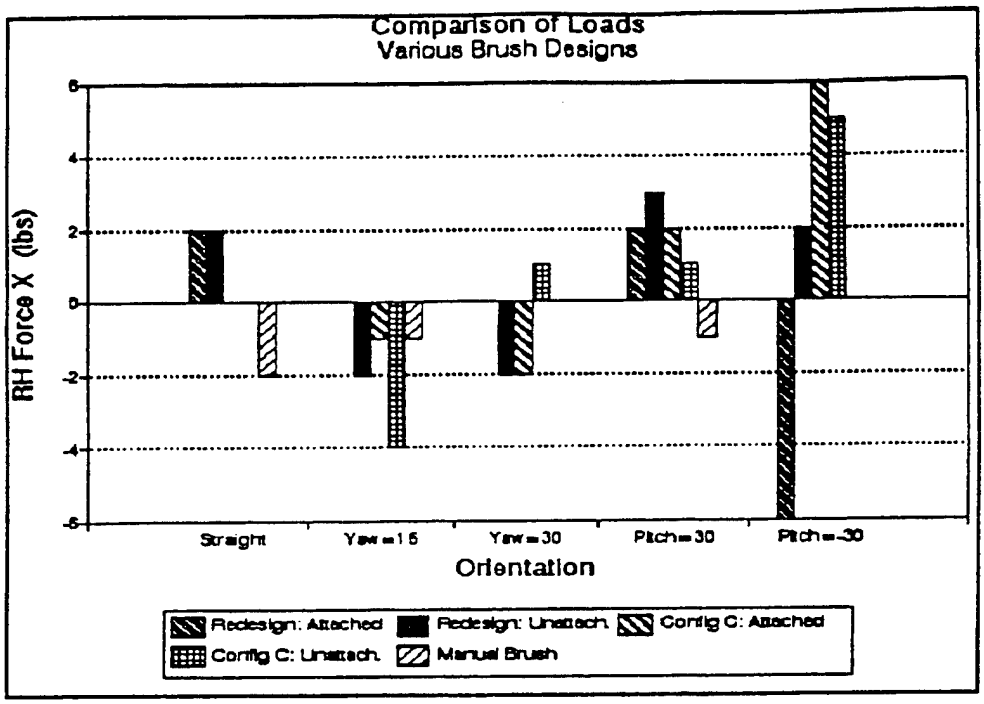

Figure B-25. Comparison of various brush configurations. Force - X at right hip.

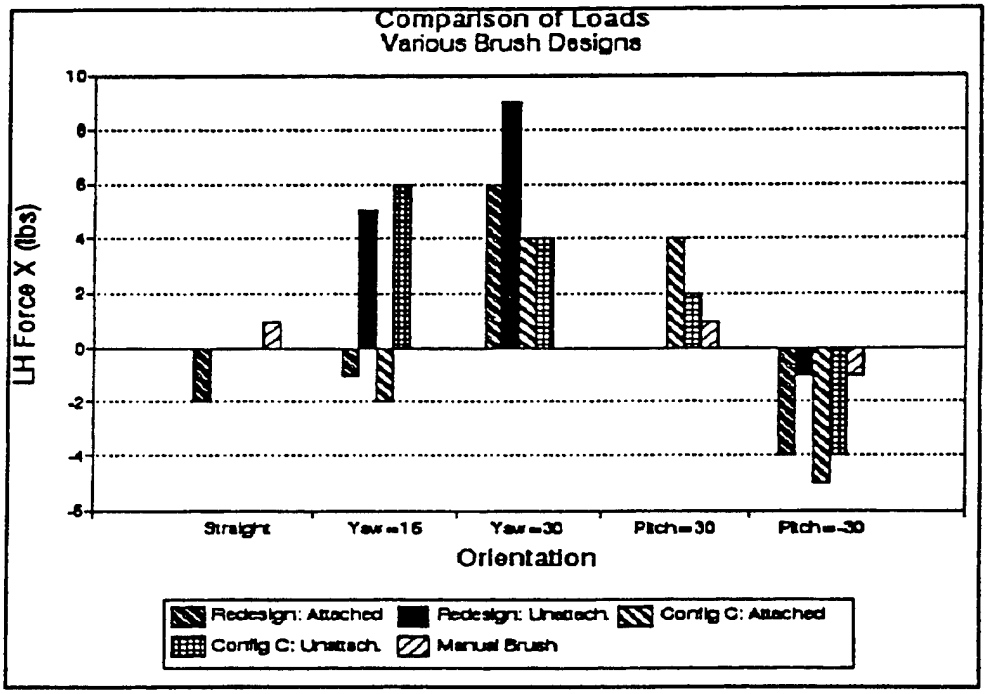

Figure B-26. Comparison of various brush configurations. Force - X at left hip.

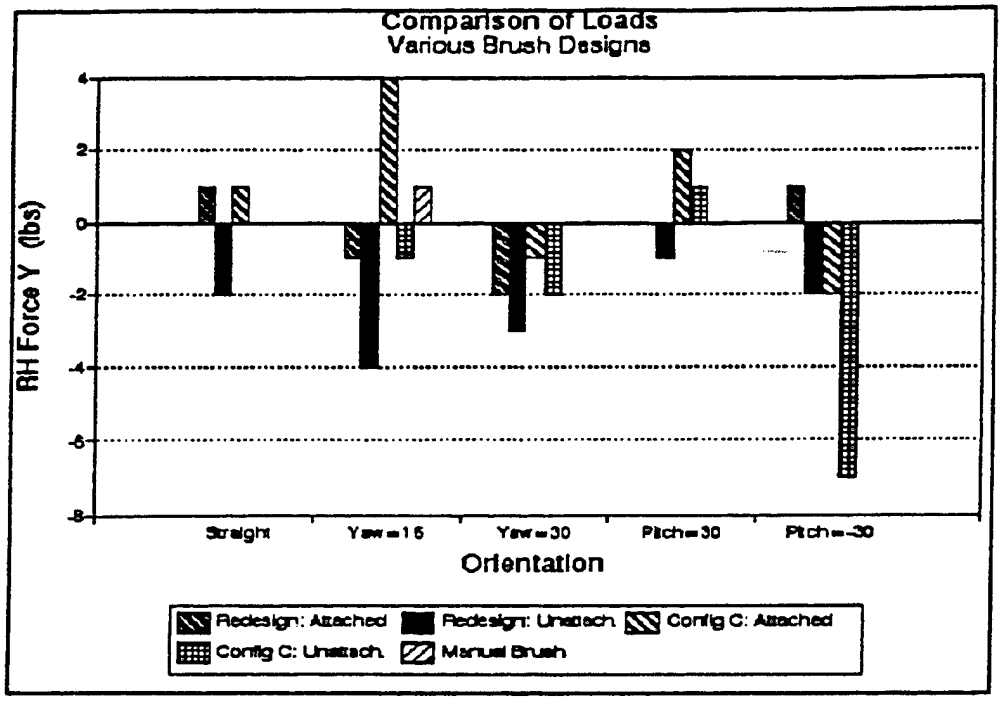

Figure B-27. Comparison of various brush configurations. Force - Y at right hip.

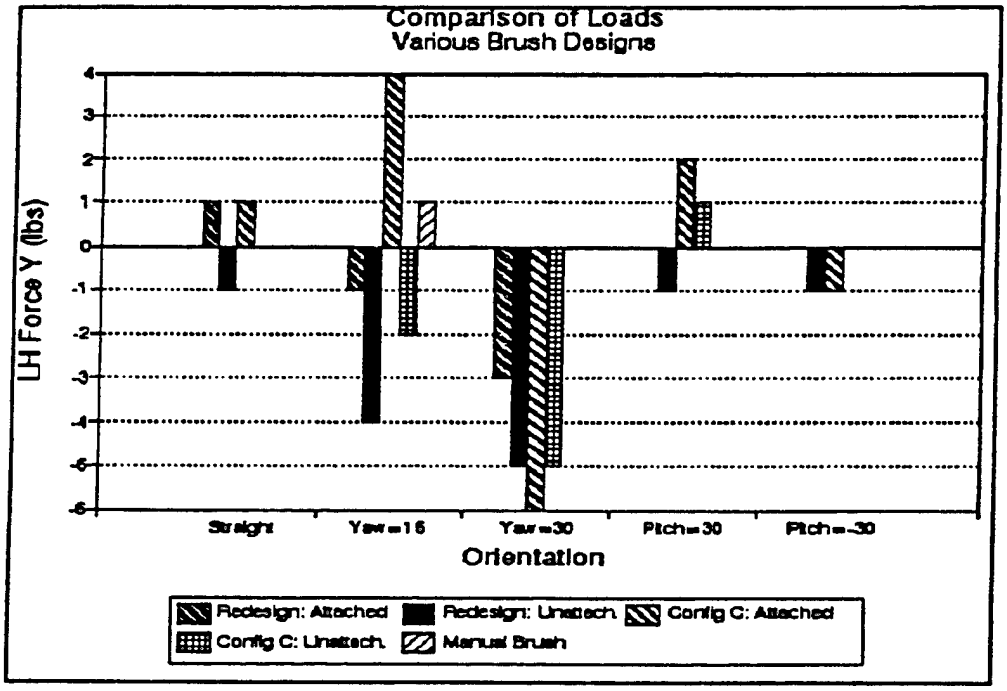

Figure B-28. Comparison of various brush configurations. Force - Y at left hip.

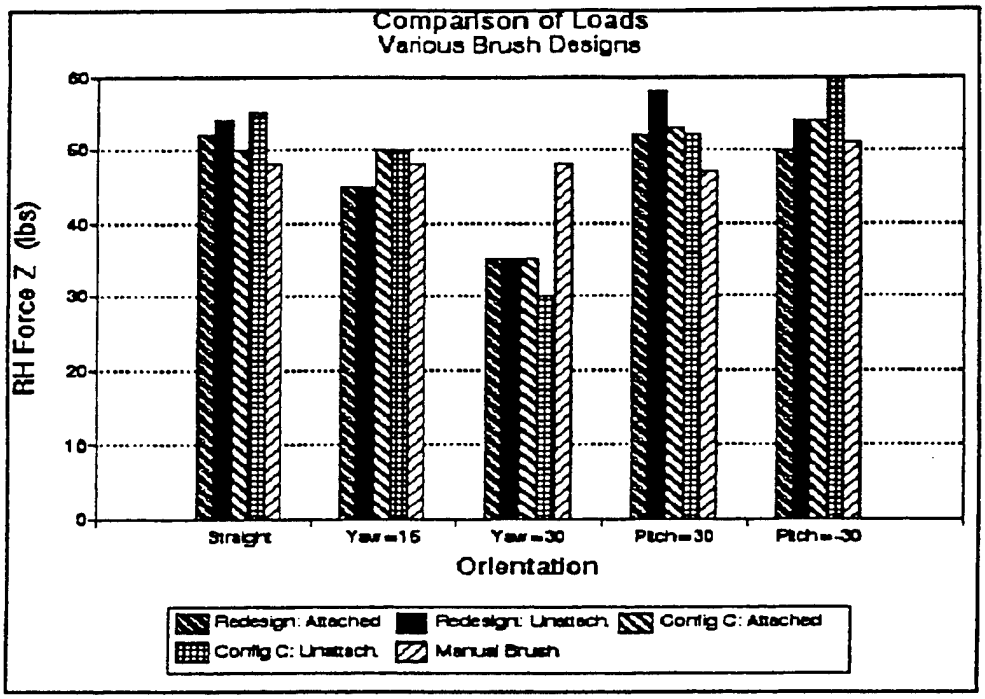

Figure B-29. Comparison of various brush configurations. Force - Z at right hip.

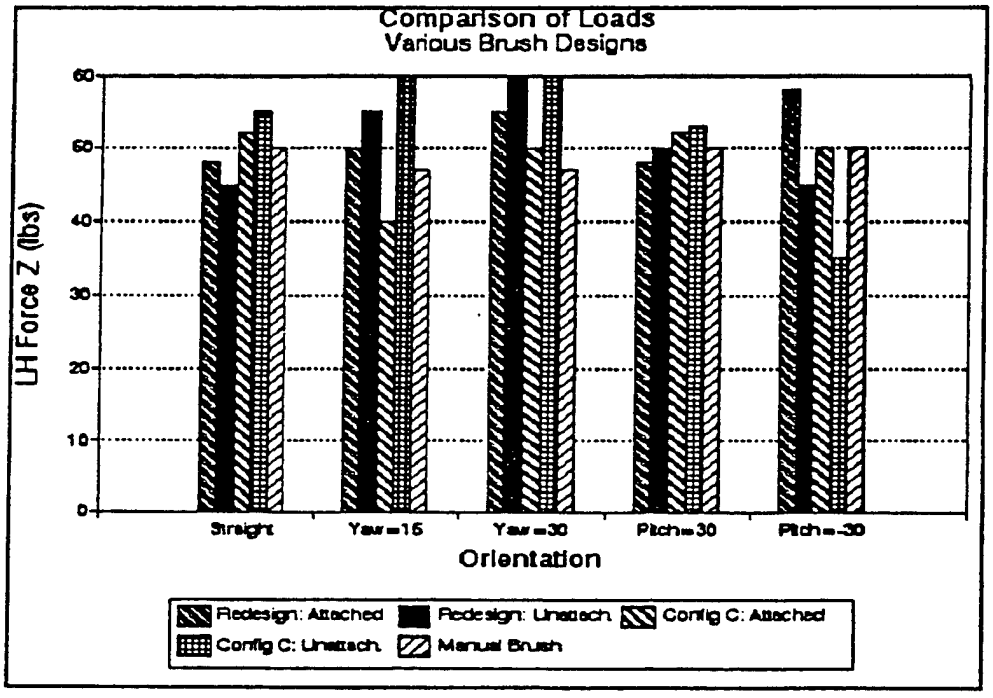

Figure B-30. Comparison of various brush configurations. Force - Z at left hip.

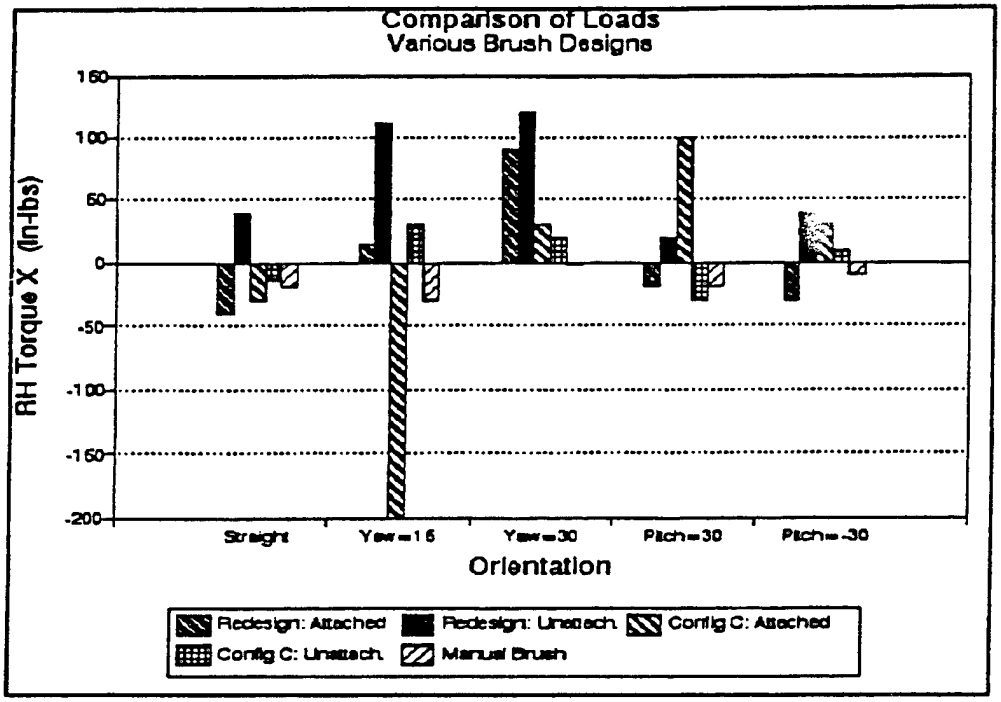

Figure B-31. Comparison of various brush configurations. Torque - X at right hip.

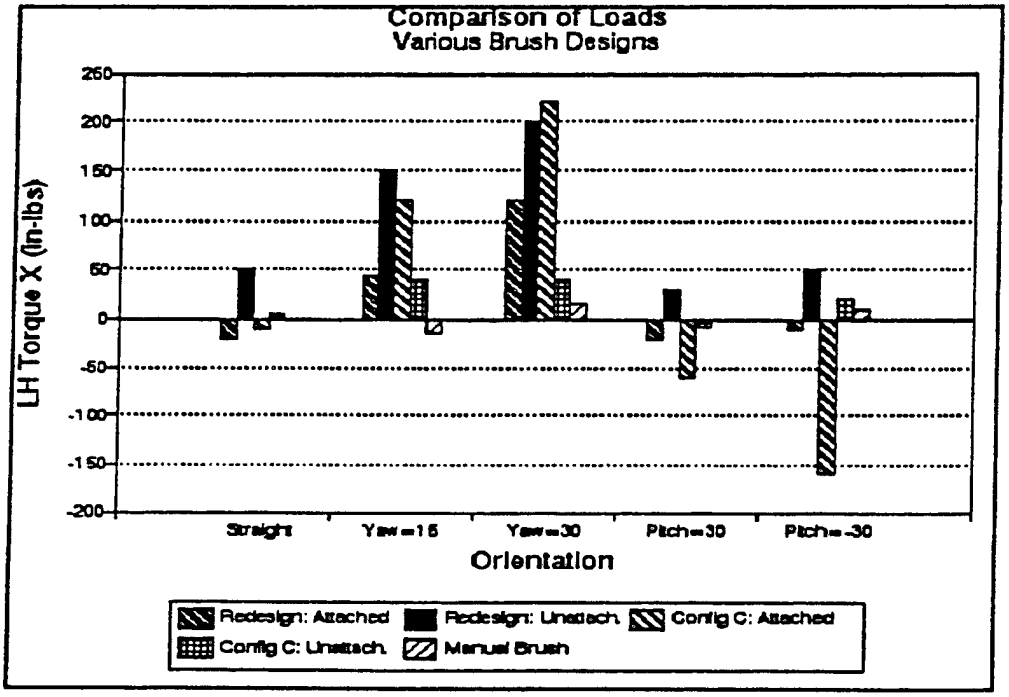

Figure B-32. Comparison of various brush configurations. Torque - X at left hip.

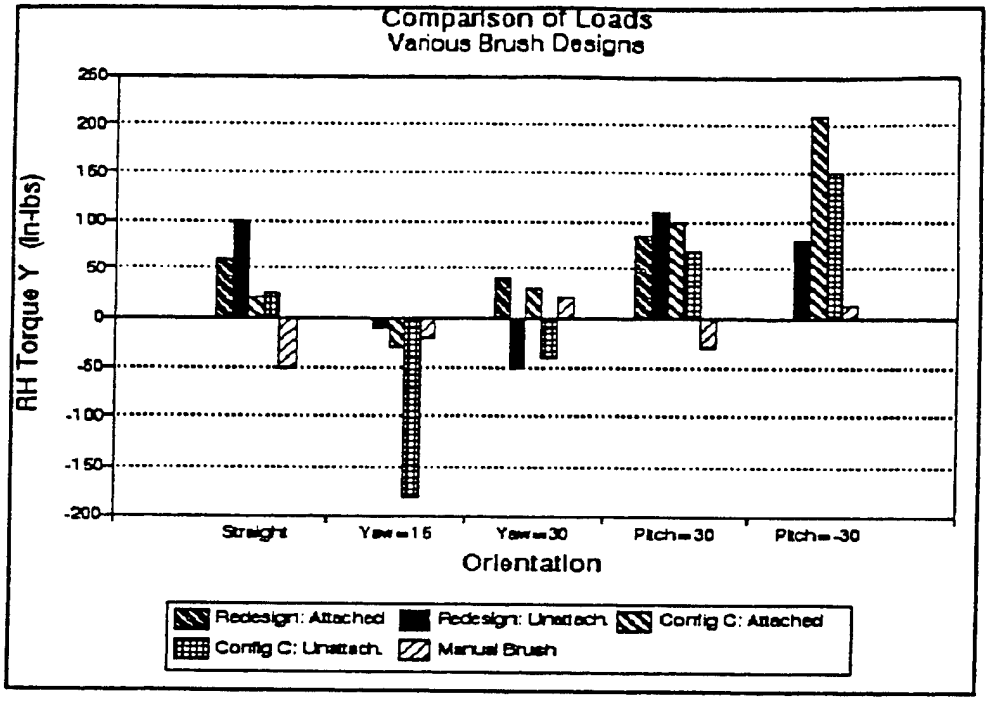

Figure B-33. Comparison of various brush configurations. Torque - Y at right hip.

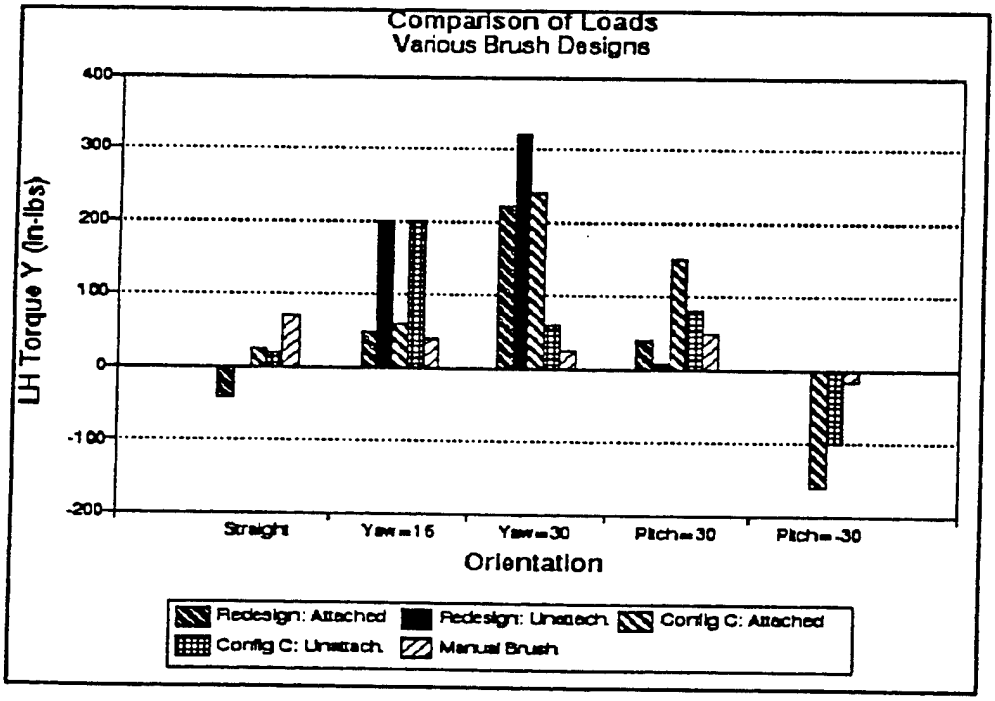

Figure B-34. Comparison of various brush configurations. Torque - Y at left hip.

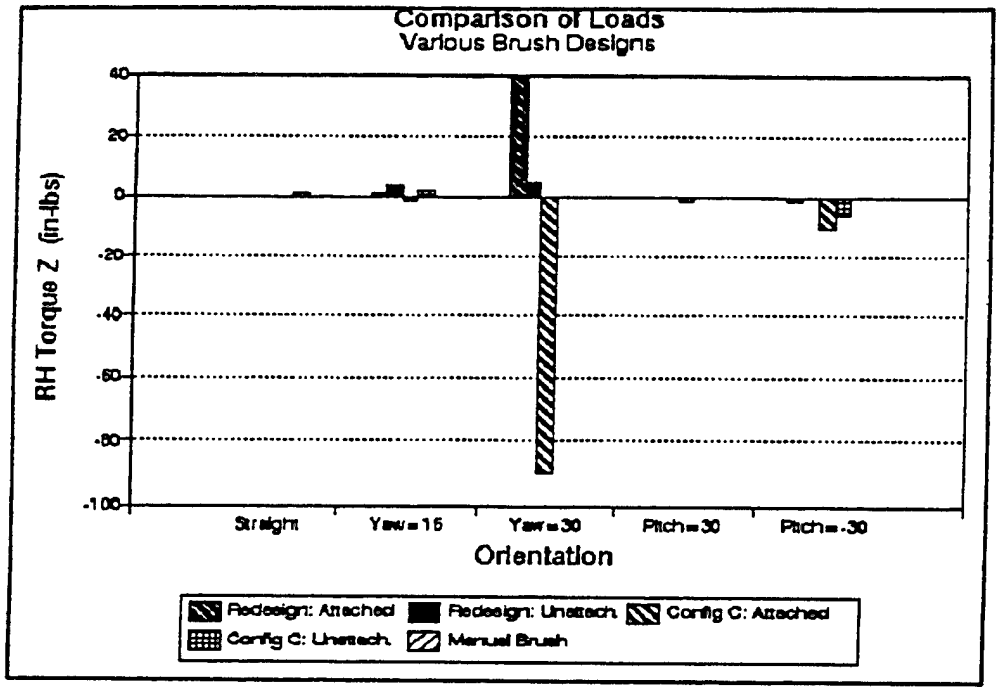

Figure B-35. Comparison of various brush configurations. Torque - Z at right hip.

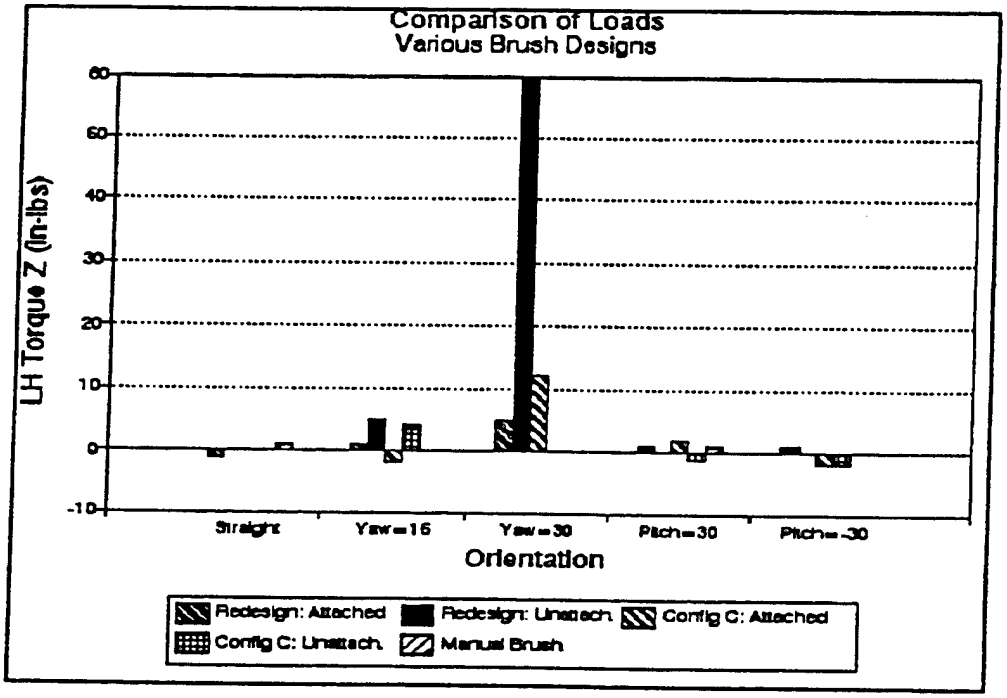

Figure B-36. Comparison of various brush configurations. Torque - Z at left hip.

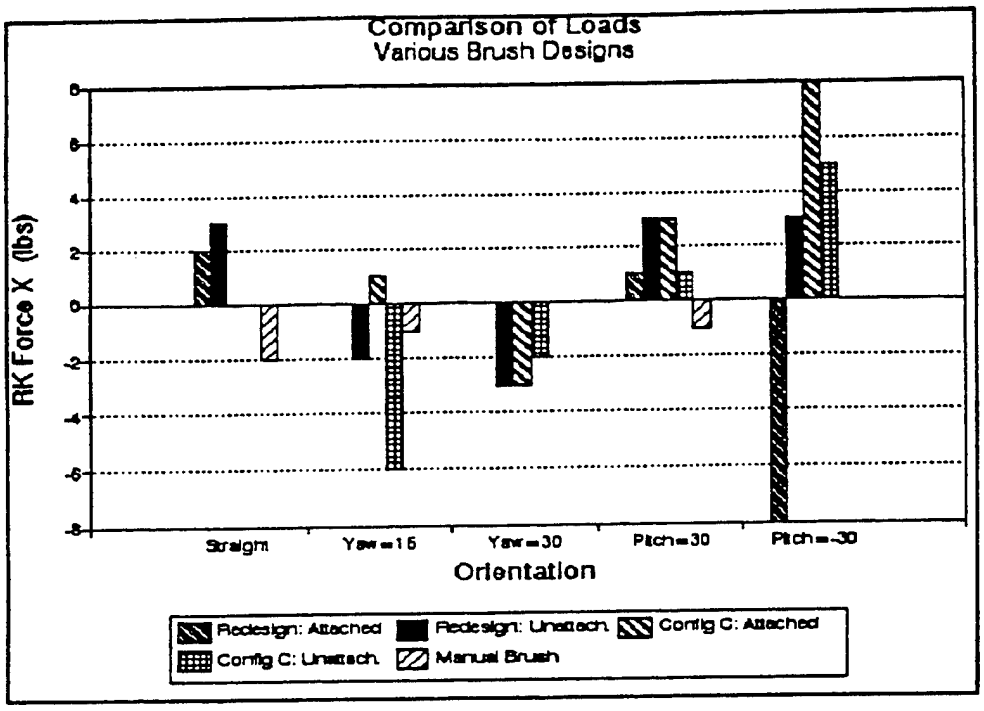

Figure B-37. Comparison of various brush configurations. Force - X at right knee.

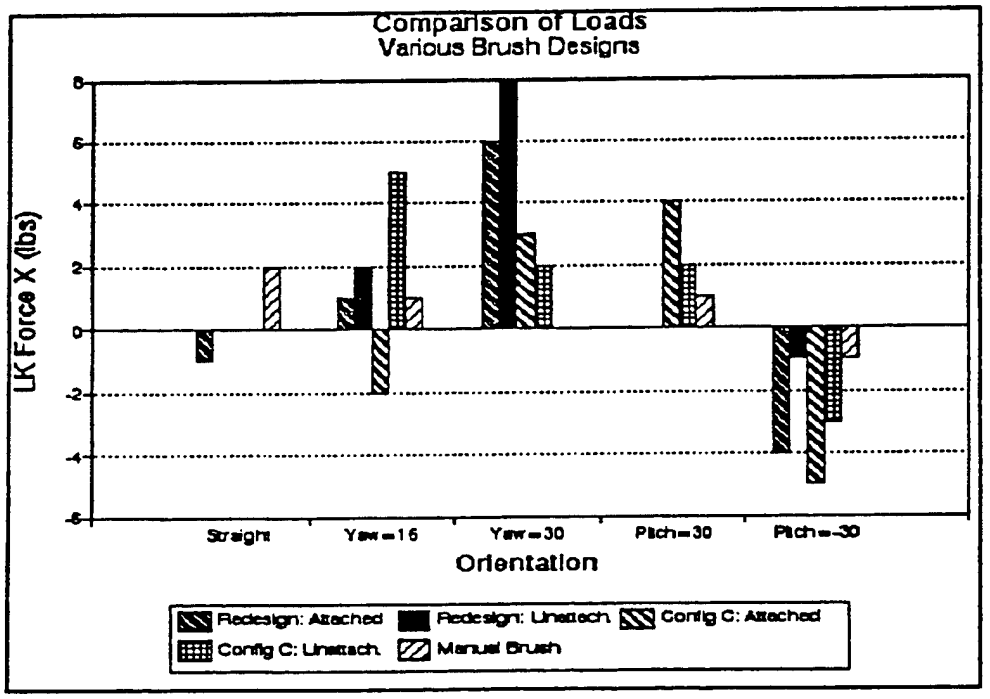

Figure B-38. Comparison of various brush configurations. Force - X at left knee.

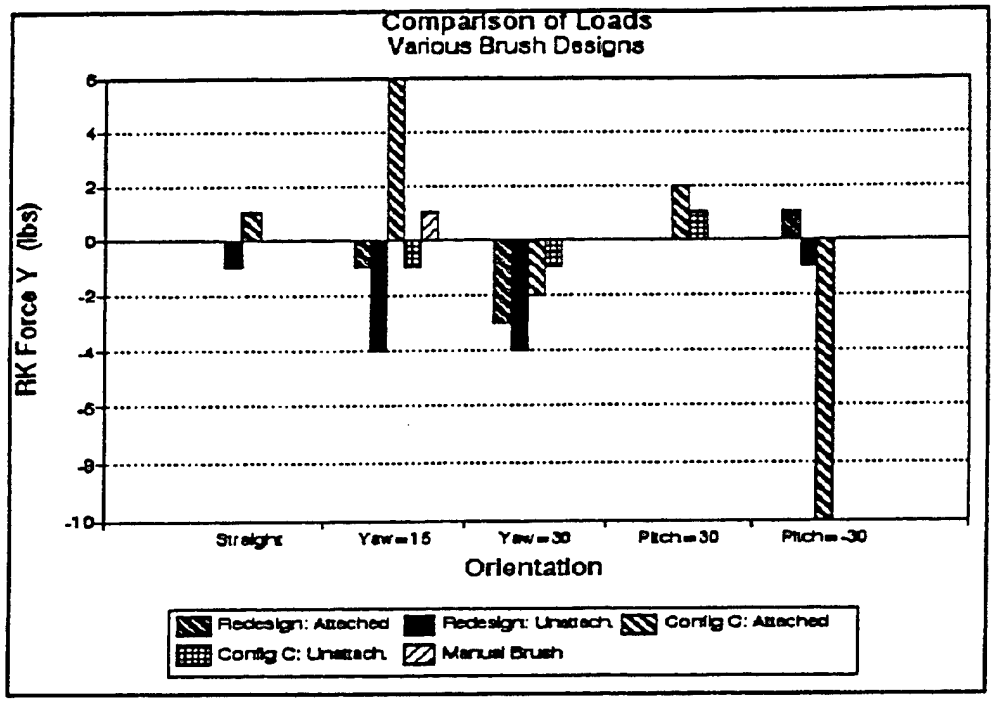

Figure B-39. Comparison of various brush configurations. Force - Y at right knee.

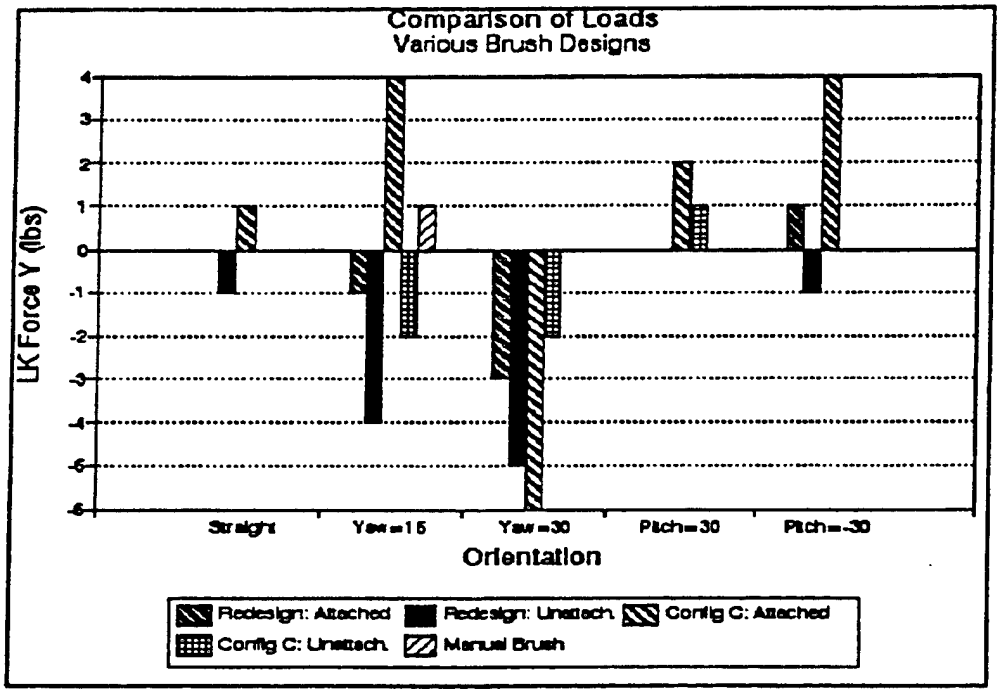

Figure B-40. Comparison of various brush configurations. Force - Y at left knee.

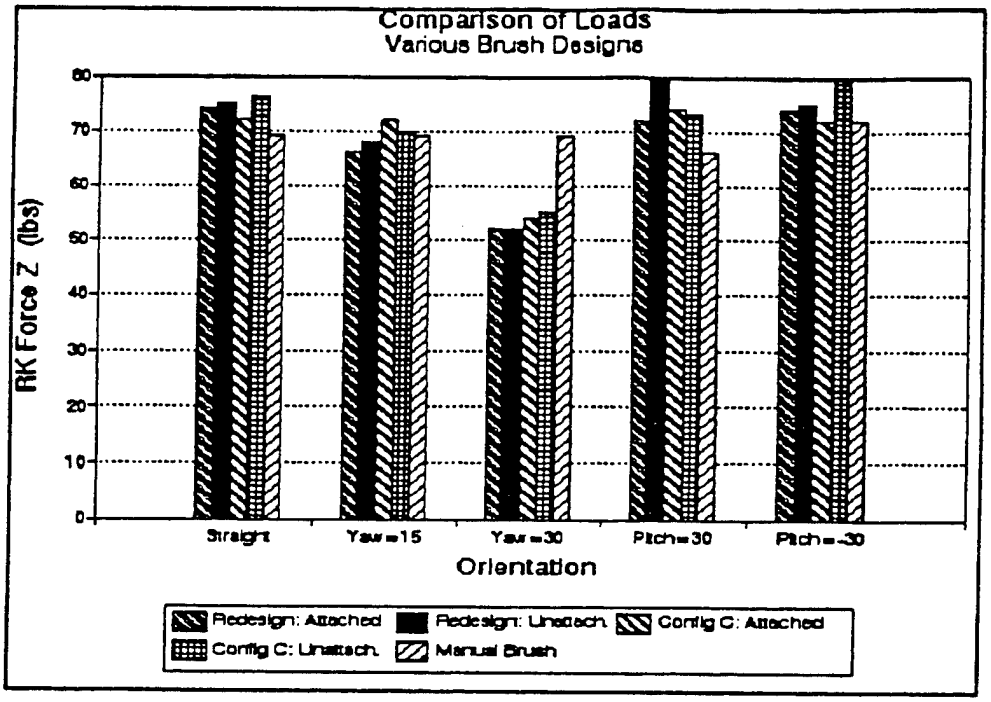

Figure B-41. Comparison of various brush configurations. Force - Z at right knee.

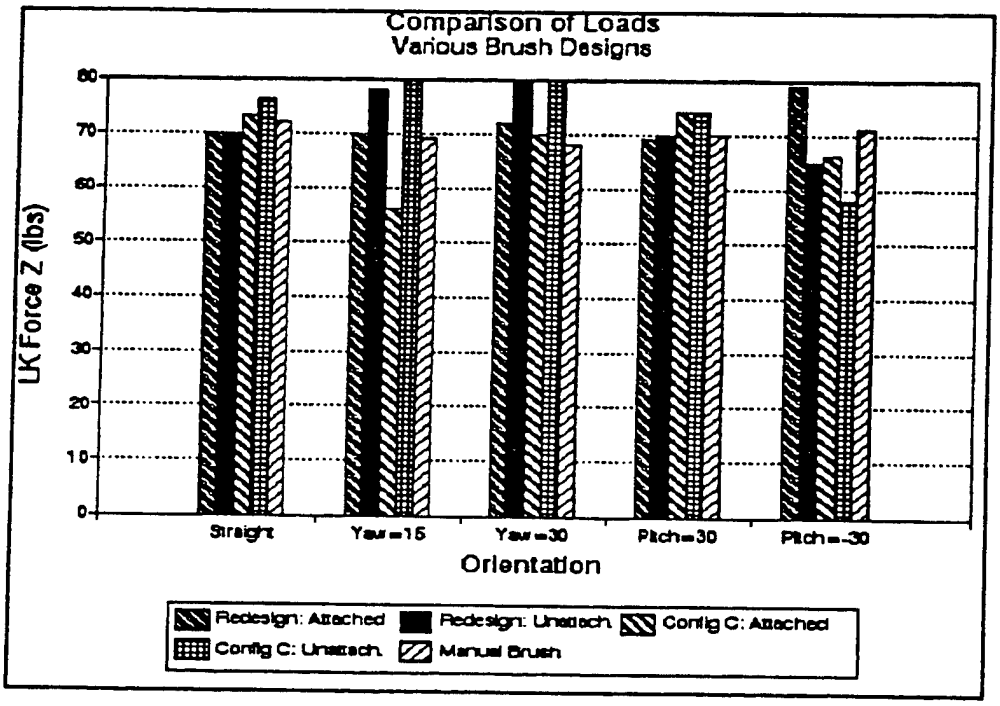

Figure B-42. Comparison of various brush configurations. Force - Z at left knee.

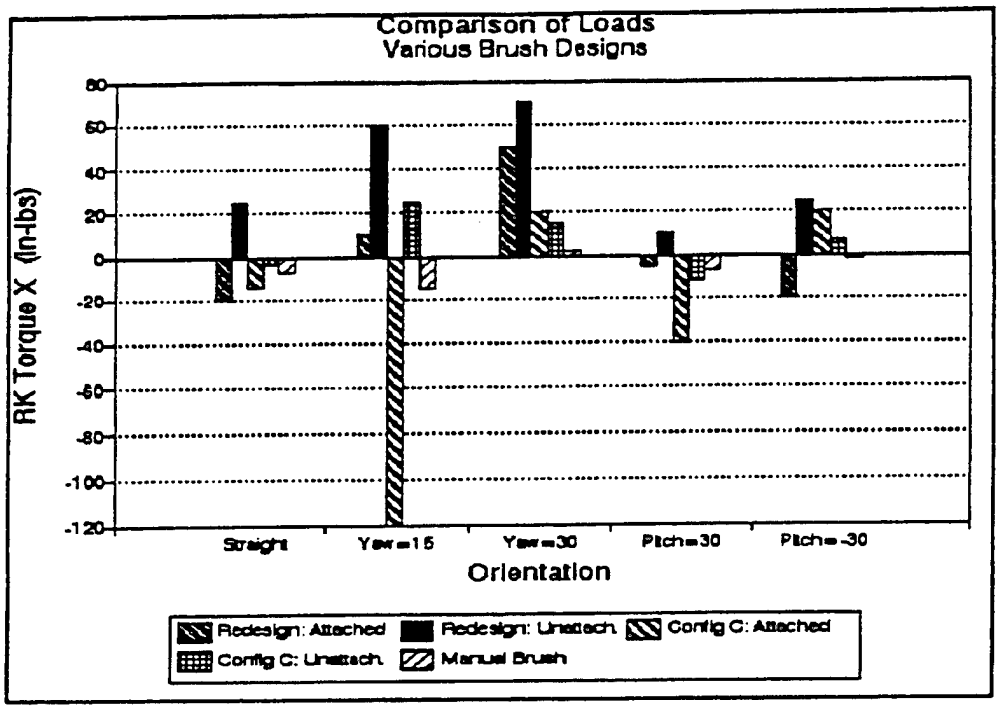

Figure B-43. Comparison of various brush configurations. Torque - X at right knee.

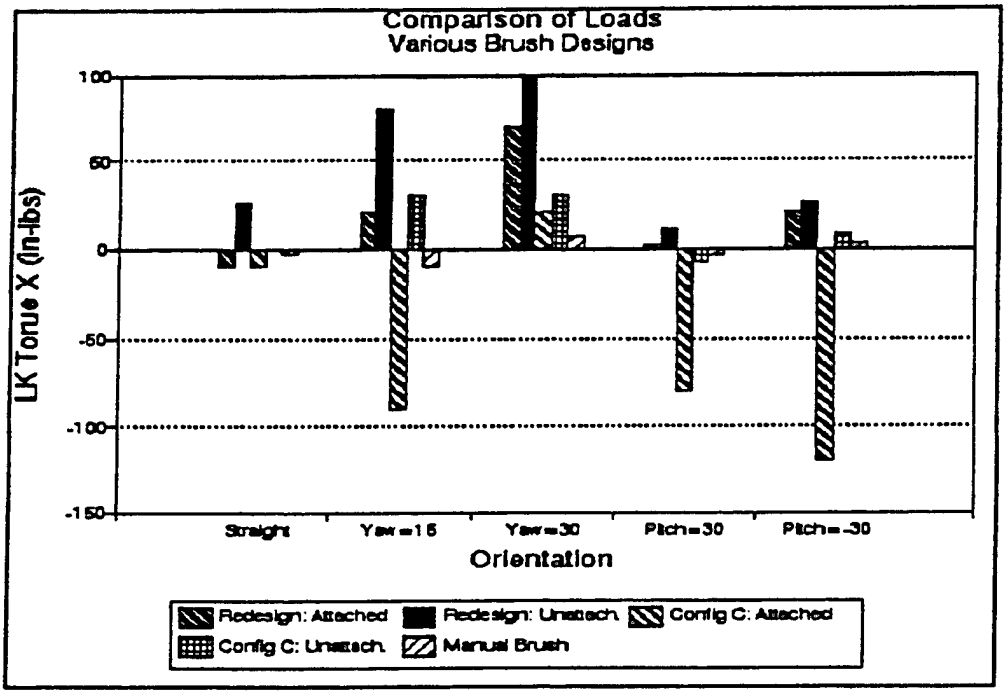

Figure B-44. Comparison of various brush configurations. Torque - X at left knee.

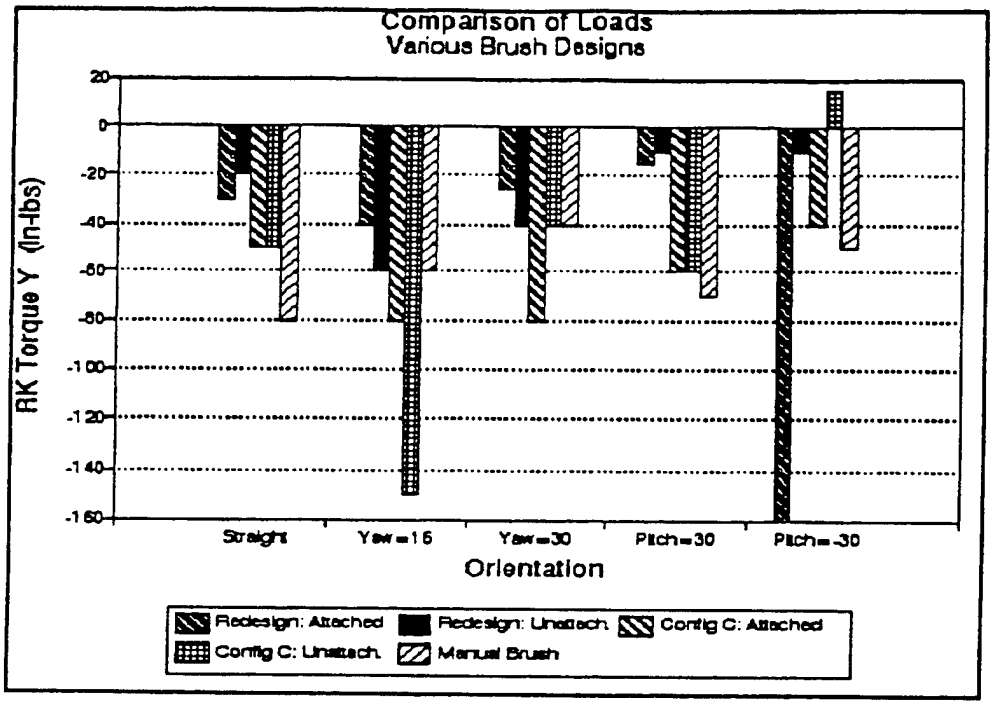

Figure B-45. Comparison of various brush configurations. Torque - Y at right knee.

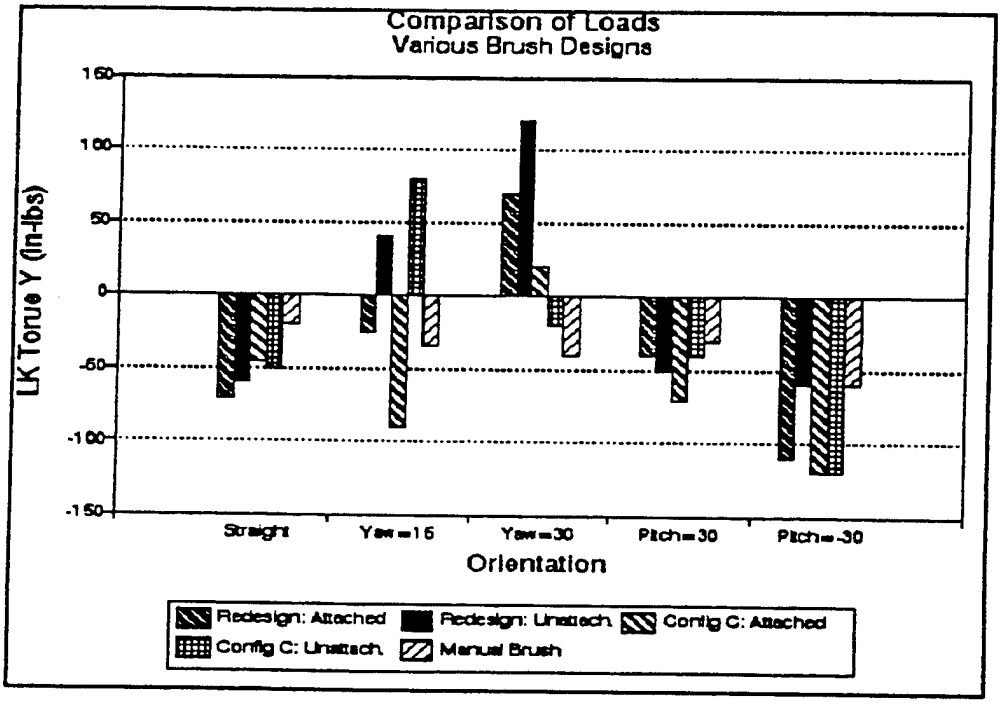

Figure B-46. Comparison of various brush configurations. Torque - Y at left knee.

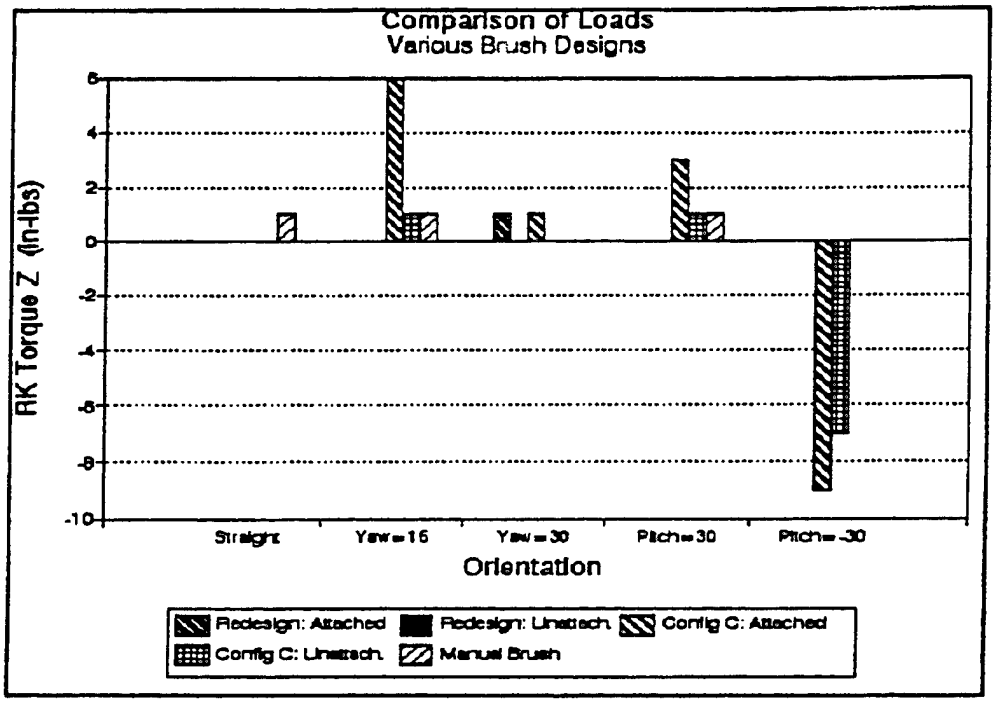

Figure B-47. Comparison of various brush configurations. Torque - Z at right knee.

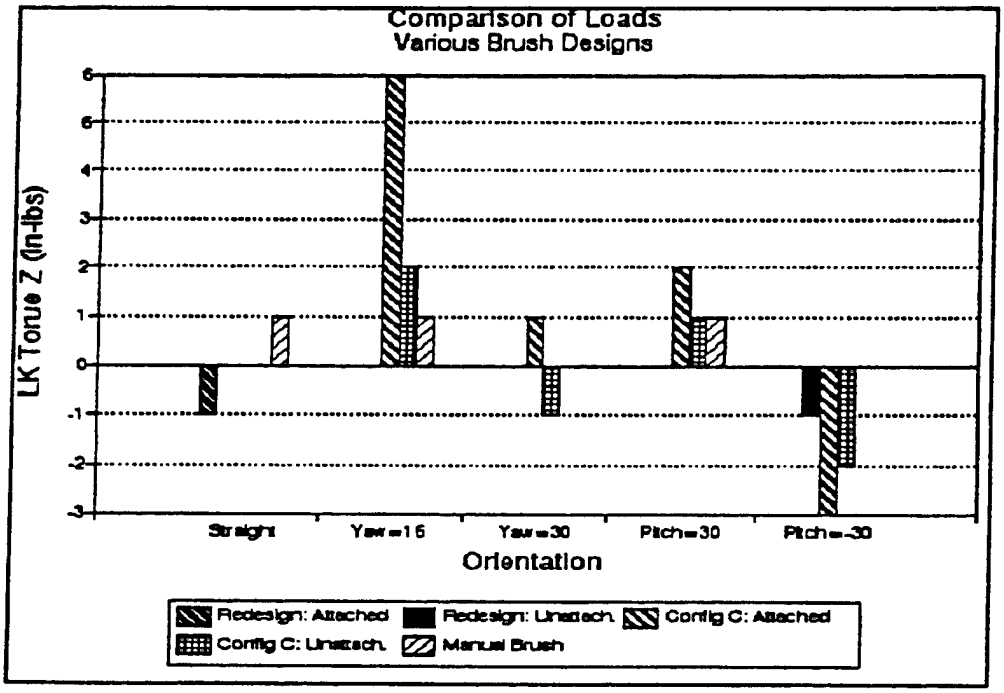

Figure B-48. Comparison of various brush configurations. Torque - Z at left knee.

APPENDIX C

PLOTS OF COMPARISON OF MAXIMUM FORCES AND TORQUES AT JOINTS

PLOTS OF COMPARISON OF MAXIMUM FORCES AND TORQUES AT JOINTS

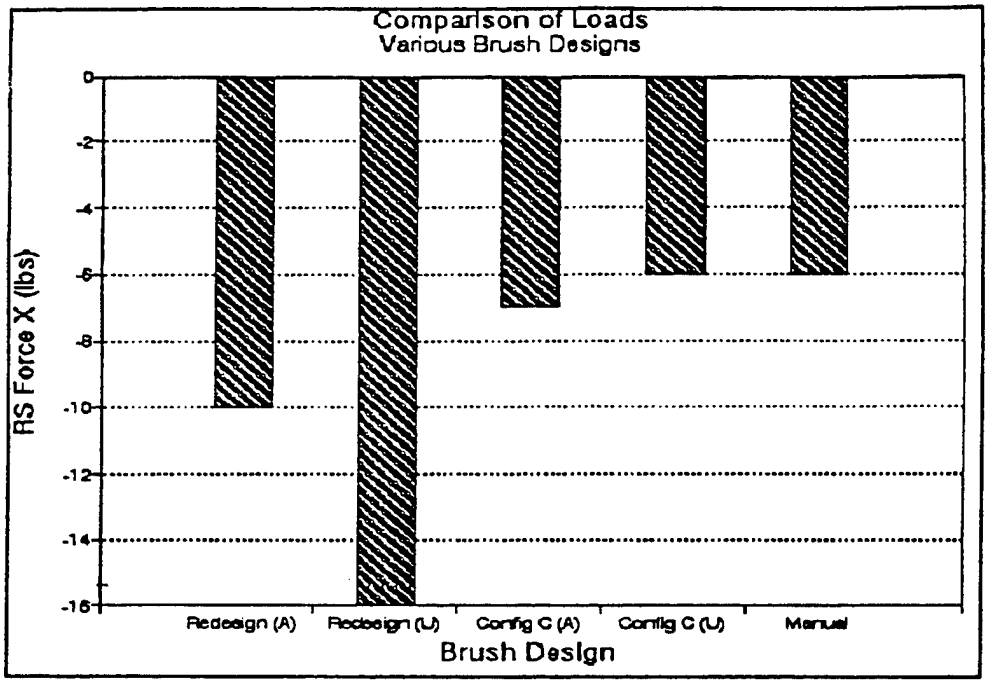

Figure C-1. Comparison of various brush configurations. Maximum force - X at right shoulder.

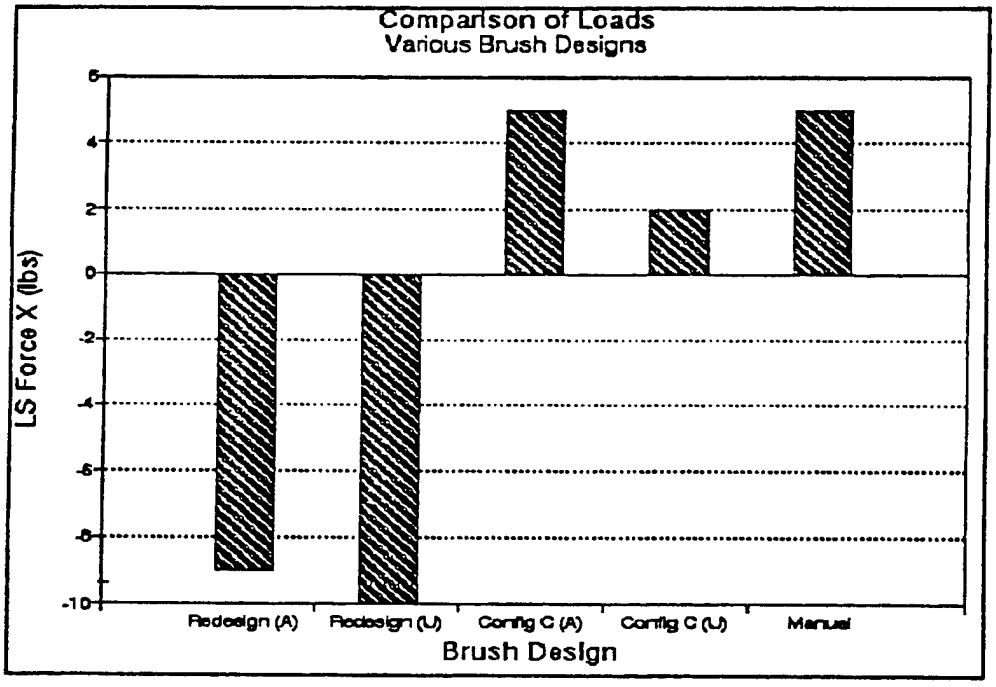

Figure C-2. Comparison of various brush configurations. Maximum force - X at left shoulder.

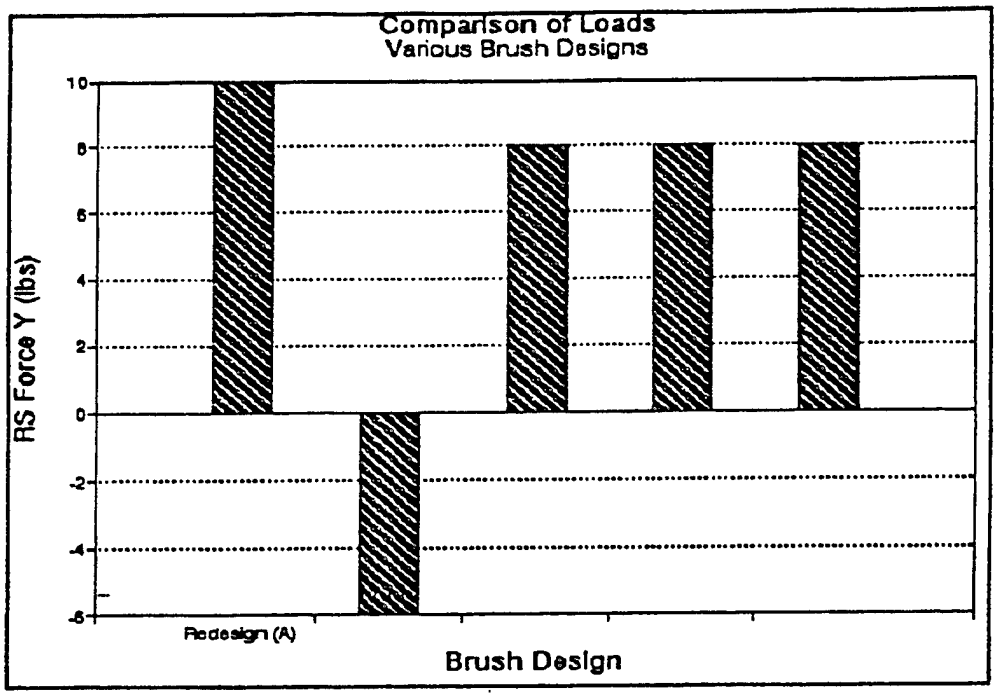

Figure C-3. Comparison of various brush configurations. Maximum force - Y at right shoulder.

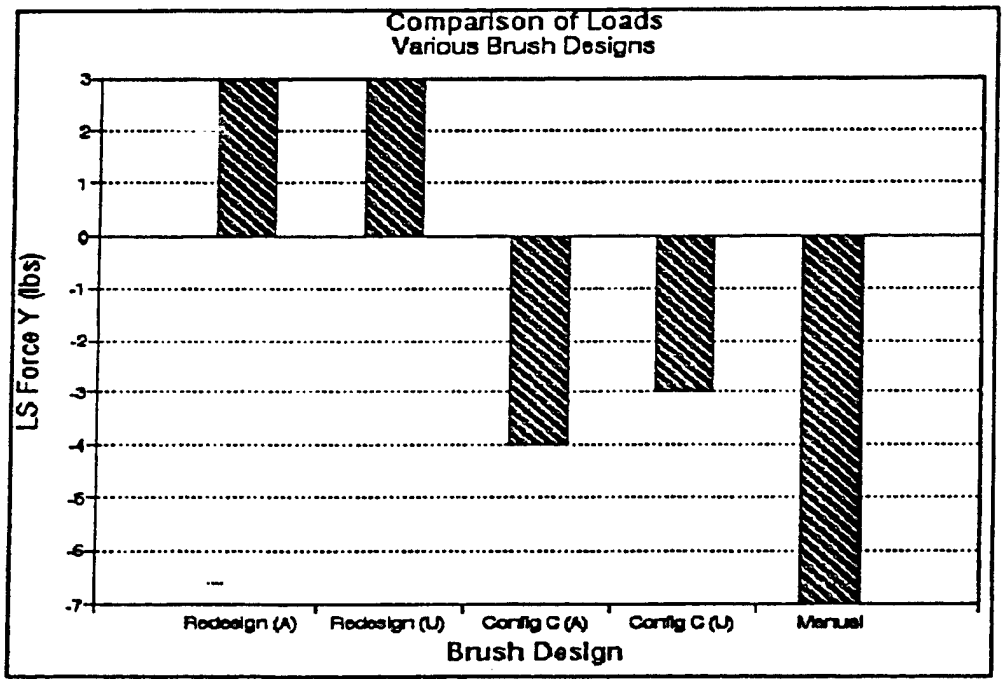

Figure C-4. Comparison of various brush configurations. Maximum force - Y at left shoulder.

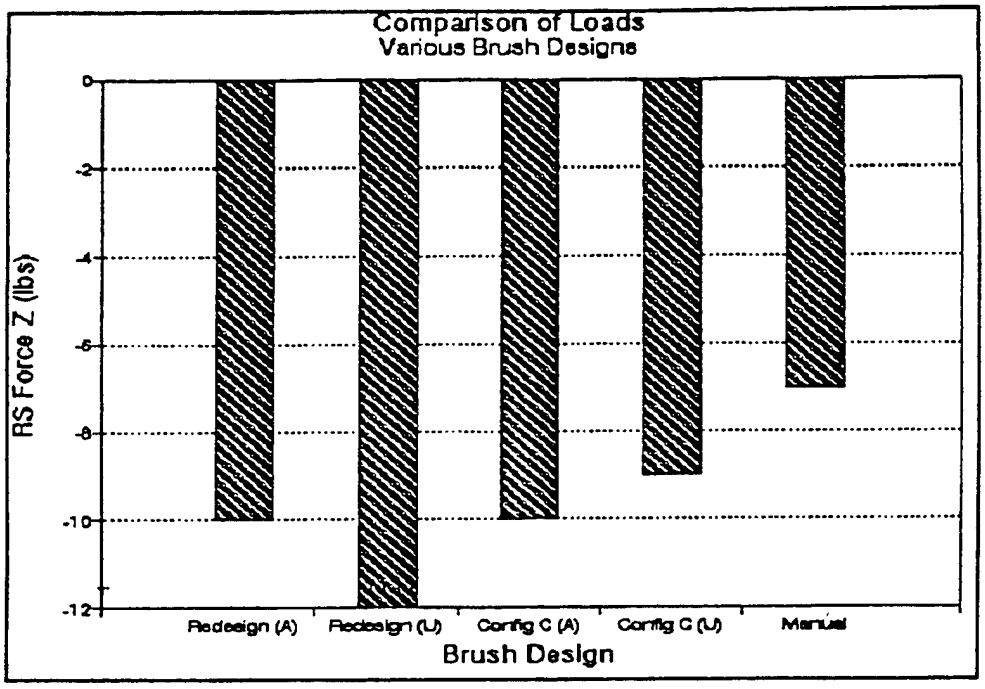

Figure C-5. Comparison of various brush configurations. Maximum force - Z at right shoulder.

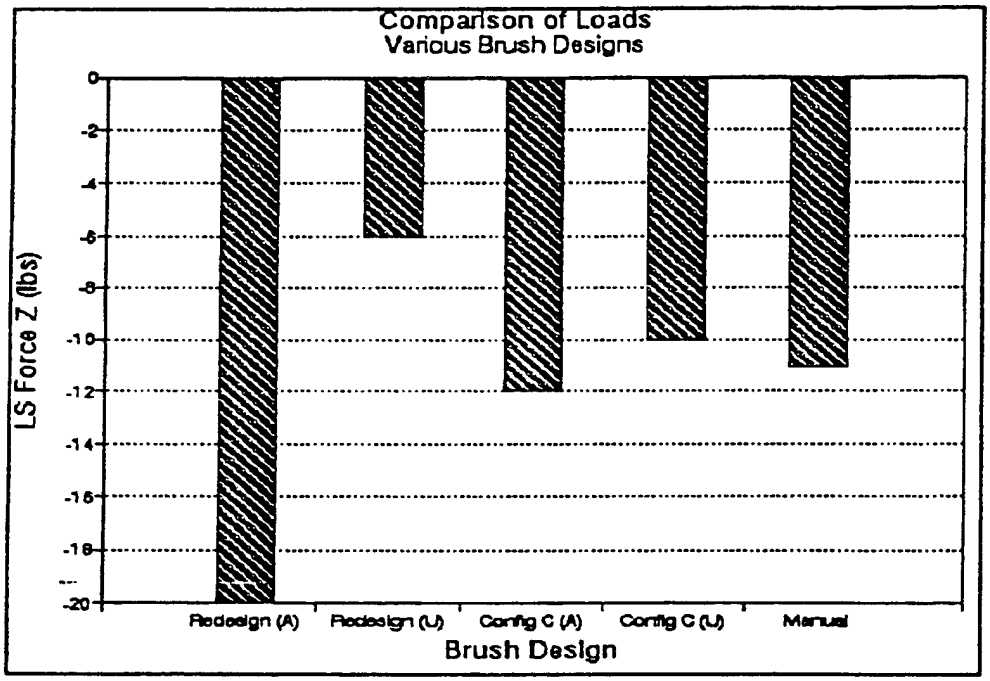

Figure C-6. Comparison of various brush configurations. Maximum force - Z at left shoulder.

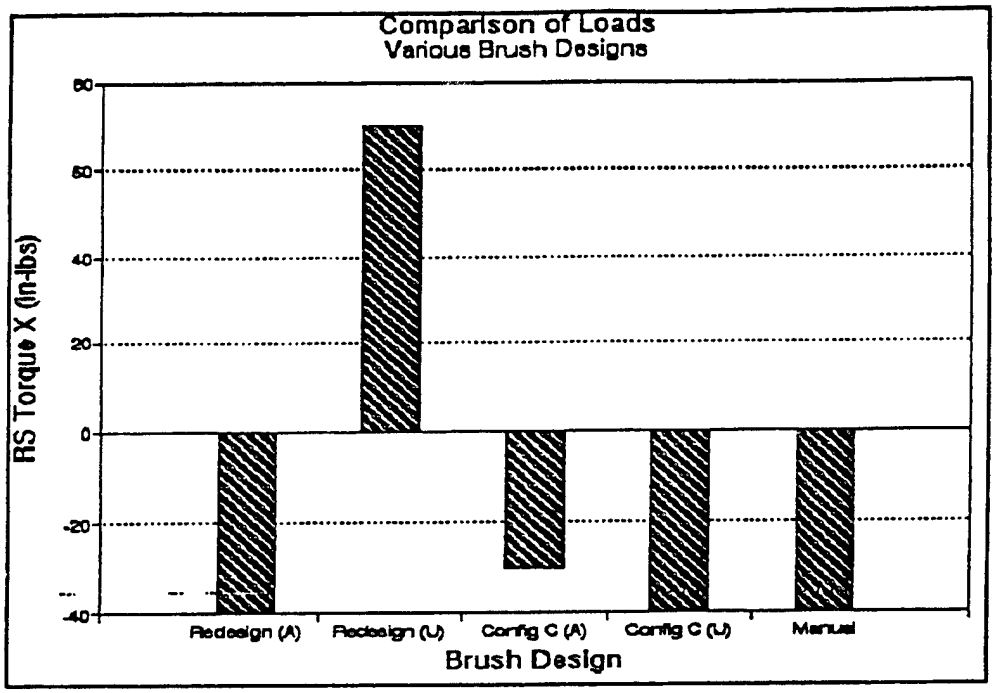

Figure C-7. Comparison of various brush configurations. Maximum torque - X at right shoulder.

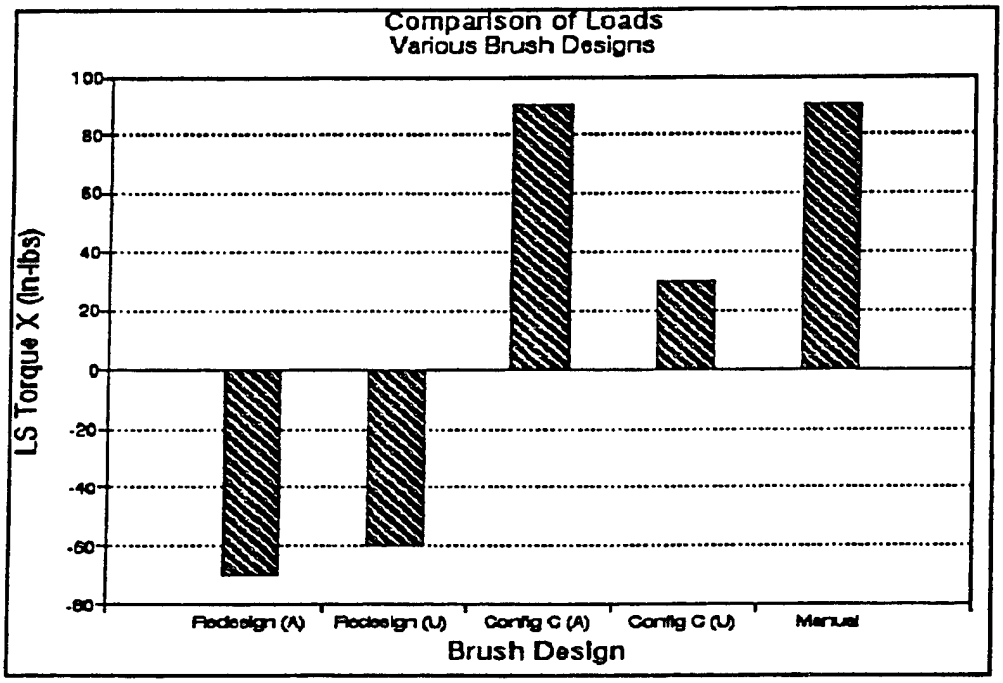

Figure C-8. Comparison of various brush configurations. Maximum torque - X at left shoulder.

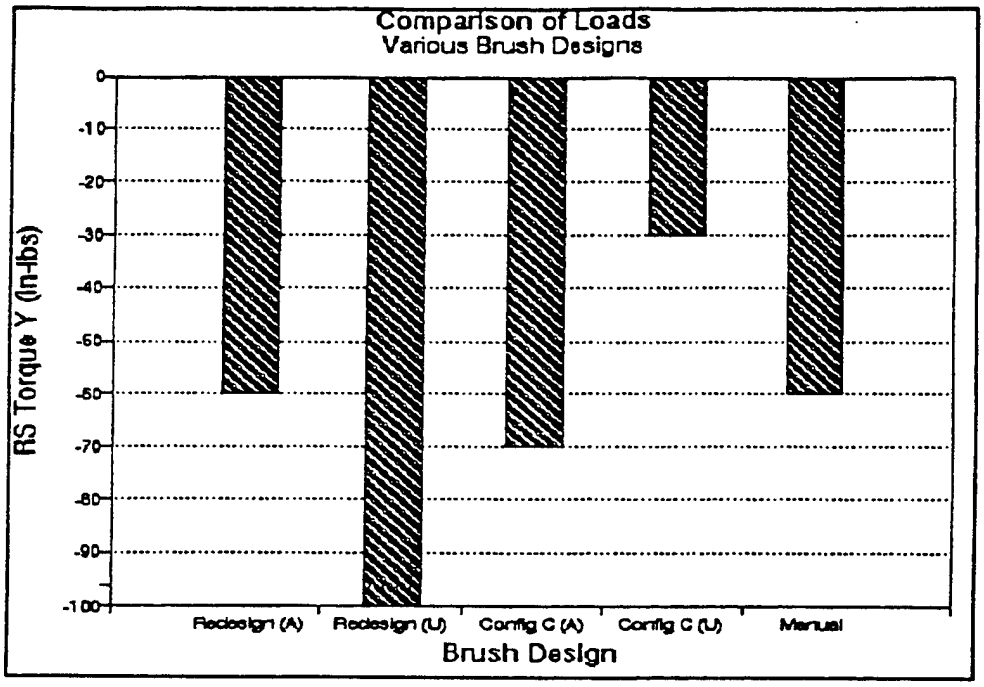

Figure C-9. Comparison of various brush configurations. Maximum torque - Y at right shoulder.

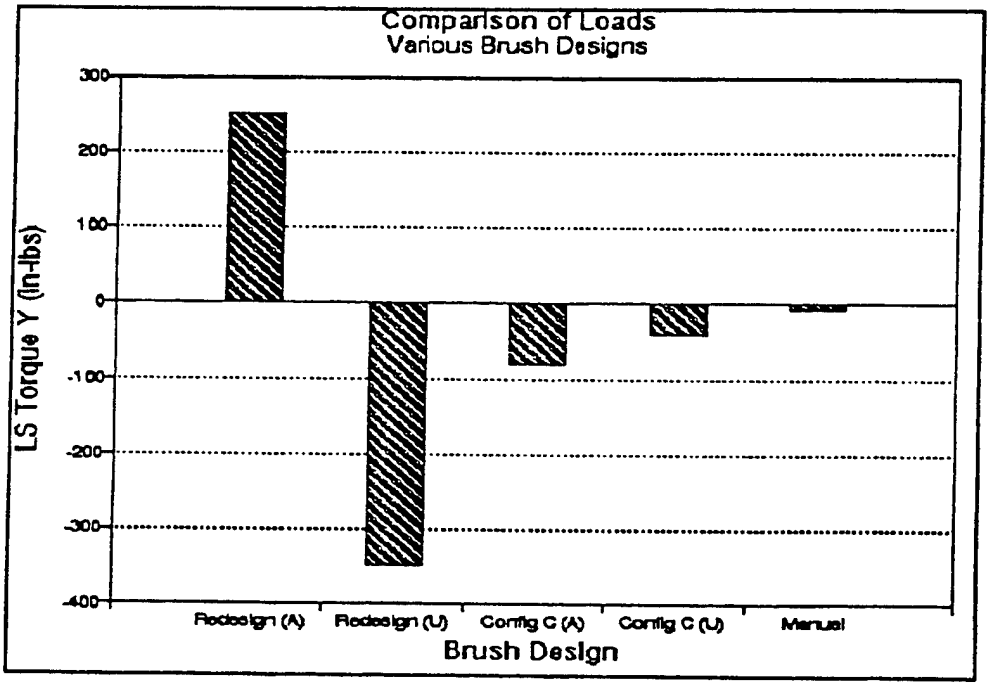

Figure C-10. Comparison of various brush configurations. Maximum torque - Y at left shoulder.

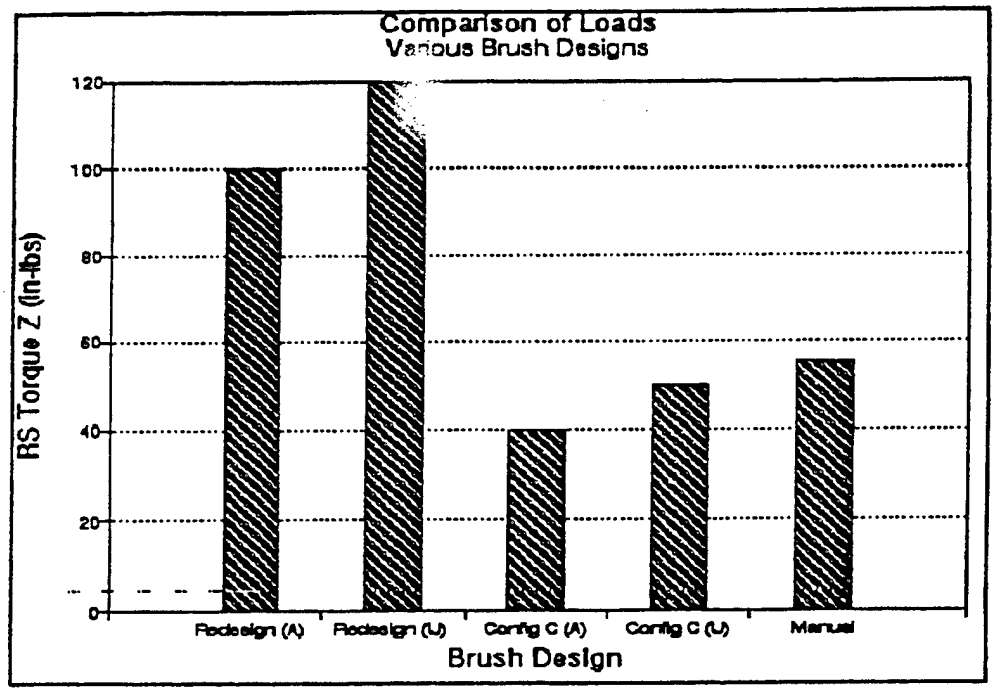

Figure C-11. Comparison of various brush configurations. Maximum torque - Z at right shoulder.

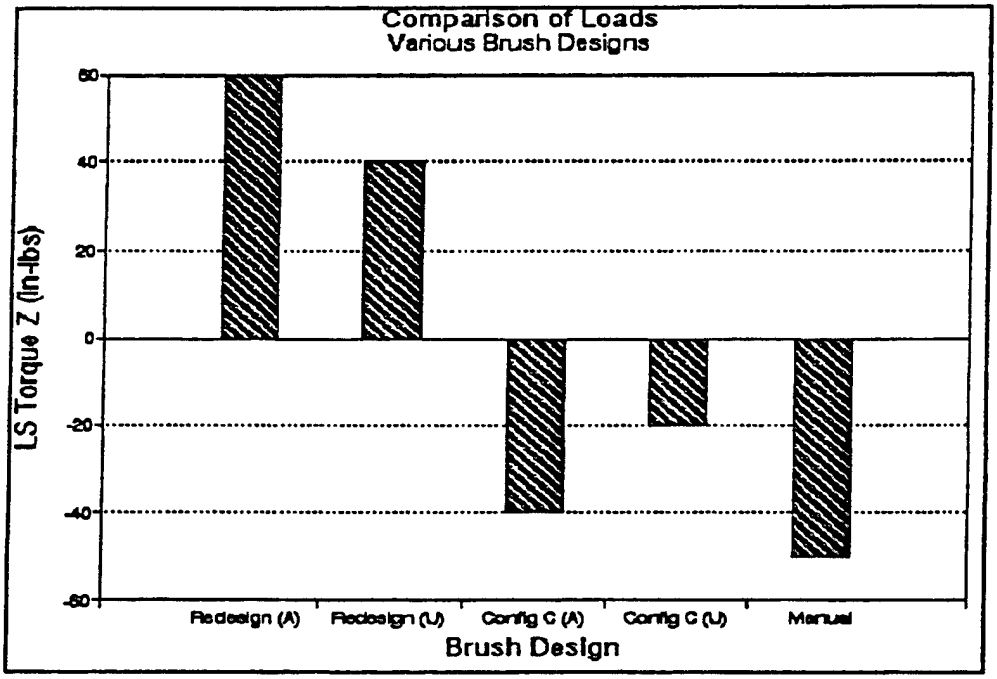

Figure C-12. Comparison of various brush configurations. Maximum torque - Z at left shoulder.

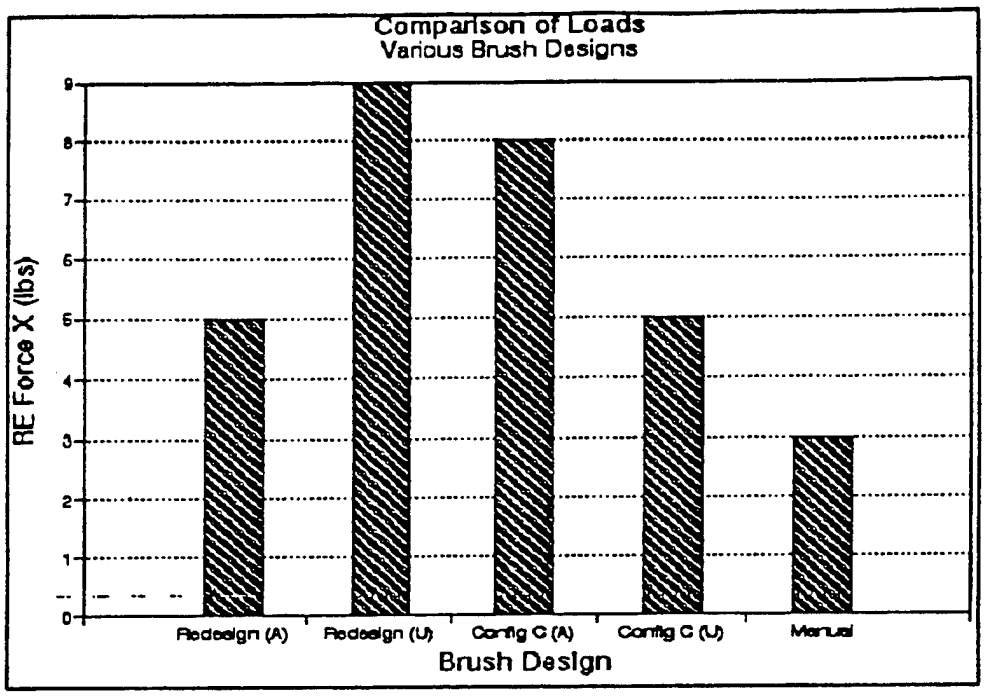

Figure C-13. Comparison of various brush configurations. Maximum force - X at right elbow.

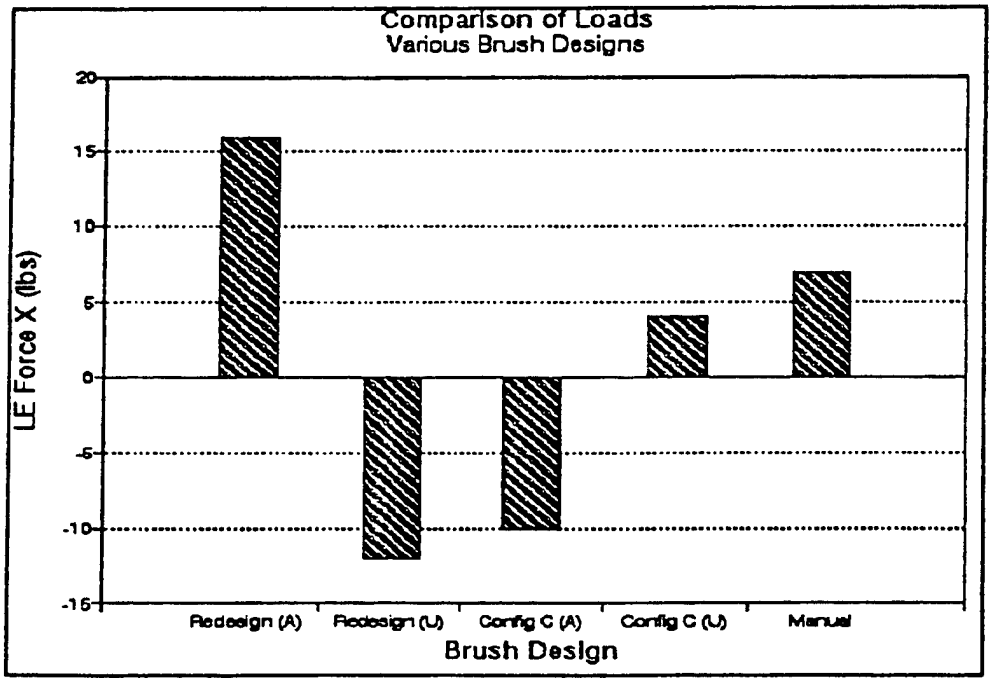

Figure C-14. Comparison of various brush configurations. Maximum force - X at left elbow.

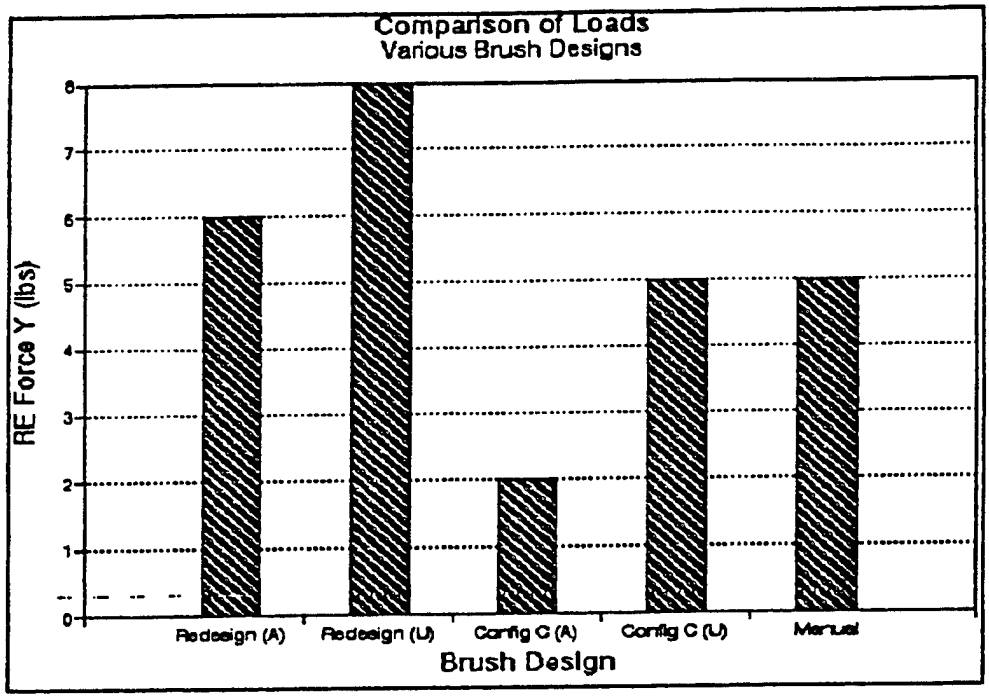

Figure C-15. Comparison of various brush configurations. Maximum force - Y at right elbow.

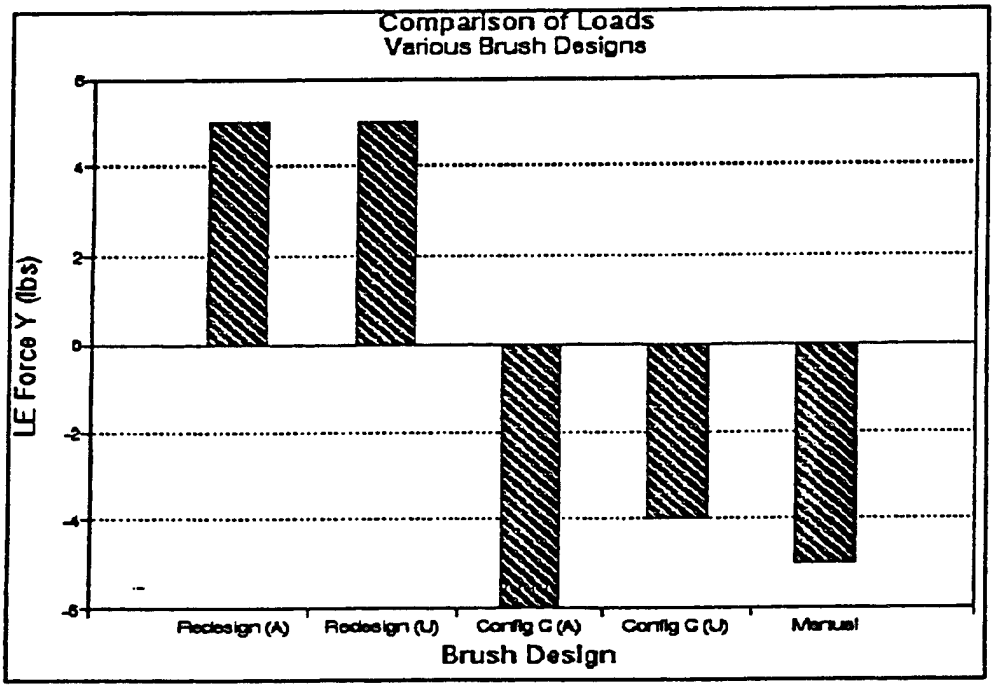

Figure C-16. Comparison of various brush configurations. Maximum force - Y at left elbow.

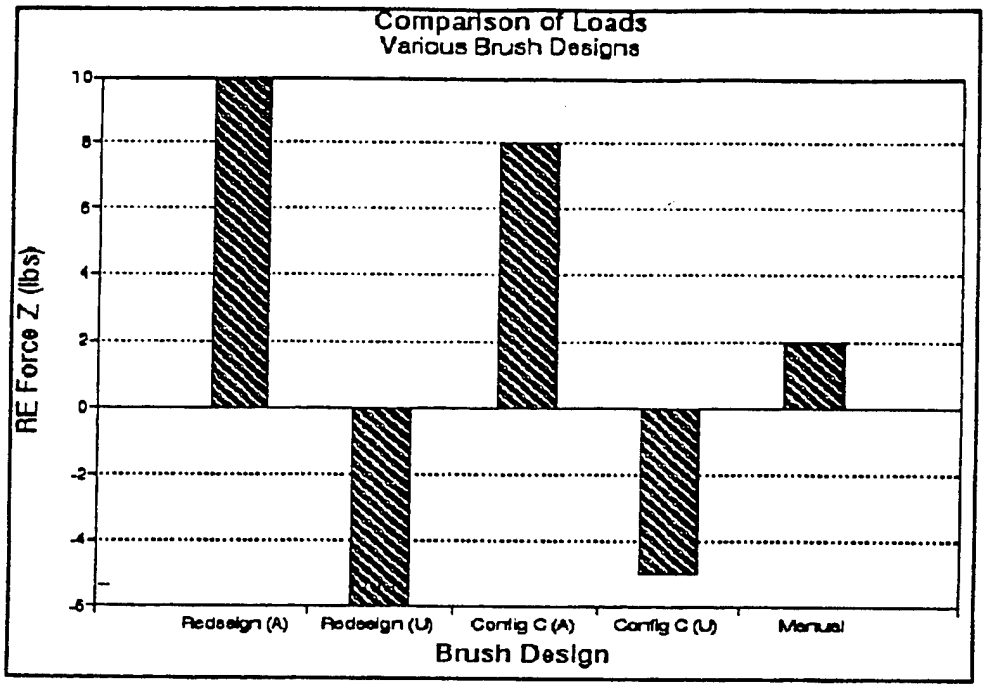

Figure C-17. Comparison of various brush configurations. Maximum force - Z at right elbow.

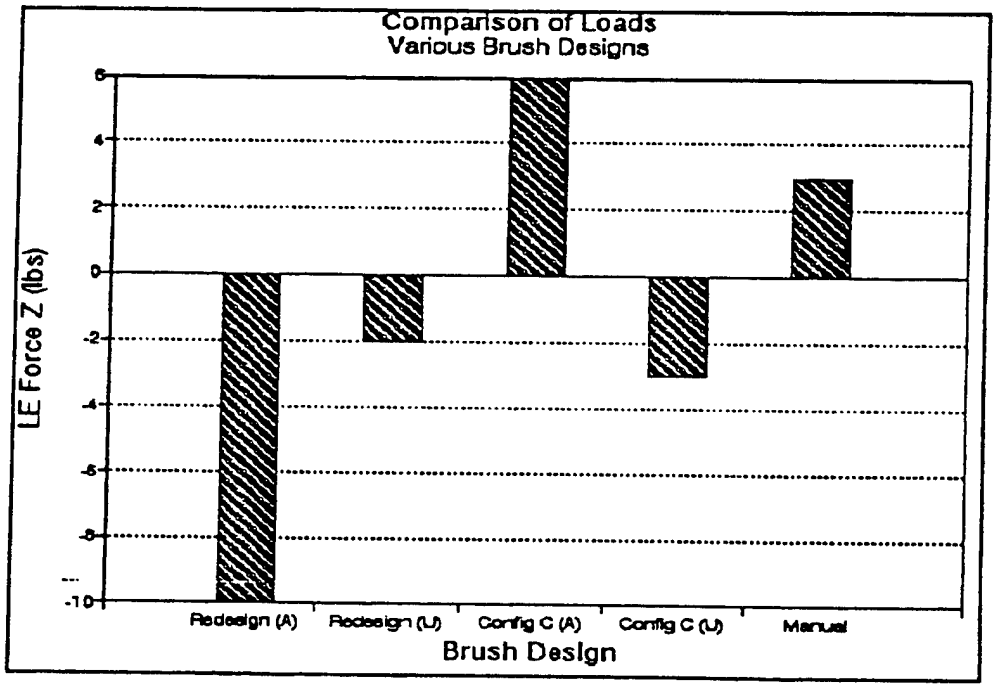

Figure C-18. Comparison of various brush configurations. Maximum force - Z at left elbow.

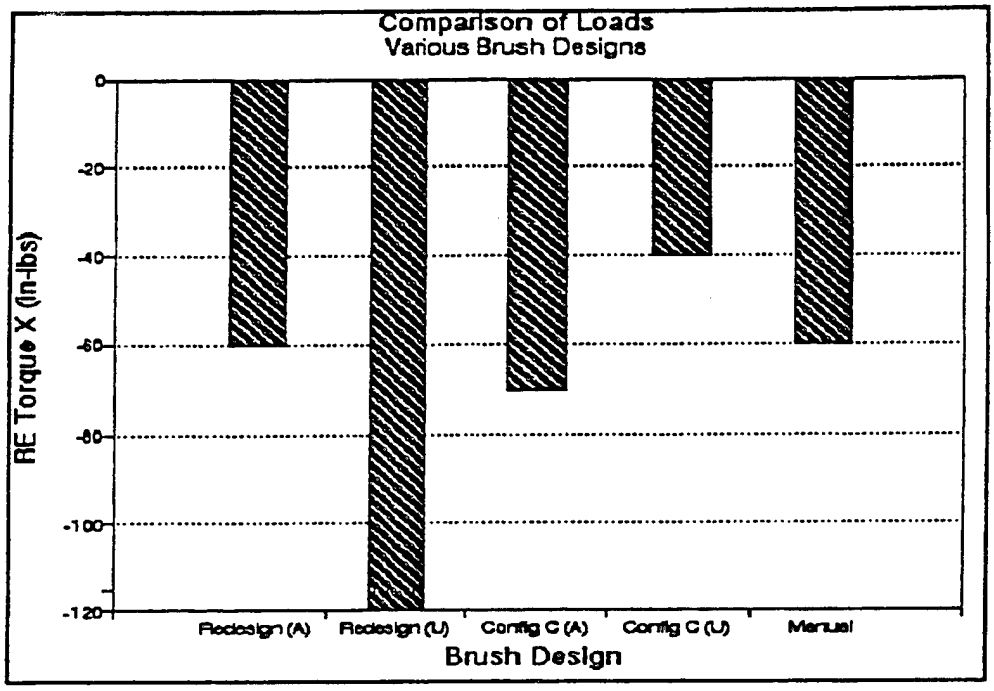

Figure C-19. Comparison of various brush configurations. Maximum torque - X at right elbow.

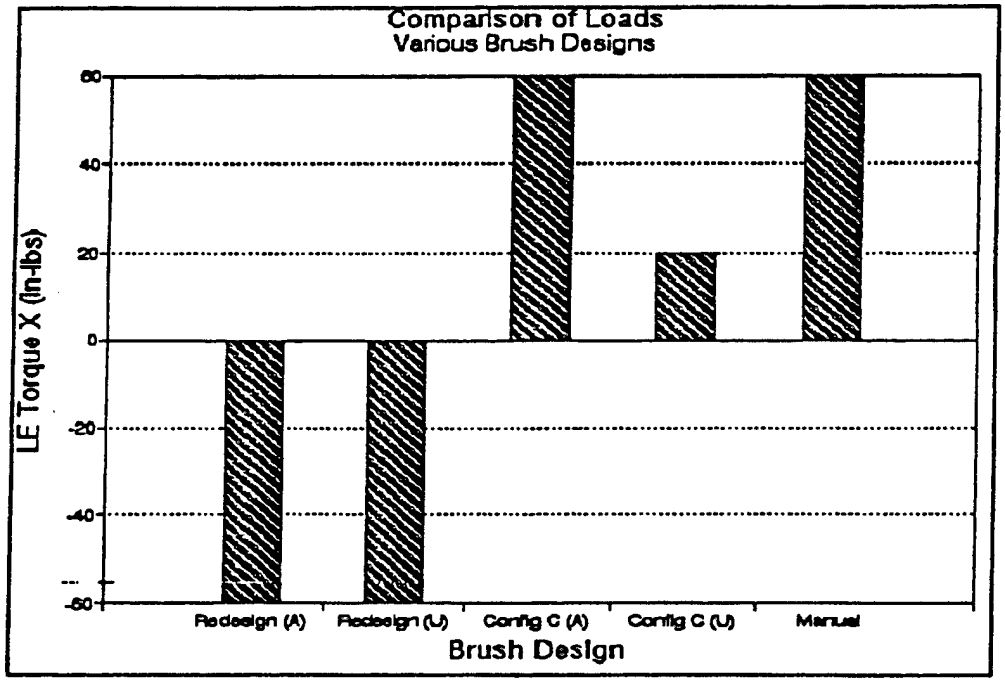

Figure C-20. Comparison of various brush configurations. Maximum torque - X at left elbow.

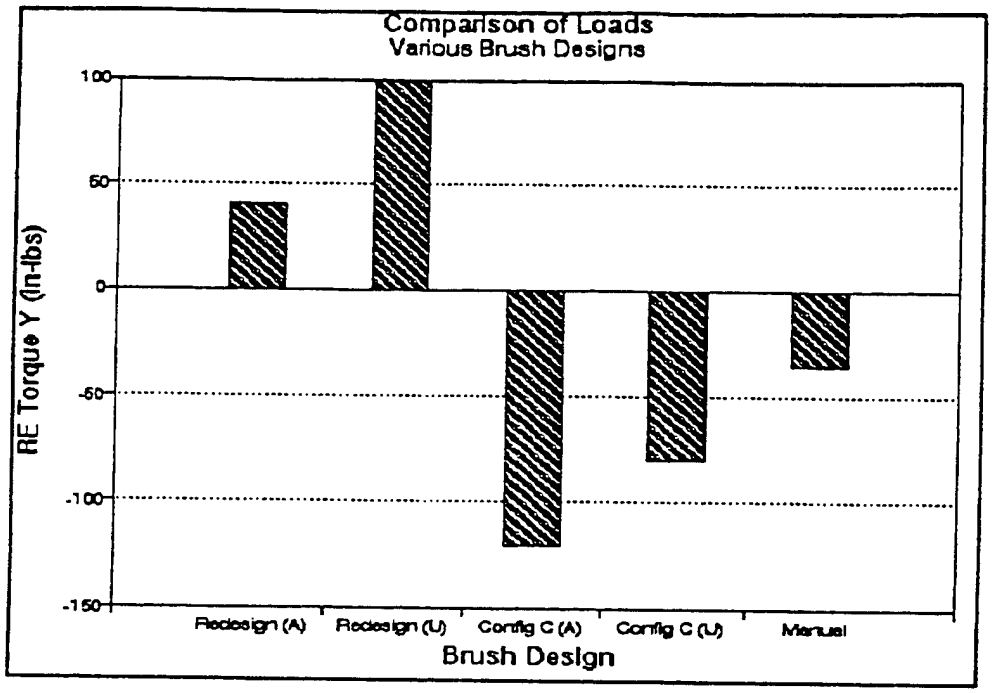

Figure C-21. Comparison of various brush configurations. Maximum torque - Y at right elbow.

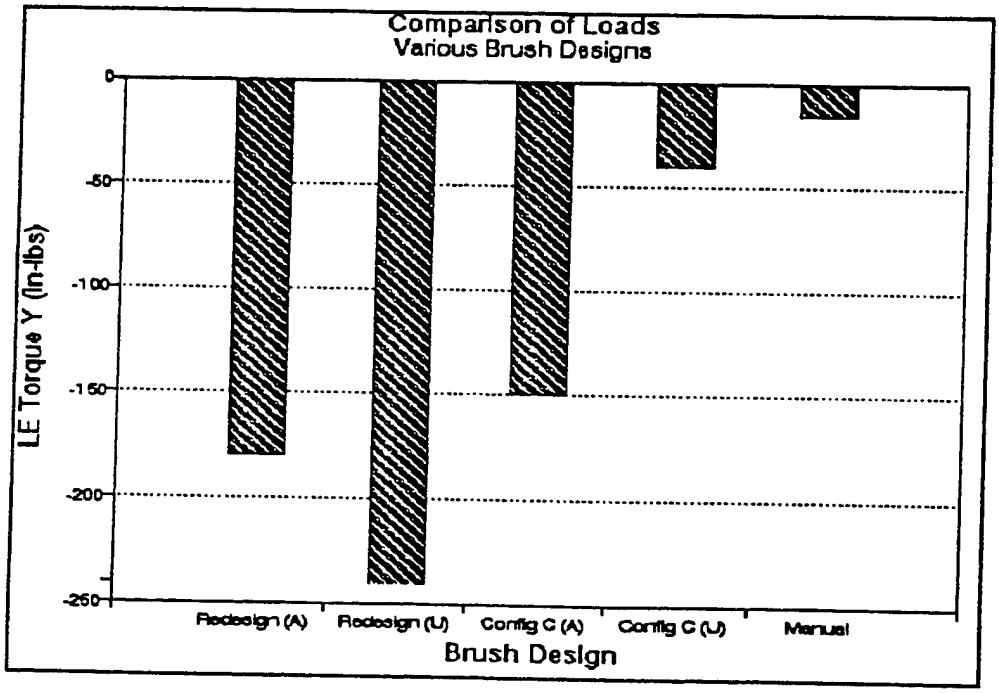

Figure C-22. Comparison of various brush configurations. Maximum torque - Y at left elbow.

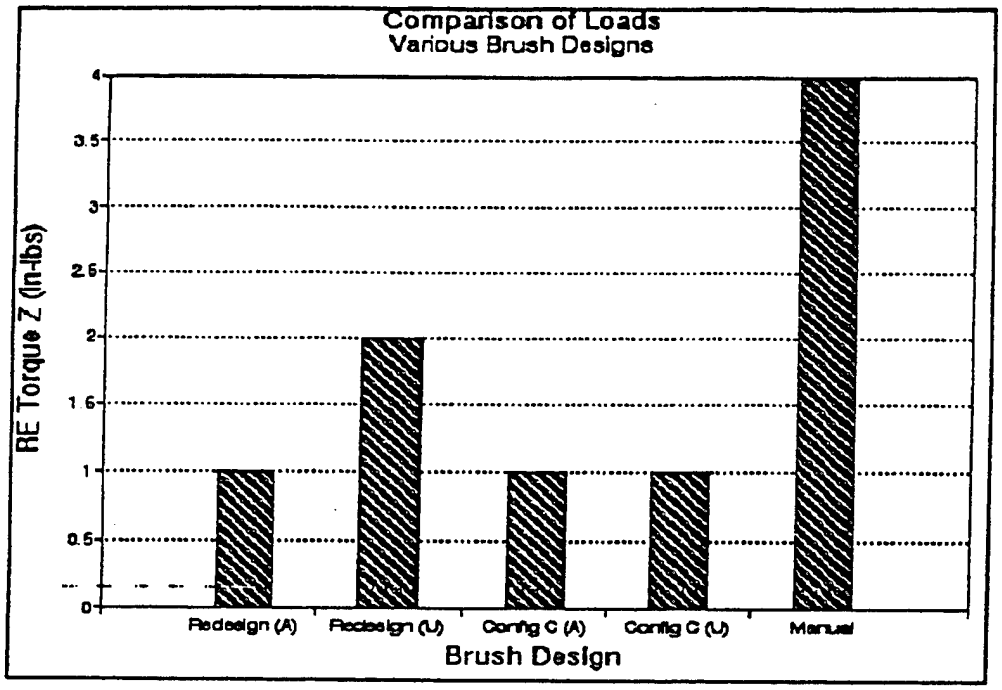

Figure C-23. Comparison of various brush configurations. Maximum torque - Z at right elbow.

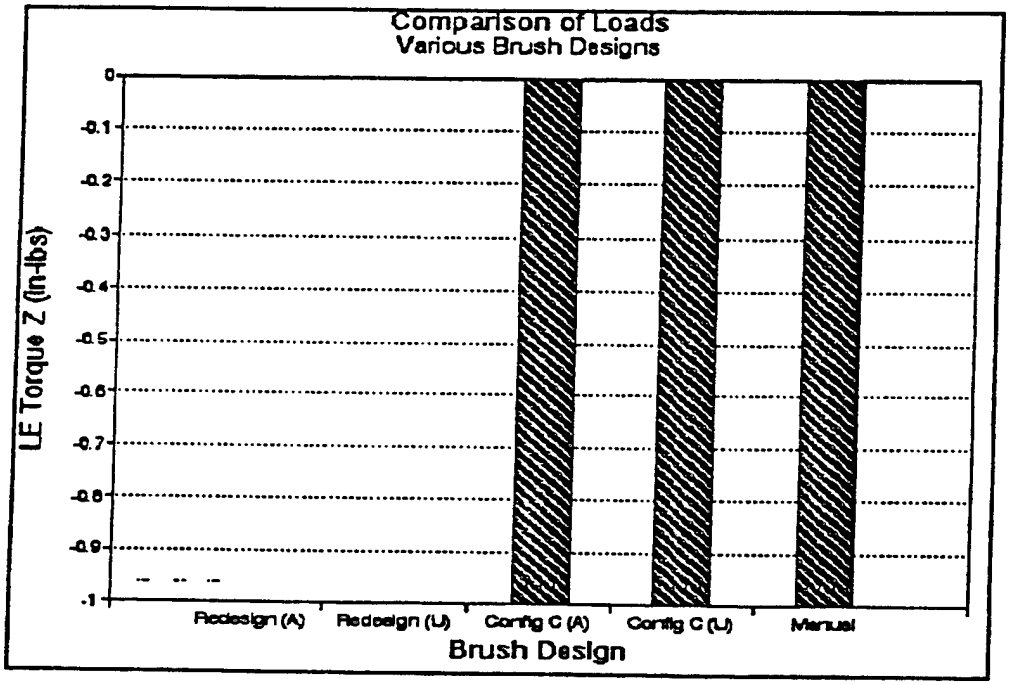

Figure C-24. Comparison of various brush configurations. Maximum torque - Z at left elbow.

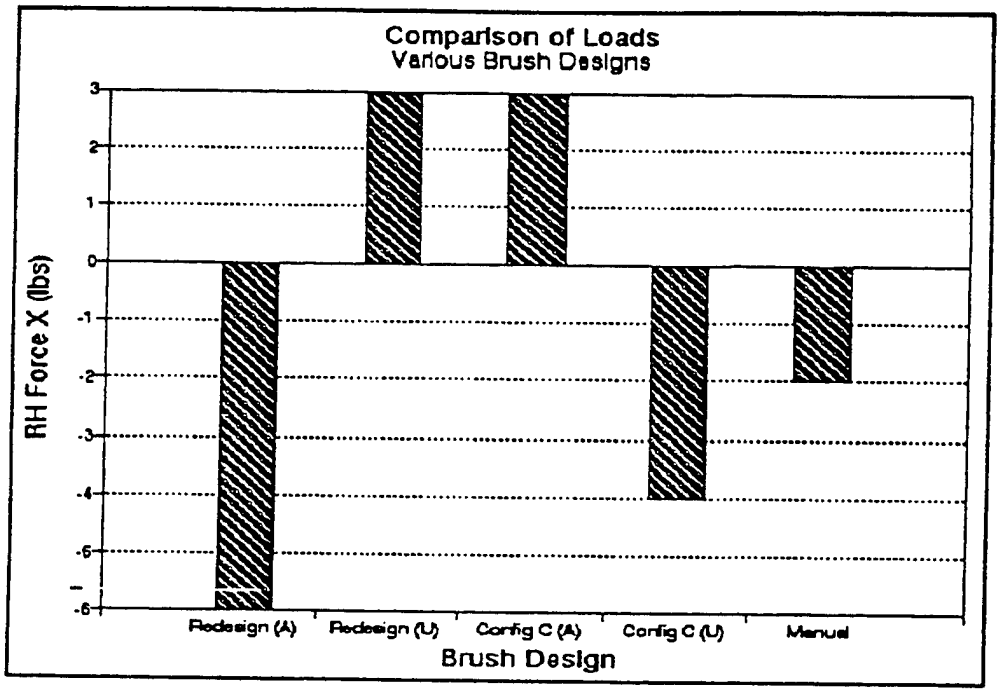

Figure C-25. Comparison of various brush configurations. Maximum force - X at right hip.

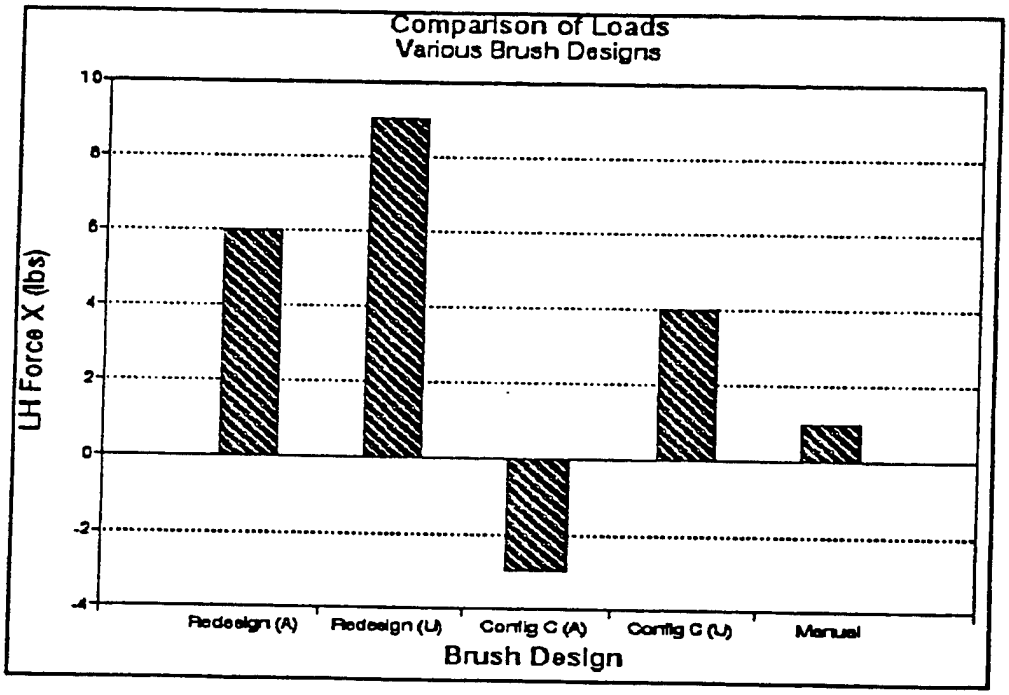

Figure C-26. Comparison of various brush configurations. Maximum force - X at left hip.

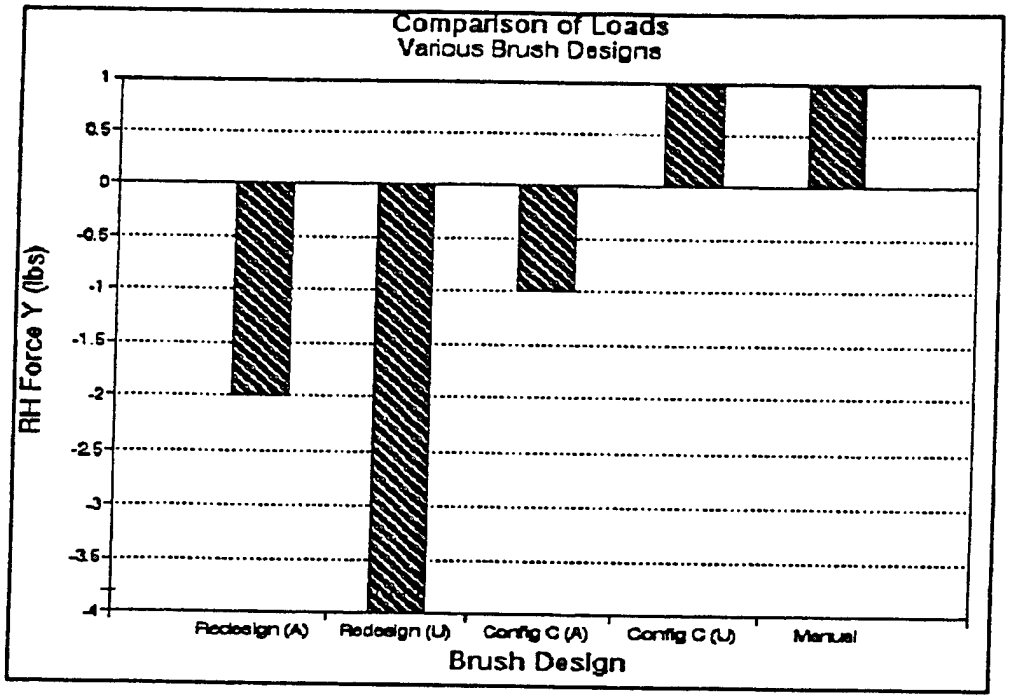

Figure C-27. Comparison of various brush configurations. Maximum force - Y at right hip.

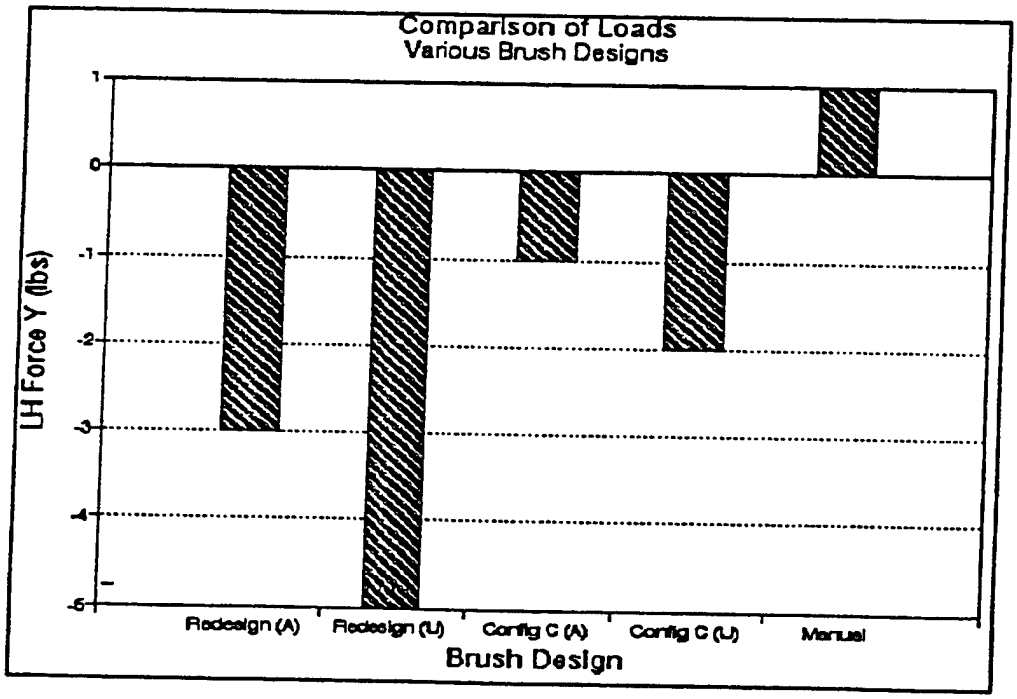

Figure C-28. Comparison of various brush configurations. Maximum force - Y at left hip.

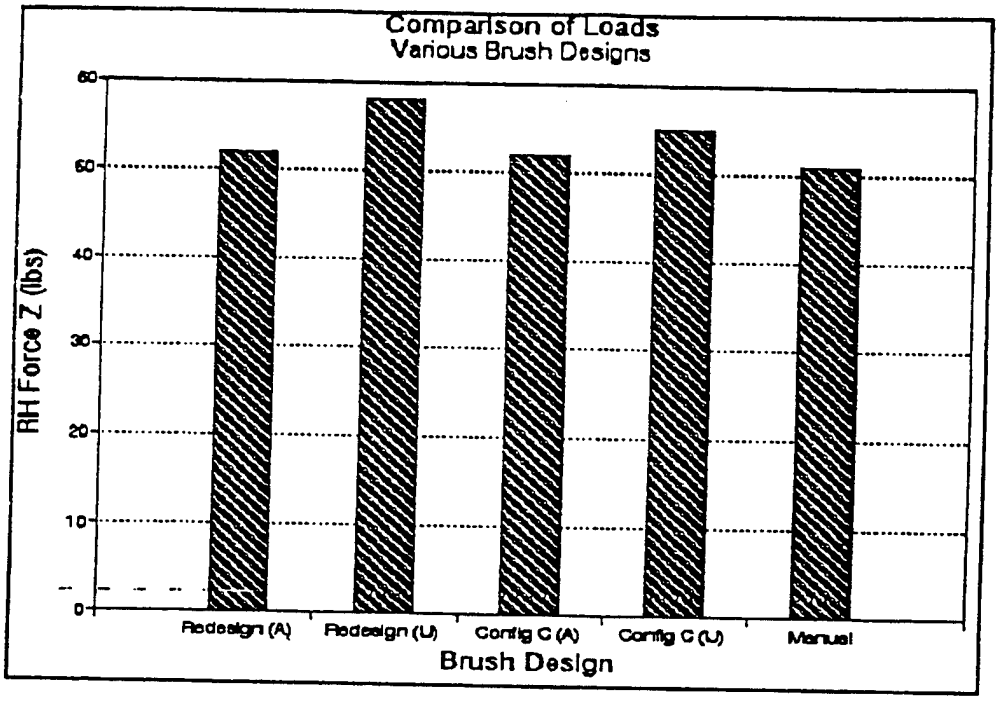

Figure C-29. Comparison of various brush configurations. Maximum force - Z at right hip.

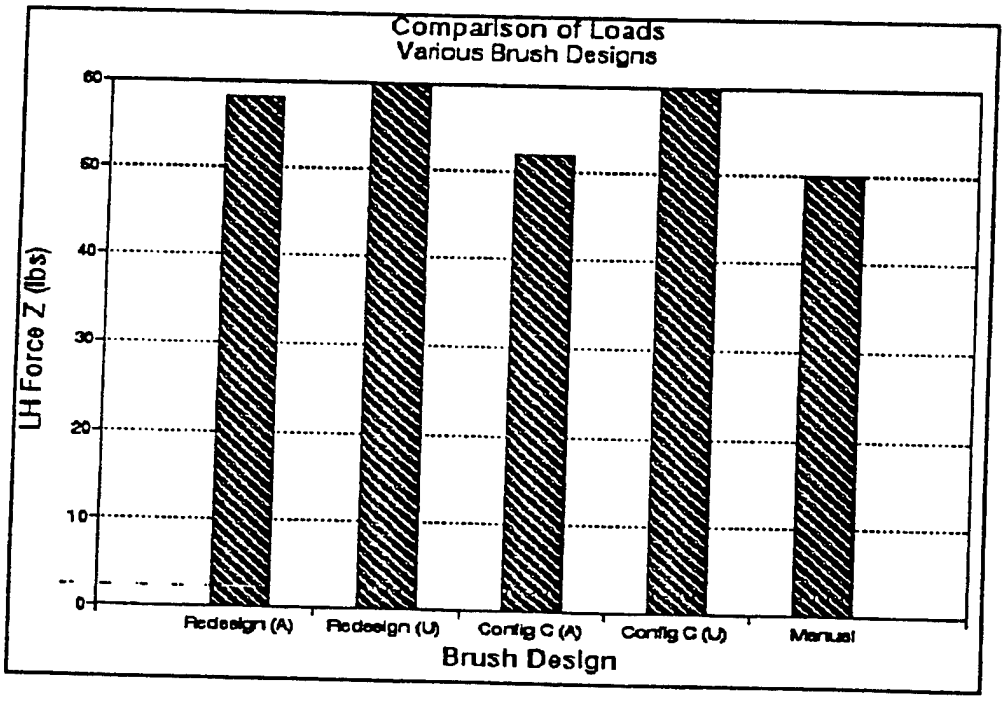

Figure C-30. Comparison of various brush configurations. Maximum force - Z at left hip.

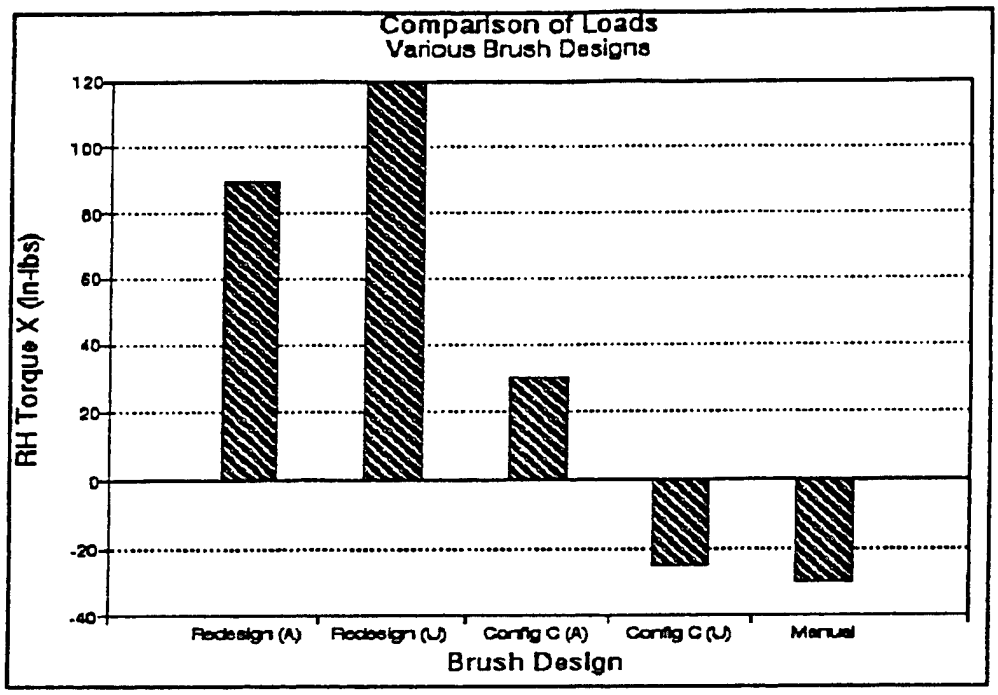

Figure C-31. Comparison of various brush configurations. Maximum torque - X at right hip.

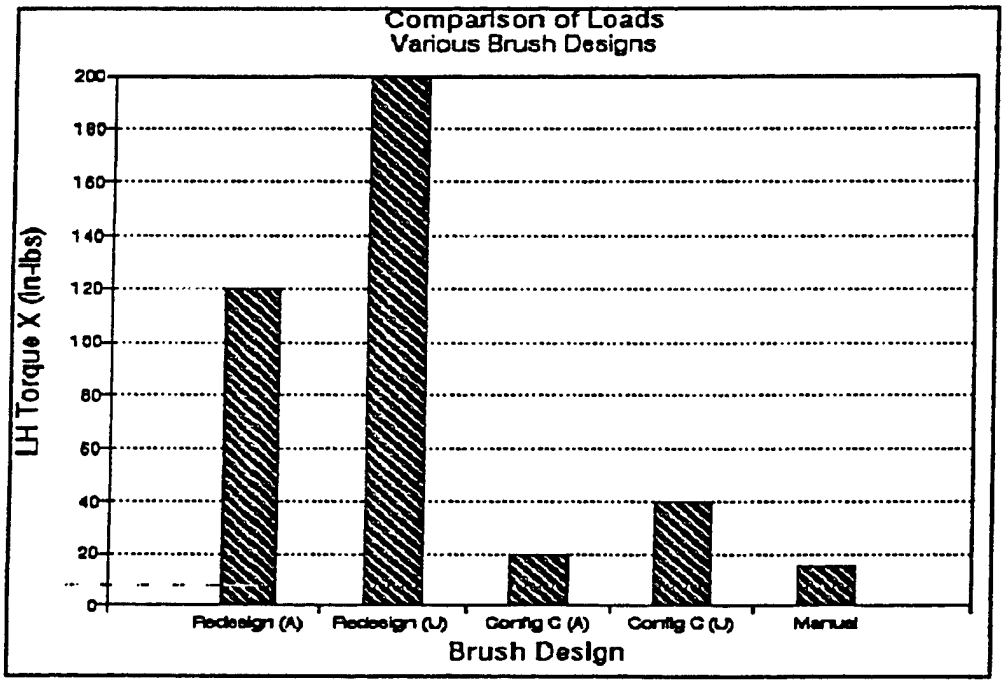

Figure C-32. Comparison of various brush configurations. Maximum torque - X at left hip.

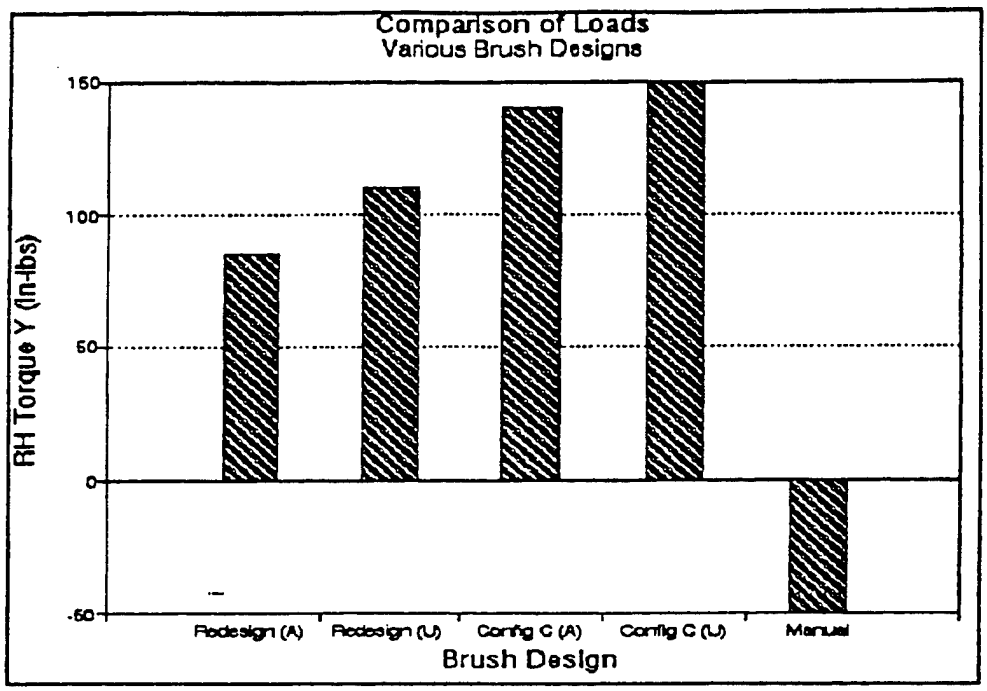

Figure C-33. Comparison of various brush configurations. Maximum torque - Y at right hip.

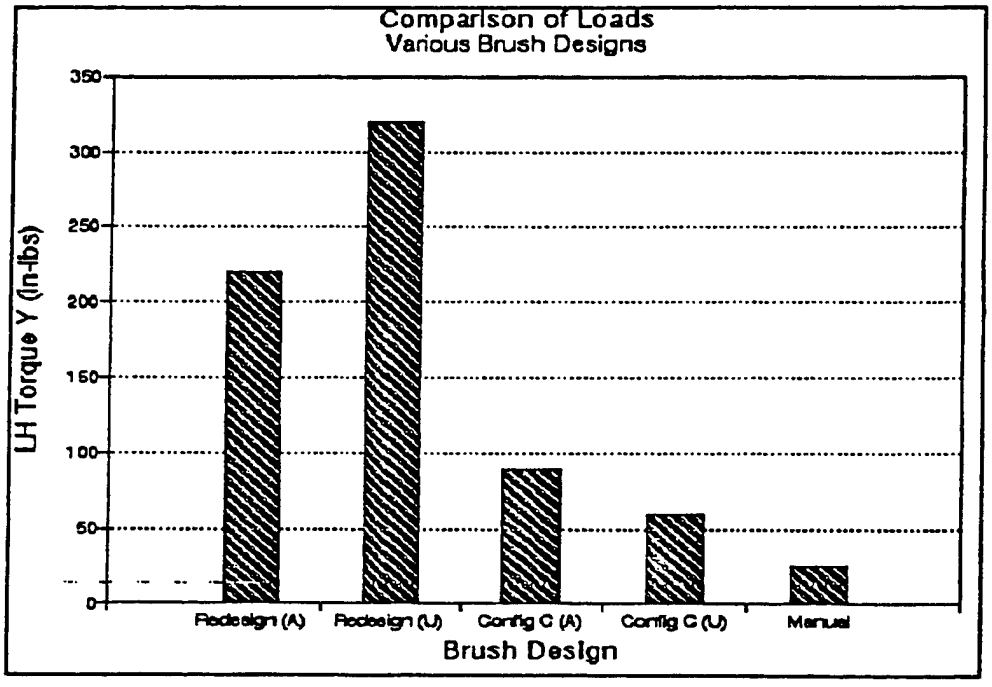

Figure C-34. Comparison of various brush configurations. Maximum torque - Y at left hip.

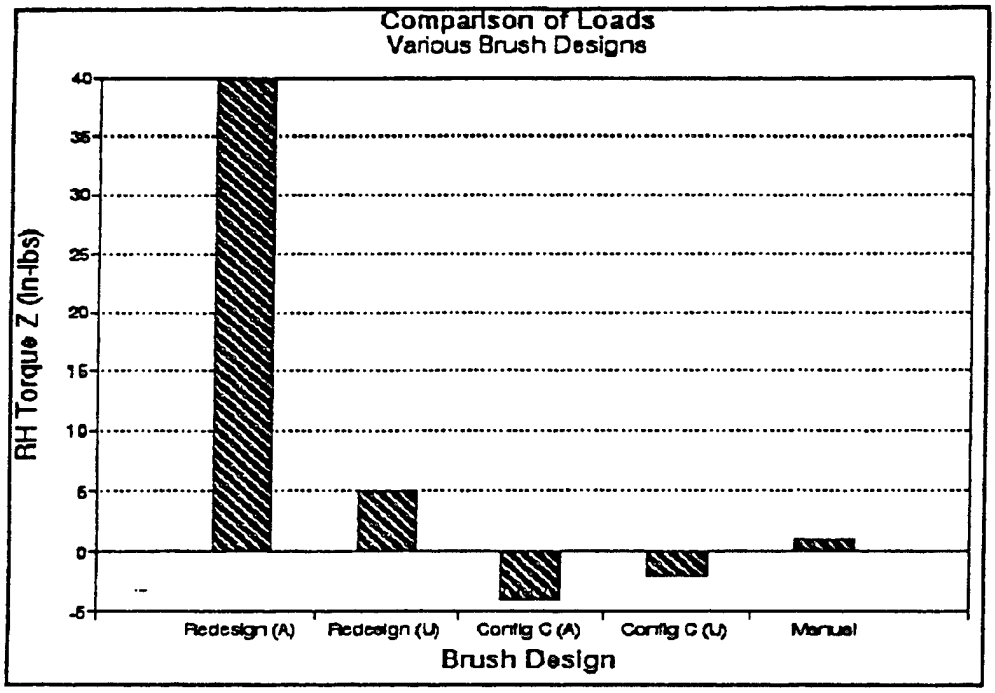

Figure C-35. Comparison of various brush configurations. Maximum torque - Z at right hip.

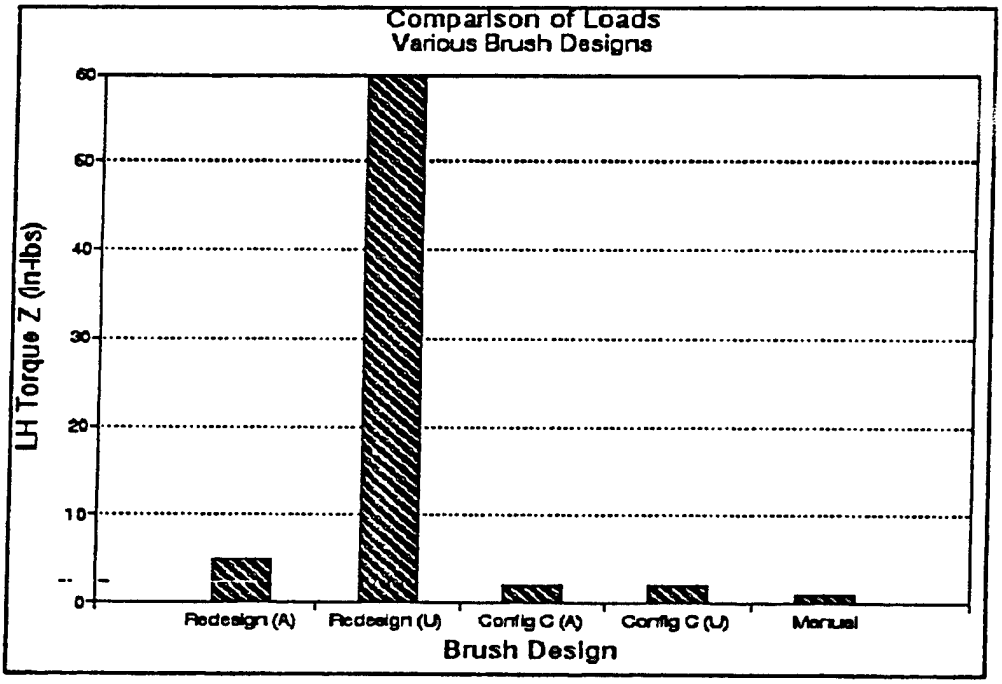

Figure C-36. Comparison of various brush configurations. Maximum torque - Z at left hip.

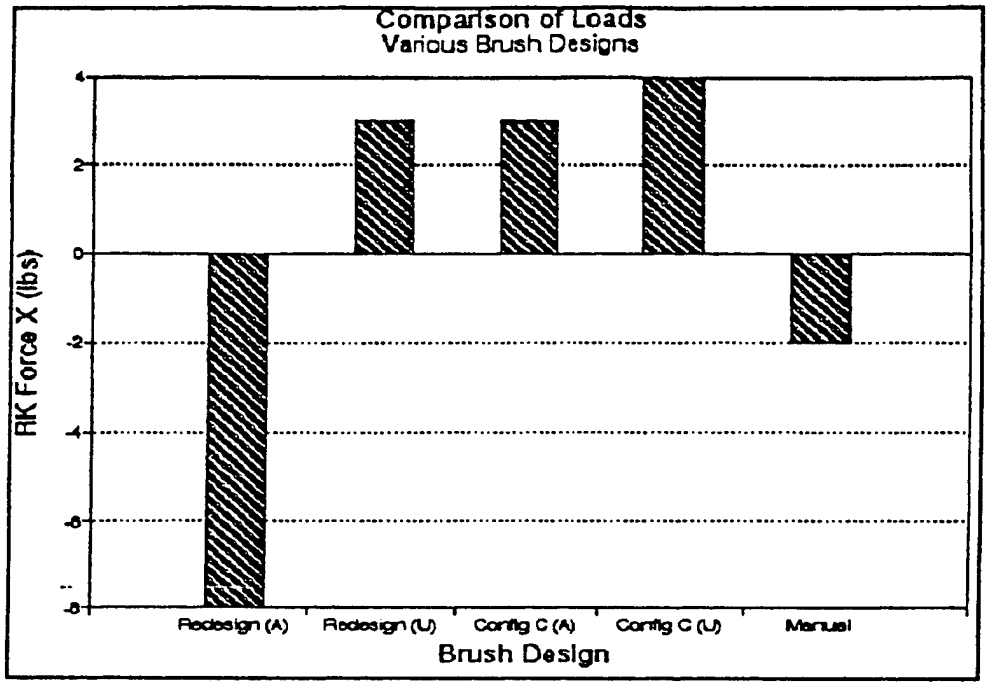

Figure C-37. Comparison of various brush configurations. Maximum force - X at right knee.

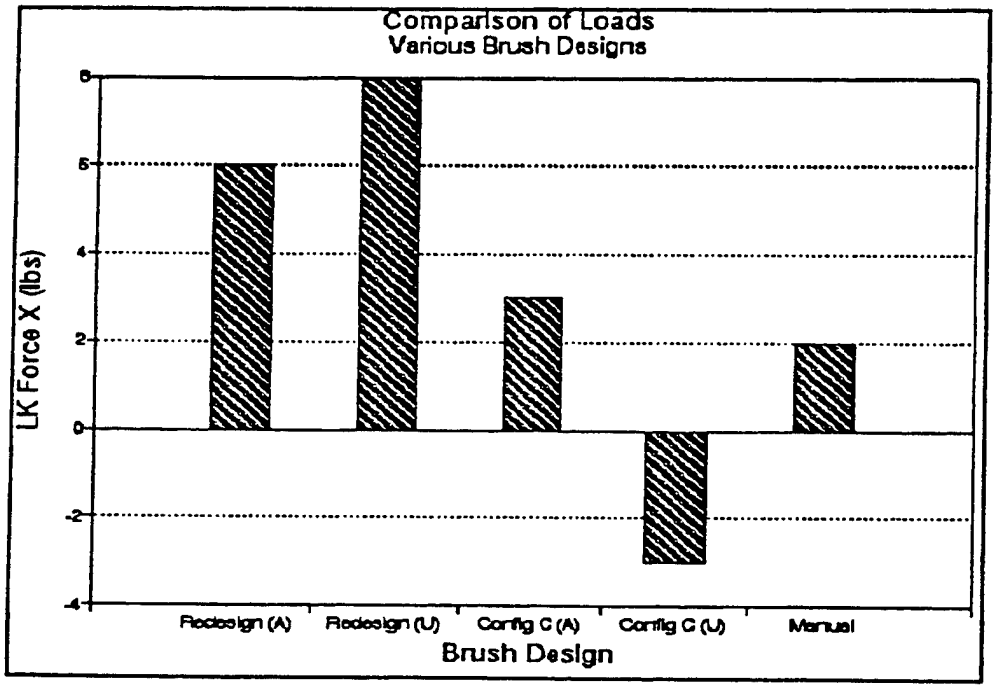

Figure C-38. Comparison of various brush configurations. Maximum force - X at left knee.

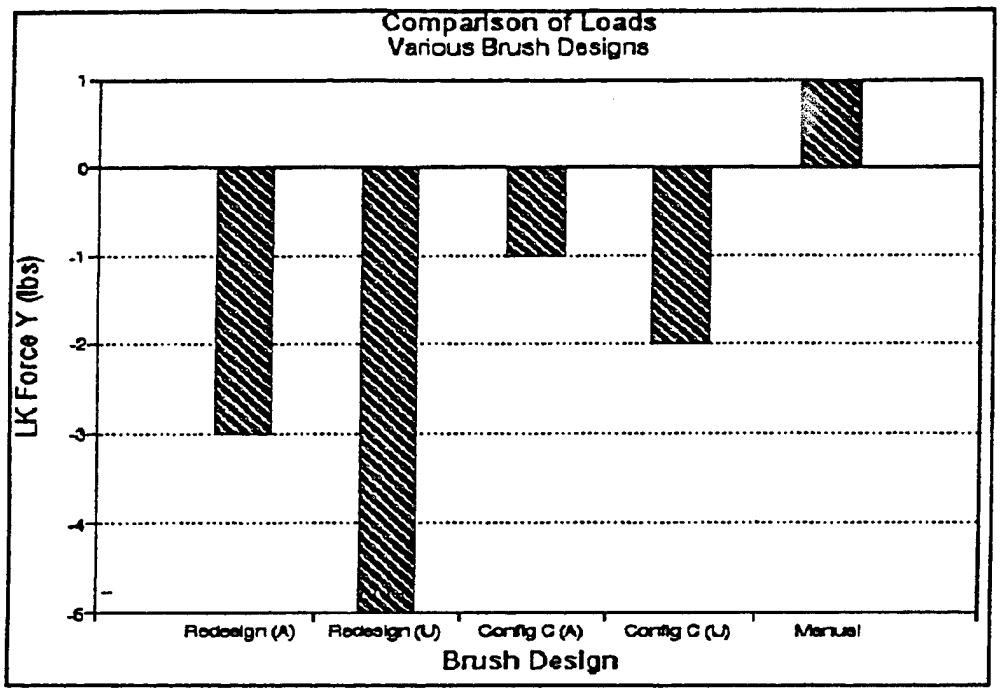

Figure C-39. Comparison of various brush configurations. Maximum force - Y at right knee.

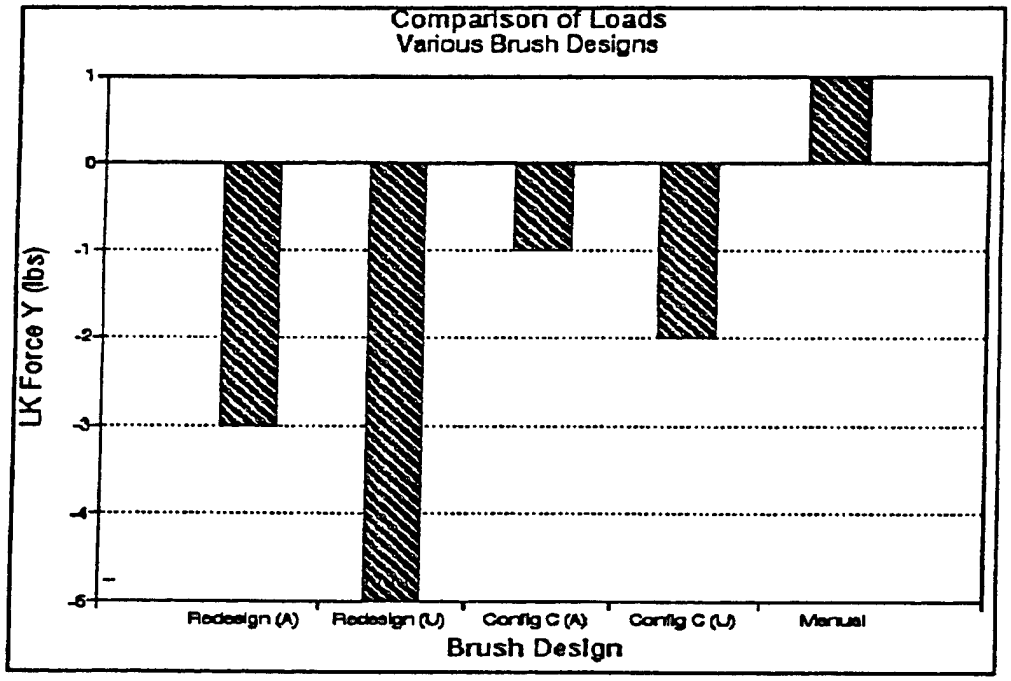

Figure C-40. Comparison of various brush configurations. Maximum force - Y at left knee.

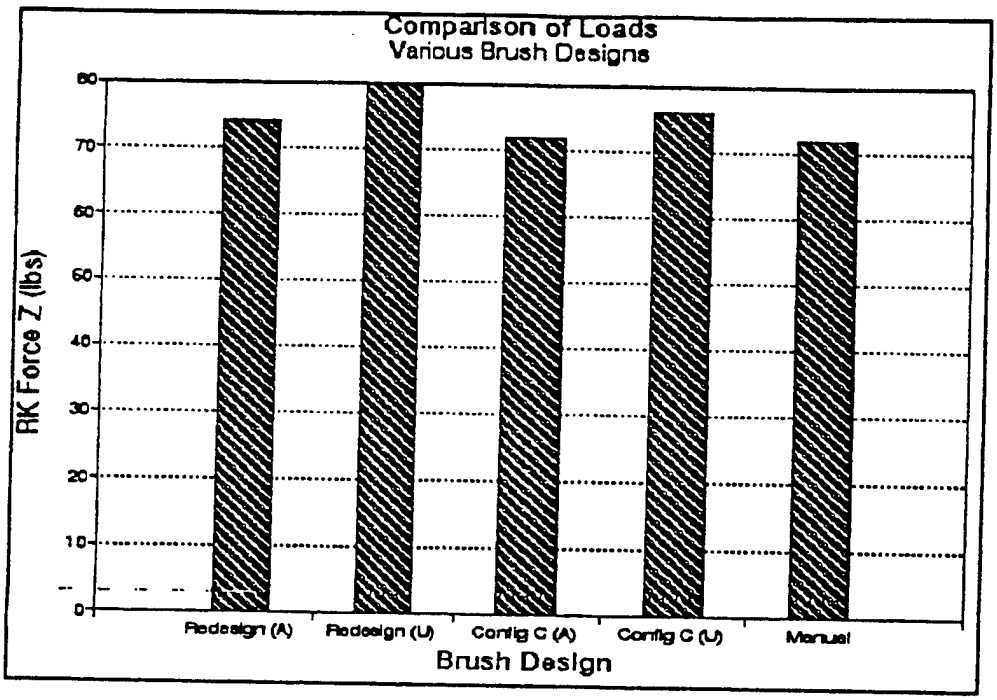

Figure C-41. Comparison of various brush configurations. Maximum force - Z at right knee.

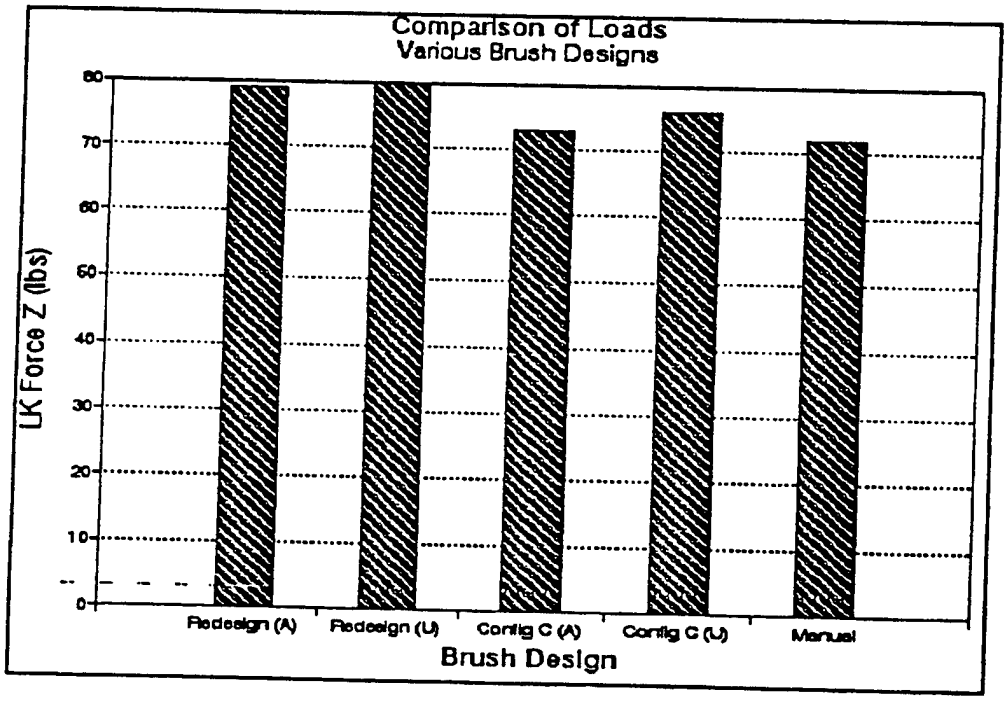

Figure C-42. Comparison of various brush configurations. Maximum force - Z at left knee.

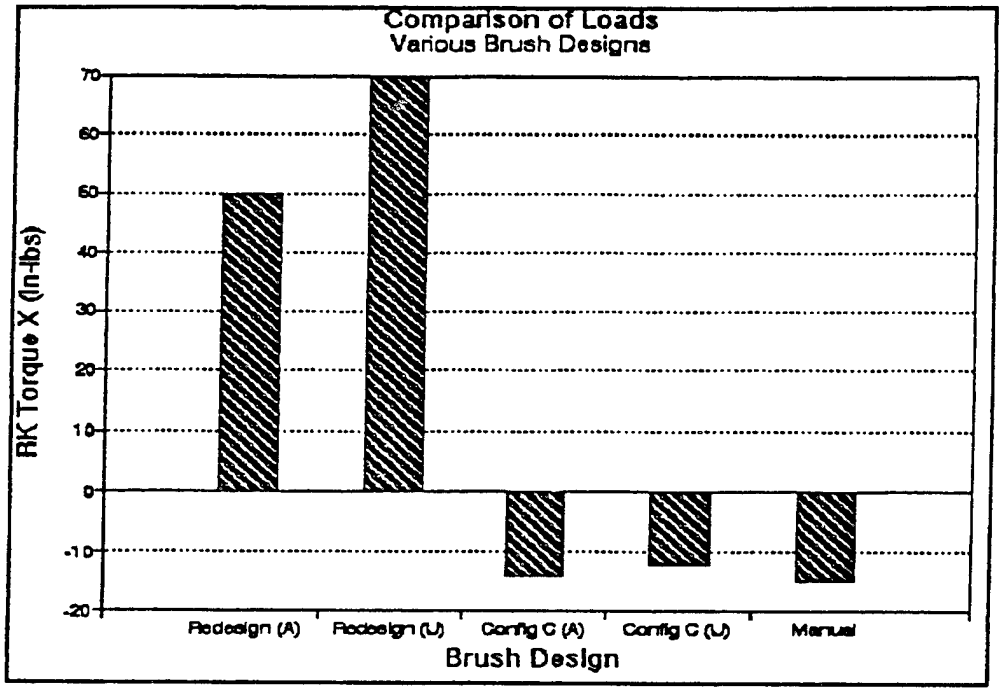

Figure C-43. Comparison of various brush configurations. Maximum torque - X at right knee.

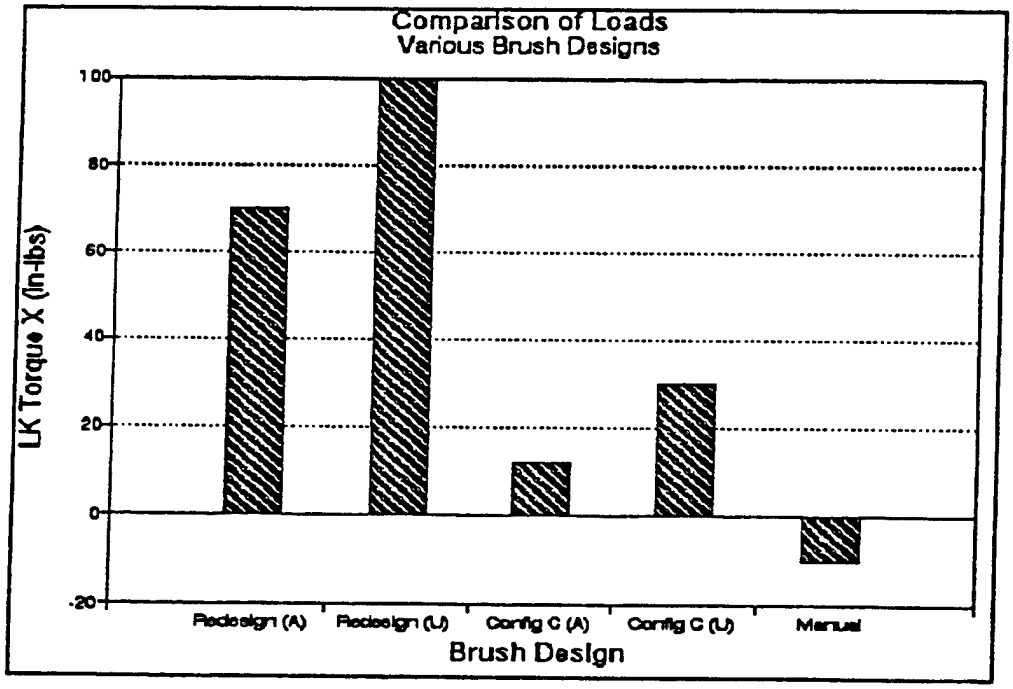

Figure C-44. Comparison of various brush configurations. Maximum torque - X at left knee.

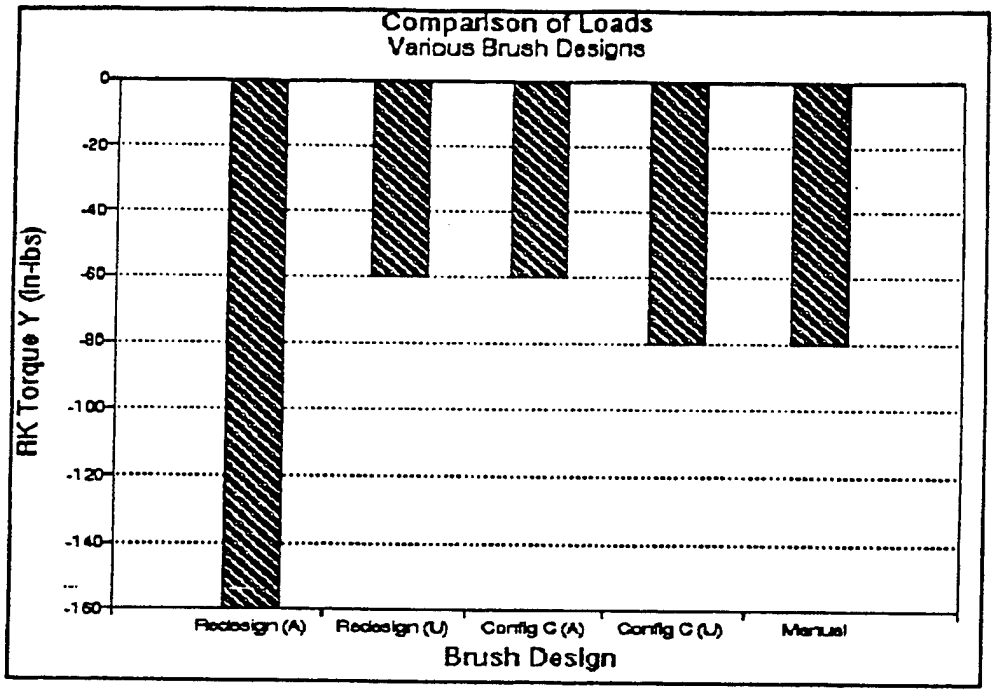

Figure C-45. Comparison of various brush configurations. Maximum torque - Y at right knee.

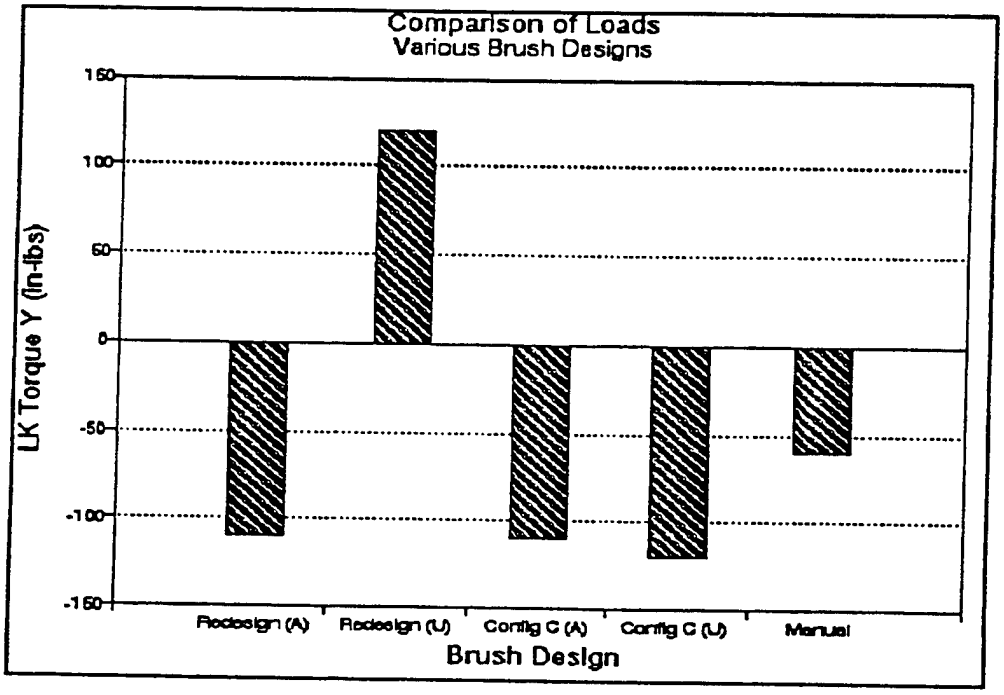

Figure C-46. Comparison of various brush configurations. Maximum torque - Y at left knee.

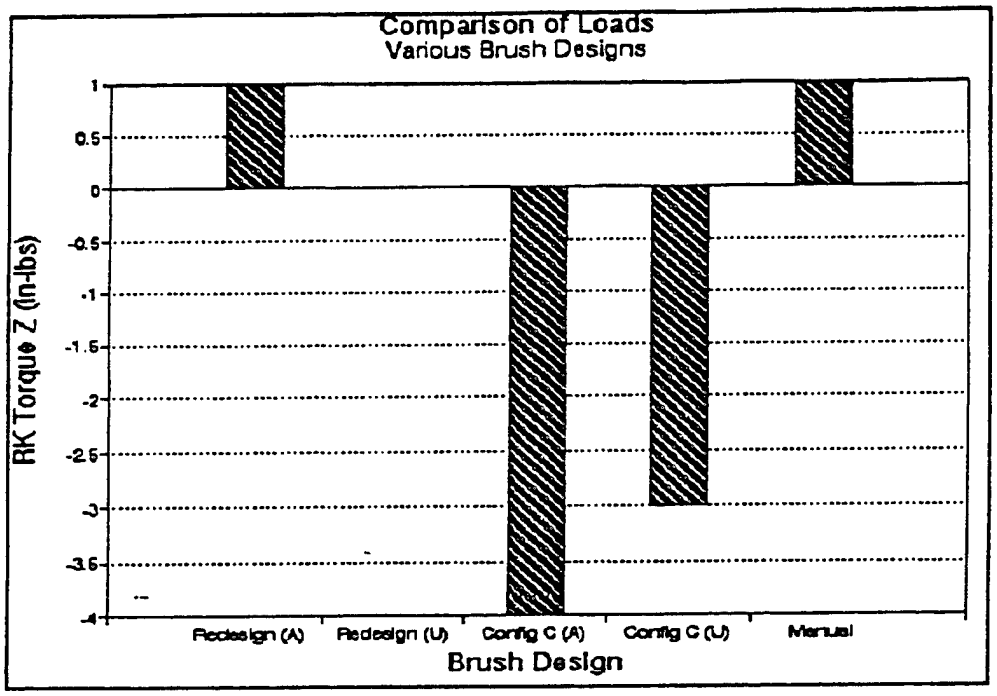

Figure C-47. Comparison of various brush configurations. Maximum torque - Z at right knee.

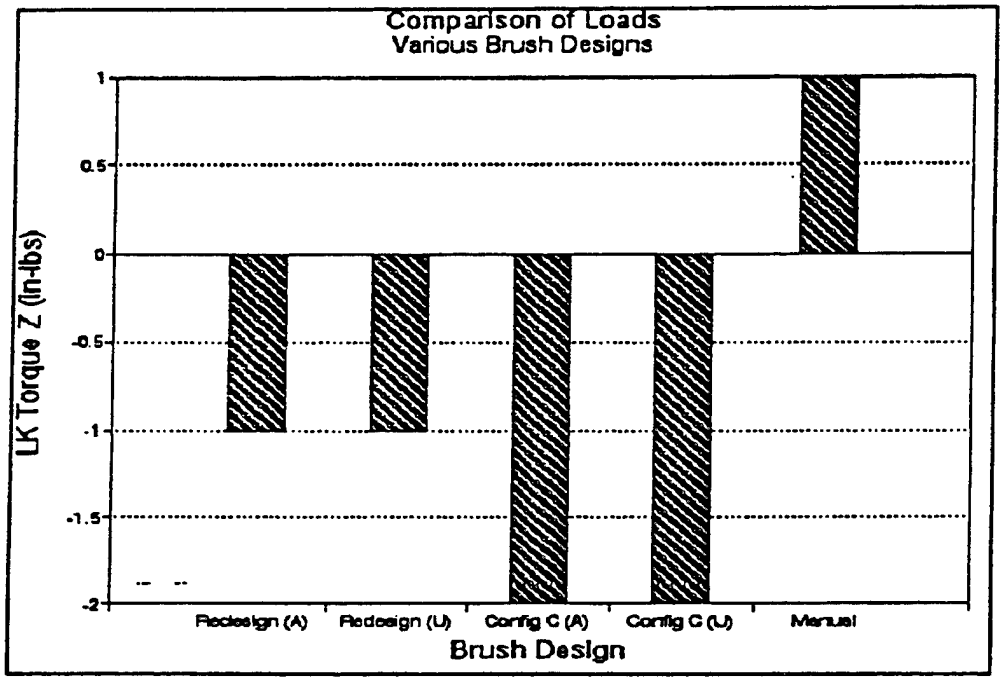

Figure C-48. Comparison of various brush configurations. Maximum torque - Z at left knee.

NO. OF COPIES	ORGANIZATION
2	ADMINISTRATOR DEFENSE TECHNICAL INFO CENTER ATTN DTIC DDA 8725 JOHN J KINGMAN RD STE 0944 FT BELVOIR VA 22060-6218
1	DIRECTOR US ARMY RESEARCH LABORATORY ATTN AMSRL CS AL TA RECORDS MANAGEMENT 2800 POWDER MILL RD ADELPHI MD 20783-1197
1	DIRECTOR US ARMY RESEARCH LABORATORY ATTN AMSRL CI LL TECHNICAL LIBRARY 2800 POWDER MILL RD ADELPHI MD 207830-1197
1	DIRECTOR US ARMY RESEARCH LABORATORY ATTN AMSRL CS AL TP TECH PUBLISHING BRANCH 2800 POWDER MILL RD ADELPHI MD 20783-1197
1	DIRECTORATE FOR MANPRINT ATTN DAPE MR DEPUTY CHIEF OF STAFF PERSONNEL 300 ARMY PENTAGON WASHINGTON DC 20310-0300
1	CODE 1142PS OFFICE OF NAVAL RESEARCH 800 N QUINCY STREET ARLINGTON VA 22217-5000
1	WALTER REED ARMY INST OF RSCH ATTN SGRD UWI C (COL REDMOND) WASHINGTON DC 20307-5100
1	COMMANDER US ARMY RESEARCH INSTITUTE ATTN PERI ZT (DR E M JOHNSON) 5001 EISENHOWER AVENUE ALEXANDRIA VA 22333-5600
1	DEFENSE LOGISTICS STUDIES INFORMATION EXCHANGE ATTN DIRECTOR DLSIE ATSZ DL BLDG 12500 2401 QUARTERS ROAD FORT LEE VA 23801-1705

NO. OF COPIES	ORGANIZATION
1	DEPUTY COMMANDING GENERAL ATTN EXS (Q) MARINE CORPS RD&A COMMAND QUANTICO VA 22134
1	HEADQUARTERS USATRADOC ATTN ATCD SP FORT MONROE VA 23651
1	COMMANDER USATRADOC COMMAND SAFETY OFFICE ATTN ATOS (MR PESSAGNO/MR LYNE) FORT MONROE VA 23651-5000
1	COMMANDER US ARMY MATERIEL COMMAND ATTN AMCAM 5001 EISENHOWER AVENUE ALEXANDRIA VA 22333-0001
1	COMMANDER USA OPERATIONAL TEST & EVAL AGENCY ATTN CSTE TSM 4501 FORD AVE ALEXANDRIA VA 22302-1458
1	USA BIOMEDICAL R&D LABORATORY ATTN LIBRARY FORT DETRICK BUILDING 568 FREDERICK MD 21702-5010
1	COMMANDER USA AEROMEDICAL RESEARCH LAB ATTN LIBRARY FORT RUCKER AL 36362-5292
1	US ARMY SAFETY CENTER ATTN CSSC SE FORT RUCKER AL 36362
1	CHIEF ARMY RESEARCH INSTITUTE AVIATION R&D ACTIVITY ATTN PERI IR FORT RUCKER AL 36362-5354
1	AIR FORCE FLIGHT DYNAMICS LAB ATTN AFWAL/FIES/SURVIAC WRIGHT PATTERSON AFB OH 45433
1	AAMRL/HE WRIGHT PATTERSON AFB OH 45433-6573

NO. OF COPIES	ORGANIZATION
1	US ARMY NATICK RD&E CENTER ATTN STRNC YBA NATICK MA 01760-5020
1	US ARMY TROOP SUPPORT CMD NATICK RD&E CENTER ATTN BEHAVIORAL SCI DIV SSD NATICK MA 01760-5020
1	US ARMY TROOP SUPPORT CMD NATICK RD&E CENTER ATTN TECH LIBRARY (STRNC MIL) NATICK MA 01760-5040
1	HQ USA RESEARCH INST OF ENVIRONMENTAL MEDICINE ATTN MEDRI CL (DR J KOBRICK) NATICK MA 01760-5007
1	DR RICHARD JOHNSON HEALTH & PERFORMANCE DIVISION US ARIEM NATICK MA 01760-5007
1	MEDICAL LIBRARY BLDG 148 NAVAL SUBMARINE MEDICAL RSCH LAB BOX 900 SUBMARINE BASE NEW LONDON GROTON CT 06340
1	USAF ARMSTRONG LAB/CFTO ATTN DR F WESLEY BAUMGARDNER SUSTAINED OPERATIONS BRANCH BROOKS AFB TX 78235-5000
1	AFHRL/PRTS BROOKS AFB TX 78235-5601
1	DR JON FALLESEN ARI FIELD UNIT PO BOX 3407 FORT LEAVENWORTH KS 66027-0347
1	ARI FIELD UNIT FORT KNOX BUILDING 2423 PERI IK FORT KNOX KY 40121-5620
1	COMMANDANT USA ARTILLERY & MISSILE SCHOOL ATTN USAAMS TECH LIBRARY FORT SILL OK 73503

NO. OF COPIES	ORGANIZATION
1	COMMANDER WHITE SANDS MISSILE RANGE ATTN TECHNICAL LIBRARY WHITE SANDS MISSILE RANGE NM 88002
1	USA TRADOC ANALYSIS COMMAND ATTN ATRC WSR (D ANGUIANO) WHITE SANDS MISSILE RANGE NM 88002-5502
1	STRICOM 12350 RESEARCH PARKWAY ORLANDO FL 32826-3276
1	COMMANDER USA TANK-AUTOMOTIVE R&D CENTER ATTN AMSTA TSL (TECH LIBRARY) WARREN MI 48397-5000
1	US ARMY RSCH DEV STDZN GP-UK ATTN DR MIKE STOUT PSC 802 BOX 15 FPO AE 09499-1500
1	INSTITUTE FOR DEFENSE ANALYSES ATTN DR JESSE ORLANSKY 1801 N BEAUREGARD STREET ALEXANDRIA VA 22311
1	DR MM AYOUB DIRECTOR INST FOR ERGONOMICS RESEARCH TEXAS TECH UNIVERSITY LUBBOCK TX 79409
1	MR WALT TRUSZKOWSKI CODE 522.3 NASA/GODDARD SPACE FLIGHT CENTER GREENBELT MD 20771
1	COMMANDER US ARMY RESEARCH INSTITUTE OF ENVIRONMENTAL MEDICINE NATICK MA 01760-5007
1	HUMAN FACTORS ENG PROGRAM DEPT OF BIOMEDICAL ENGINEERING COLLEGE OF ENGINEERING & COMPUTER SCIENCE WRIGHT STATE UNIVERSITY DAYTON OH 45435

NO. OF COPIES	ORGANIZATION
1	COMMANDER US ARMY MATERIEL COMMAND ATTN AMCDE AQ 5001 EISENHOWER AVENUE ALEXANDRIA VA 22333
1	US ARMY RESEARCH INSTITUTE ATTN PERI IK (DOROTHY L FINLEY) 2423 MORANDE STREET FORT KNOX KY 40121-5620
1	US MILITARY ACADEMY MATHEMATICAL SCIENCES CENTER OF EXCELLENCE DEPT OF MATHEMATICAL SCIENCES ATTN MDN A MAJ DON ENGEN THAYER HALL WEST POINT NY 10996-1786
1	USARL HRED FIELD ELEMENT USAADASCH ATTN ATSA CD ATTN AMSRL HR ME (K REYNOLDS) 5800 CARTER ROAD FORT BLISS TX 79916-3802
1	ARL HRED ARDEC FIELD ELEMENT ATTN AMSRL HR MG (R SPINE) BUILDING 333 PICATINNY ARSENAL NJ 07806-5000
1	ARL HRED ARMC FIELD ELEMENT ATTN AMSRL HR MH (M BENEDICT) BUILDING 1109D (BASEMENT) FT KNOX KY 40121-5215
1	ARL HRED ATCOM FIELD ELEMENT ATTN AMSRL HR MI (A MANCE) 4300 GOODFELLOW BLVD BLDG 105 1ST FLOOR POST A-7 ST LOUIS MO 63120-1798
1	ARL HRED AVNC FIELD ELEMENT ATTN AMSRL HR MJ (R ARMSTRONG) PO BOX 620716 BUILDING 514 FT RUCKER AL 36362-0716
1	ARL HRED FIELD ELEMENT AT FORT BELVOIR STOP 5850 ATTN AMSRL HR MK (P SCHOOL) 10109 GRIDLEY ROAD SUITE A102 FORT BELVOIR VA 22060-5850

NO. OF COPIES	ORGANIZATION
1	ARL HRED CECOM FIELD ELEMENT ATTN AMSRL HR ML (J MARTIN) MYERS CENTER ROOM 3C214 FT MONMOUTH NJ 07703-5630
1	ARL HRED FT HOOD FIELD ELEMENT ATTN AMSRL HR MA (E SMOOTZ) HQ TEXCOM BLDG 91012 RM 134 FT HOOD TX 76544-5065
1	ARL HRED MICOM FIELD ELEMENT ATTN AMSRL HR MO (T COOK) BUILDING 5400 ROOM C242 REDSTONE ARSENAL AL 35898-7290
1	ARL HRED ATTN AMSRL HR MQ (M R FLETCHER) USASSCOM NRDEC BLDG 3 RM 140 NATICK MA 01760-5015
1	ARL HRED SC&FG FIELD ELEMENT ATTN AMSRL HR MS (L BUCKALEW) SIGNAL TOWERS ROOM 207 FORT GORDON GA 30905-5233
1	ARL HRED TACOM FIELD ELEMENT ATTN AMSRL HR MU (M SINGAPORE) BUILDING 200A 2ND FLOOR WARREN MI 48397-5000
1	ARL HRED STRICOM FIELD ELEMENT ATTN AMSRL HR MT (A GALBAVY) 12350 RESEARCH PARKWAY ORLANDO FL 32826-3276
1	ARL HRED USAIC FIELD ELEMENT ATTN AMSRL HR MW (E REDDEN) BUILDING 4 ROOM 349 FT BENNING GA 31905-5400
1	ARL HRED USAFAS FIELD ELEMENT ATTN AMSRL HR MF (L PIERCE) BLDG 3040 ROOM 220 FORT SILL OK 73503-5600
1	ARL HRED USASOC FIELD ELEMENT ATTN AMSRL HR MN (F MALKIN) BUILDING D3206 ROOM 503 FORT BRAGG NC 28307-5000
1	ARL HRED ATTN AMSRL HR MP (UNGVARSKY) FT LEAVENWORTH KS

NO. OF
COPIES ORGANIZATION

1 ARL HRED FT HUACHUCA FIELD
ELEMENT
ATTN AMSRL HR MY
BUILDING 84017
FORT HUACHUCA AZ 85613-7000

1 ARL HRED OPTEC FIELD ELEMENT
ATTN AMSRL HR MR (D HEADLEY)
PARK CENTER IV RM 1450
4501 FORD AVENUE
ALEXANDRIA VA 22302-1458

1 ARL HRED ERDEC FIELD ELEMENT
ATTN AMSRL HR MM (D HARRAH)
BLDG 459
APG-AA

ABERDEEN PROVING GROUND

2 DIRECTOR
US ARMY RESEARCH LABORATORY
ATTN AMSRL CI LP (TECH LIB)
BLDG 305 APG AA

1 LIBRARY
ARL BLDG 459
APG-AA

1 CHIEF ARL HRED ERDEC FIELD
ELEMENT
ATTN AMSRL HR MM (D HARRAH)
BLDG 459 APG-AA

1 USATECOM
RYAN BUILDING
APG-AA

1 COMMANDER
CHEMICAL BIOLOGICAL AND DEFENSE
COMMAND
ATTN AMSCB CI
APG-EA

REPORT DOCUMENTATION PAGE

Form Approved
OMB No. 0704-0188

1. AGENCY USE ONLY *(Leave blank)*	2. REPORT DATE	3. REPORT TYPE AND DATES COVERED
	July 1997	Final

4. TITLE AND SUBTITLE

Modeling Body Joint Loads During Equipment Decontamination Operations

5. FUNDING NUMBERS

AMS Code 622716.H700011
PR: 1L162716AH70
PE: 6.27.16

6. AUTHOR(S)

McMahon, R.W. (U.S. Army Research Laboratory); Shams, T. (General Engineering and Systems Analysis Company)

7. PERFORMING ORGANIZATION NAME(S) AND ADDRESS(ES)

U.S. Army Research Laboratory
Human Research & Engineering Directorate
Aberdeen Proving Ground, MD 21005-5425

8. PERFORMING ORGANIZATION REPORT NUMBER

9. SPONSORING/MONITORING AGENCY NAME(S) AND ADDRESS(ES)

U.S. Army Research Laboratory
Human Research & Engineering Directorate
Aberdeen Proving Ground, MD 21005-5425

10. SPONSORING/MONITORING AGENCY REPORT NUMBER

ARL-TR-1332

11. SUPPLEMENTARY NOTES

12a. DISTRIBUTION/AVAILABILITY STATEMENT

Approved for public release; distribution is unlimited.

12b. DISTRIBUTION CODE

13. ABSTRACT *(Maximum 200 words)*

The General Engineering and Systems Analysis Company (GESAC), Inc., under contract with the Human Research and Engineering Directorate of the U.S. Army Research Laboratory (ARL), (contract number DAAL01-94-P-0906) estimated body joint loading using a computer simulation program called DYNAMAN©. This work was performed in support of the U.S. Army Chemical and Biological Defense Command (CBDCOM) modular decontamination system (MDS) development program.

The objective of this effort was to model the loading imposed by each of five different scrub brush systems on various human body joints and compare the resulting force and torque values. Of primary interest was information concerning how electric motor placement affected joint loading and how the joint loads of the powered brush systems compared with those of the manual brush.

The results of this modeling effort identified several limitations with the current model, identified several key aspects of power scrub brush design and operator interface, and were used to aid in the selection of brush designs for continued development. In addition, the results indicate that the counterweight offered by attaching the motor to the brush helps to slightly reduce the torque imposed on the operator's body.

It is recommended that future efforts to model the effects of force and torque on humans include a highly definitive description of simulation conditions to allow for improved comparison. Finally, it is recommended that a research effort be undertaken to improve our understanding of the biodynamical tolerance of human joints to external loading. This effort should include determinations of human joint safety as well as comfort tolerance to joint loading.

14. SUBJECT TERMS

acceleration	computer simulation	external loads	modeling
anthropometry	decontamination	force	power brush design
body joint loads	DYNAMAN©	linked bodies	torque

15. NUMBER OF PAGES 105

16. PRICE CODE

17. SECURITY CLASSIFICATION OF REPORT	18. SECURITY CLASSIFICATION OF THIS PAGE	19. SECURITY CLASSIFICATION OF ABSTRACT	20. LIMITATION OF ABSTRACT
Unclassified	Unclassified	Unclassified	